Spring 5-7-2016

Genetic Predisposition and M1 Macrophage Polarization Created by Elastin-Derived Peptides Drive Abdominal Aortic Aneurysm Formation

Matthew A. Dale
University of Nebraska Medical Center

GENETIC PREDISPOSITION AND M1 MACROPHAGE POLARIZATION CREATED BY ELASTIN-DERIVED PEPTIDES DRIVE ABDOMINAL AORTIC ANEURYSM FORMATION

By

Matthew Dale

A DISSERTATION

Presented to the Faculty of

the University of Nebraska Graduate College

in Partial Fullfilment of the Requirements

for the Degree of Doctor in Philosophy

Pathology & Microbiology
Graduate Program

(Surgery)

Under the Supervision of Professor Bernard Timothy Baxter, M.D.

University of Nebraska Medical Center
Omaha, Nebraska

April, 2016

Supervisory Committee:

Tammy L. Kielian, Ph.D. Andrew T. Dudley, Ph.D.

Thomas L. McDonald, Ph.D. Stephen I. Rennard, M.D.

Acknowledgements

To my wife, my family,

and everyone in the B. Timothy Baxter laboratory

Abstract

Abdominal aortic aneurysm (AAA) is a dynamic vascular disease characterized by inflammatory cell invasion and extracellular matrix (ECM) degradation. Evidence has demonstrated a profound influence of genetic background on AAA formation. The work presented herein discusses two studies: the first demonstrates how genetic components can enhance the susceptibility to AAA formation and the second demonstrates how ECM degradation enhances AAA progression by influencing inflammatory cell phenotypes. An understanding of the pathways involved in AAA pathogenesis can help not only to identify potential patients at risk of AAA development, a heritable disease in which the incriminating component has yet to be discovered, but also to identify therapeutic targets for medical therapy. By using the $CaCl_2$ model of aneurysm formation, we were able to induce aneurysms in two different strains of mice, C57Bl/6 and 129/SvEv. While both strains developed aneurysms, 129/SvEv mice developed larger aneurysms, increased inflammatory cell infiltration, and had higher MMP expression compared to C57Bl/6 mice. We believe this increased susceptibility is due to increased ProMMP-2 expression at baseline. This increase in MMP expression may help to explain why some patients develop aneurysms at faster rates than others or why some patients may be predisposed to aneurysm formation while others form atherosclerotic plaque.

Furthermore, our study examines how products released from damage to the aortic wall, particularly the breakdown of elastin and the release of elastin-derived peptides (EDPs), influence the surrounding microenvironment. Pro-inflammatory M1 macrophages initially are recruited to sites of injury but, if their effects are prolonged, can lead to chronic inflammation that prevents normal tissue repair. The EDPs released from aortic wall damage create a pro-inflammatory M1 macrophage phenotype. By using $CaCl_2$ to induce AAA formation, we show how manipulation of this pro-inflammatory response by direct injection of anti-inflammatory M2 macrophages can reduce aortic

dilation. Antibody-mediated neutralization of EDPs can attenuate aortic dilation by preventing macrophage recruitment to the damaged aortic wall, reducing MMP upregulation, and influencing the M1/M2 phenotype ratio. By manipulating the M1/M2 ratio, we identify a potential therapeutic target in the fight to discover a medical therapy and minimize the need for invasive mechanical intervention in AAA.

TABLE OF CONTENTS

ACKNOWLEDGEMENTS……ii

ABSTRACT……...iii

LIST OF TABLES……,,vii

LIST OF FIGURES……viii

LIST OF ABBREVIATIONS……x

INTRODUCTION……1

CHAPTER 1: Inflammatory cell phenotypes in AAAs……3

Brief review: Innate and Adaptive Immune System……..4

Inflammatory Cells in AAAs……...4

Inflammatory Cells in Atherosclerosis……8

Inflammatory Cells in Diabetic Atherosclerosis……8

$CD4^+$ and $CD8^+$ T cells……...9

T cell phenotypes: Th1, Th2, Th17, and T_{reg}……..…..9

Macrophage Phenotypes: M1 and M2……17

Neutrophils and Mast Cells……23

Discussion……23

CHAPTER 2: Genetic differences in MMP levels influence AAA susceptibility……25

Introduction……26

Methods……..28

Results……31

Discussion……52

CHAPTER 3: Elastin-derived peptides enhance M1 macrophage polarization leading to AAA formation……..56

Introduction……57

Methods……..59

Results……67

Discussion……90

DISSERTATION DISCUSSION……..94

BIBLIOGRAPHY……...101

LIST OF TABLES

Table 1.1. Th Cell Differentiation, Function, and Role in Disease……...11

Table 1.2. Th Cell Differentiation in Human and Experimental AAA……13

Table 1.3 Macrophage Differentiation, Function, and Role in Disease……...19

Table 1.4 Macrophage Differentiation in Human and Experimental AAA……..21

Table 2.1. Changes in aortic diameter in C57Bl/6 and 129/ SvEv mice after treatment of NaCl and $CaCl_2$……..35

Table 2.2 The number of macrophages in $CaCl_2$-treated aorta of 129/SvEv and C57Bl/6 mice……..43

Table 2.3. Changes in aortic diameter in chimeric mice after treatment of NaCl and $CaCl_2$……..50

LIST OF FIGURES

Figure 1.1. Schematic representation of inflammatory cell infiltration in AAAs……6

Figure 2.1. Aortic changes after NaCl and $CaCl_2$ treatment in C57Bl/6 and 129/SvEv mice……..33

Figure 2.2. Elastic modulus of aortic tissues from C57Bl/6 and 129/SvEv mice……..36

Figure 2.3. Aortic tropoelastin content……49

Figure 2.4. Aortic MMP-2 and MMP-9 expression……...41

Figure 2.5. Aortic elastase activity and neutrophil elastase expression……45

Figure 2.6. The role of myelogenous cells in AAA susceptibility……...48

Figure 3.1. Aortic tissue mRNA levels of Ym1, CD206, and iNOS after aneurysm induction with $CaCl_2$……62

Figure 3.2. Elastin-derived peptides polarize macrophages to a pro-inflammatory M1 phenotype……..68

Figure 3.3. M1 and M2 macrophage influence on aortic size six weeks after aneurysm induction……..70

Figure 3.4. Active MMP-2 and MMP-9 levels are decreased in mice injected with M2 macrophages……73

Figure 3.5. M1 and M2 macrophage influence on aortic size three days after aneurysm induction……...75

Figure 3.6. BA4 attenuates aortic dilation and elastin degradation……78

Figure 3.7. BA4 increases $CD206^+$ macrophages in aortic tissue……81

Figure 3.8. BA4 reduced macrophage migration, MMP production, and the ratio of M1/M2 markers in aortic tissue one week after aneurysm induction……..83

Figure 3.9. BA4 treatment promotes an anti-inflammatory environment in aortic tissue one week after aneurysm induction……86

Figure 3.10. Aortic tissue protein levels of Ym1 one week after BA4 treatment……...88

LIST OF ABBREVIATIONS

AAA	abdominal aortic aneurysm
AGE	advanced glycation end products
AP	activator protein
Arg	arginase
BMDM	bone marrow-derived macrophage
CREB	cAMP response element-binding protein
ECM	extracellular matrix
EDP	elastin-derived peptides
FIZZ	found in inflammatory zone
Fox	forkhead box
IFN	interferon
IL	interleukin
ILT	intraluminal thrombus
iNOS	inducible nitric oxide synthase
LDL	low-density lipoproteins
LPS	lipopolysaccharide
MCP	monocyte chemotactic protein
MFS	Marfan Syndrome
MHC	major histocompatibility complex
MMP	matrix metalloproteinase
NF-κB	nuclear factor-κB
NK	natural killer
PPAR	peroxisome proliferator-activated receptor
ROR	retinoic acid receptor-related orphan receptor
SMC	smooth muscle cell

STAT	signal transducer and activator of transcription
T_{eff}	T effector
Th	T helper
TGF	transforming growth factor
TLR	toll-like receptor
TNF	tumor necrosis factor
T_{reg}	T regulatory
VVG	Verhoeff-Van Geison
Ym1	chitinase 3-like-3

INTRODUCTION

Abdominal aortic aneurysms (AAAs) are permanent dilations of the abdominal aorta that, if left untreated, can lead to fatal aortic rupture. Death results from exsanguination into the retroperitoneum or abdominal cavity and may be rapid. Approximately 15,000 deaths due to aneurysm rupture are reported each year in the U.S. [1] Most AAAs are diagnosed serendipitously since they are asymptomatic until the time of rupture. Therefore, screening programs have been employed to identify the disease in high-risk populations. [2] Risk factors include male gender, increased age (> 65 years), and a positive family history. [3-5] Additionally, smoking history is one of the major risk factors associated with aneurysm formation. A positive smoking history predicts a larger aneurysm size at diagnosis[6] as well as a higher risk of aneurysm progression with continued smoking. [7] Other associated risk factors for AAA formation include Caucasian race, presence of other aneurysms, and atherosclerosis.[8,9]

An aortic aneurysm is defined as a 50% increase in aortic diameter. Many screening studies use an infrarenal aortic diameter greater than 3.0 cm to define an aneurysm. Surgical intervention is not recommended until the aorta reaches a diameter of 5.5 cm in men and 5.0 cm in women, where the risk of rupture exceeds the risk of repair. Currently, there are no pharmacological therapies for slowing AAA progression, so patient management is a matter of watching and waiting until the aorta reaches a size where repair is indicated. Animal studies using statins, β-blockers, angiotensin-converting enzyme inhibitors, angiotensin receptor blockers, and tetracyclines have been shown to have a beneficial effect by delaying progression of aortic dilation. [10-17] Despite this, none of these drugs have proven benefit in humans. The only known approach to slow aneurysm progression is smoking cessation.

The pathogenesis of AAA is a highly complex process that is undoubtedly multifactorial with, an as yet uncertain, genetic contribution. Histological features of AAA include smooth muscle cell (SMC) apoptosis, elastin fragmentation, as well as chronic adventitial and medial inflammatory cell infiltration. [18] Elastin fragmentation is triggered by upregulation of various elastin-degrading enzymes such as matrix metalloproteinases (MMPs), cysteine proteases, and serine proteases. These elastin and extracellular matrix (ECM) fragments recruit inflammatory cells to the artery wall triggering an innate immune response that attempts to resolve the damage. The adaptive immune response later develops and is associated with aneurysm progression through antigen specific antibody production. [19,20]

Studies of human aortic aneurysm tissue obtained at surgery are informative but likely reflect the end stage of the disease process. To investigate the cause of aneurysmal disease and to determine early pathophysiological changes in AAA, animal models are commonly used. Studies with animal models have led to advances including recognition that chronic inflammation, increased expression of endogenous proteinases, degradation of structural matrix proteins, and medial smooth muscle cell depletion all play a role in the process of aneurysm development. [21,22] Genetically engineered mice have been increasingly used to investigate the molecular mechanisms of AAA. Important insights pertaining to inflammatory cytokines and MMPs have been obtained from mouse studies involving targeted disruptions of genes such as interferon-γ (IFN-γ), tumor necrosis factor-α (TNF-α), MMP-2, and -9. [23-26]

CHAPTER 1

Inflammatory cell phenotypes in AAAs

The following is a modified version of an article published in *Arteriosclerosis, Thrombosis, and Vascular Biology* 2015 Aug;35(8):1746-55. The work was coauthored by Melissa K Ruhlman, B. Timothy Baxter, and myself.

Brief review: Innate and adaptive immune system

The immune system is a complex arrangement of many cell types and molecules interacting to maintain homeostasis. The first basic distinction is the difference between innate and adaptive immunity. The innate immune system comprises all of the immune responses present from birth whereas the adaptive immune system consists of those responses generated after exposure to specific new antigens. The innate immune system is considered the first line of defense against invading microorganisms and is made up of the cells and molecules that act as first responders in the face of an insult. [27] It has been conserved throughout evolution with similar molecular components found in simple eukaryotes and more complex organisms including humans. [27] The adaptive immune system developed later in evolution and can acquire what is considered immunologic "memory." After exposure to a novel pathogen, the adaptive immune system tailors its response while maintaining self-tolerance (except in autoimmune diseases). These responses are typically controlled with an acute phase and subsequent resolution. In aneurysmal disease, it is believed that there is ongoing, poorly regulated inflammation resulting in progressive tissue damage and aneurysm expansion.

Inflammatory cells in AAAs

The transmural inflammation seen in AAA involves a variety of inflammatory cell types, where macrophages and lymphocytes are the most prominent with mast cells and neutrophils migrating to a lesser extent. [28-31] Ocana et al. demonstrated that both T- and B-lymphocytes are present in AAA tissue, where the majority of the infiltrating lymphocytes are cluster of differentiation four positive ($CD4^+$) T cells. [32] No natural killer (NK) cells were detected in tissue from AAA patients; [32] however, peripheral blood levels of NK cells were significantly higher in AAA patients compared to controls. [33] The presence of B- and T- lymphocytes suggests antibody-mediated humoral immunity and

potentially an autoimmune process driving AAA formation or progression. Previous animal studies have reported that without the presence of $CD4^+$ T cells, AAA formation does not occur.[34] Furthermore, experimental AAA formation is mediated by interleukin (IL)-17, a cytokine notably produced by pro-inflammatory $CD4^+$ T cells.[35] These pro-inflammatory $CD4^+$ T cells exacerbate AAA disease progression and play a role in creating chronic inflammation in the damaged aortic wall (Figure 1.1).

Macrophages have also been shown to play a key role in AAA progression. Macrophages are key components of the inflammatory process. Tumor necrosis factor (TNF)-α, IL-6, IL-1β, and interferon (IFN)-γ are pro-inflammatory macrophage-associated cytokines studied as biomarkers of AAA progression.[36,37] Although all of these cytokine levels are elevated in patients with AAA compared to controls, only IFN-γ levels had a positive correlation with AAA progression. Macrophages are recruited to injury sites by ECM degradation products and numerous chemokines. These chemokines, monocyte chemotactic protein (MCP)-1, IL-8, and TNF-α, are colocalized to infiltrating macrophages.[38-40] Macrophages recruited to AAA tissue begin a positive feedback loop creating chronic inflammation, but they may not always be harmful in AAA development (Figure 1.1). Macrophages, like T cells, display plasticity and have the ability to polarize to various phenotypes, such as the classically activated (M1) phenotype or the alternatively activated (M2) phenotype. M1 macrophages are typically characterized by pro-inflammatory cytokine production and initiate tissue degradation, whereas M2 macrophages are implicated in inflammation resolution and tissue repair. An M1/M2 imbalance may be occurring in AAA, where strategies targeting a stronger M2 response may prove a potential therapeutic target to reduce chronic inflammation in AAAs.

Figure 1. Schematic representation of inflammatory cell infiltration in AAAs. A normal aorta is represented on the left with intact endothelial and elastin layers. The wall of the aneurysmal aorta consists of robust inflammatory cell infiltration. T cells and macrophages primarily migrate to the adventitia, with lesser infiltration into the media. Pro-inflammatory Th1 and Th17 cells predominate whereas infiltration of anti-inflammatory T_{regs} and Th2 cells occurs to a lesser extent. A macrophage phenotype imbalance exists with more pro-inflammatory M1 macrophages (M1 MΦ) than anti-inflammatory M2 macrophages (M2 MΦ) in the aneurysmal aortic wall. During the initial aortic growth phase, thickening of the adventitial layer occurs, resulting in increased total wall thickness. Aneurysm formation and inflammation results in breakdown of medial elastin and smooth muscle cell (SMC) apoptosis, causing a thinning of the medial layer. Loss of the endothelial cell (EC) layer is replaced by an intraluminal thrombus (ILT).

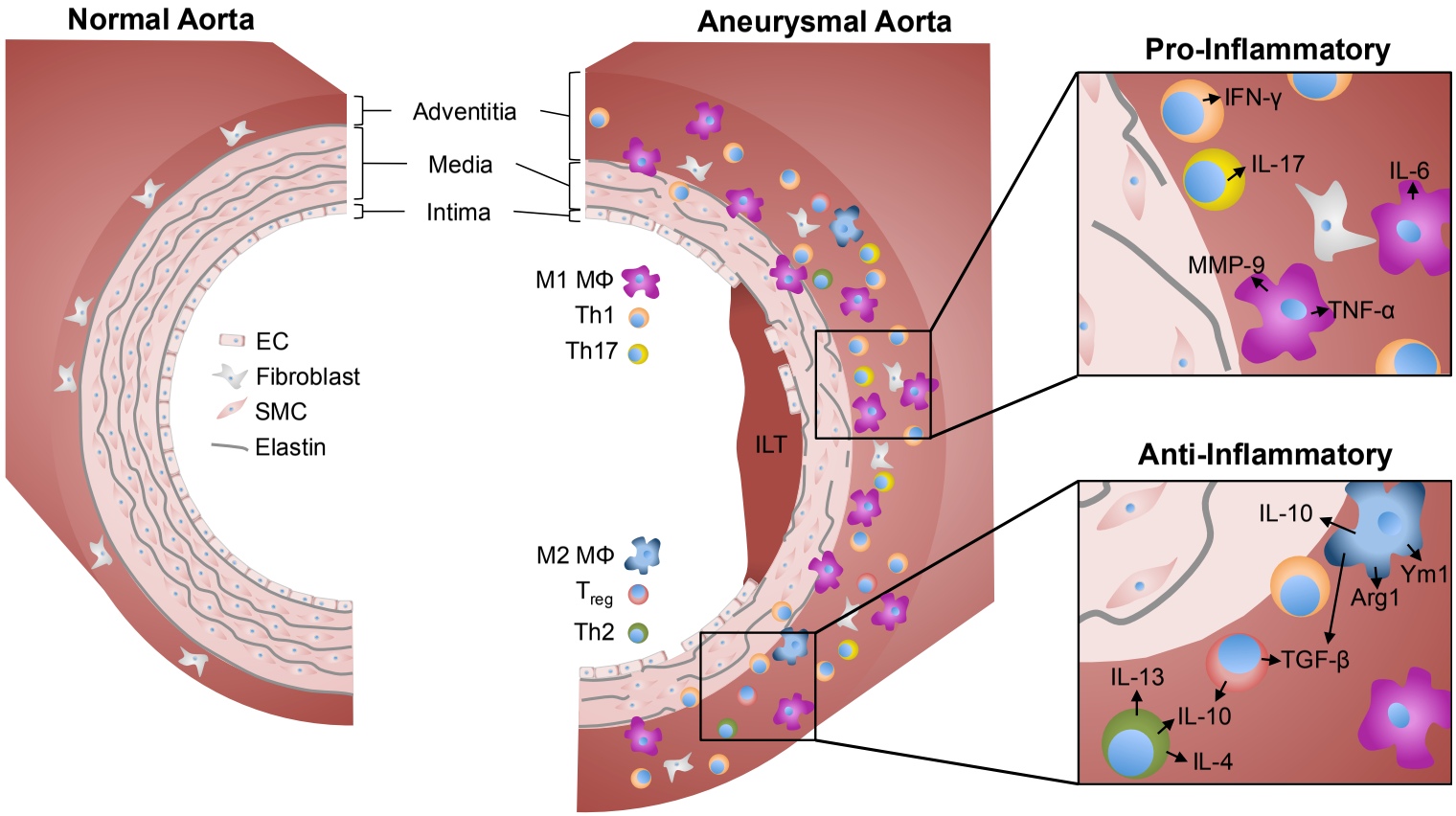
Normal Aorta
Aneurysmal Aorta
Adventitia
Media
Intima
EC
Fibroblast
SMC
Elastin
M1 MΦ
Th1
Th17
ILT
M2 MΦ
Treg
Th2
Pro-Inflammatory
IFN-γ
IL-17
IL-6
MMP-9
TNF-α
Anti-Inflammatory
IL-10
Ym1
Arg1
TGF-β
IL-13
IL-10
IL-4

Inflammatory cells in atherosclerosis

Atherosclerosis is an inflammatory disease beginning in the intima of large and medium sized arteries caused by accumulations of low-density lipoproteins (LDL). A wide range of inflammatory cell types has been found in advanced atherosclerotic lesions including but not limited to macrophages/monocytes, lymphocytes, and dendritic cells.[41] Infiltration of these inflammatory cells occurs primarily in the neointima, aiding in the inward rather than outward remodeling in atherosclerosis. Glagov et al. were the first to describe compensatory outward remodeling that partially compensated for intimal expansion.[42] A recent study proposed that IL-1 is an important factor that enhances outward remodeling, protecting the artery from stenosis.[43] Inhibition of the IL-1 pathway actually enhanced macrophage infiltration and caused further narrowing of the arterial lumen. MMPs assist in the outward remodeling process and are implicated as a cause of AAA formation, but in atherosclerosis, MMPs are predominantly expressed in the atherosclerotic plaque, leading to plaque instability.[44,45] In contrast, Figure 1 demonstrates that the inflammatory lesions in AAA tend to occur in the outer layers of the media and adventitia, where they may be expected to have a greater impact on outward remodeling. The presence of inflammatory cells and their associated cytokines and proteases may protect from arterial narrowing by promoting outward remodeling. Taken to the extreme, this inflammatory response may promote overcompensation in the outward remodeling process by causing aneurysm formation.[46]

Inflammatory cells in diabetic atherosclerosis

Diabetes is an important risk factor for the development of atherosclerotic lesions. Irreversible formation of advanced glycation end products (AGEs) is implicated as a cause of accelerated atherosclerosis.[47] The interaction of AGEs with mononuclear phagocytes induces a pro-inflammatory macrophage phenotype, resulting in production

of various pro-inflammatory cytokines such as TNF-α and IL-1β. [48-50] Interestingly, diabetes is negatively associated with AAAs. [6,51] This negative correlation may be related to the formation of AGEs and alterations to ECM proteins. Golledge et al. found that aortic tissue from patients with diabetes have decreased activities of MMP-2 and MMP-9. [52] Modification of collagen lattices by glycation or treatment with glutaraldehyde reduced MMP activity. These findings suggest that modification of ECM proteins reduces protease activity, potentially preventing aortic wall degeneration and aneurysm formation.

$CD4^+$ and $CD8^+$ T cells

A review of the cell types involved is critical to understanding the role of inflammation in AAA development and progression. T cells are a heterogeneous group of lymphocytes with a diverse classification system and multitude of physiologic actions. They are initially classified based on surface expression of CD4 or CD8 molecules. $CD4^+$ cells recognize antigens presented by major histocompatibility complex (MHC) Class II, while $CD8^+$ cells recognize antigens presented by MHC Class I, important in cell-mediated toxicity. [53] Most modulatory T cells express CD4 while most cytotoxic T cells express CD8. The $CD4^+$ T cell has been found to be the predominant cell type in human aneurysm tissue. Through its profile of secreted cytokines, the $CD4^+$ T cell indirectly controls matrix metabolism by recruitment of macrophages and regulation of ECM and protease synthesis.

T cell phenotypes: Th1, Th2, Th17, and T_{reg}

$CD4^+$ T cells can be further subdivided into the T helper (Th) or T effector (T_{eff}) subsets: Th1, Th2, and Th17 and the regulatory subset: T regulatory (T_{reg}) cells. Each subset is classified by the cytokine profile required for stimulation, their secreted

products, and their physiologic actions. In human disease, there is rarely polarization to one specific cell phenotype but an imbalance between pro-inflammatory and anti-inflammatory $CD4^+$ cells may enhance aneurysmal disease progression.

Th1

The Th1 cell has been linked to many chronic auto-inflammatory disorders including: [54,55] rheumatoid arthritis, [56] emphysema, [57] and systemic lupus erythematosis. [58] Th1 cells are characteristically activated by IL-12, triggering the signal transducer and activator of transcription 4 (STAT4) and T-bet pathway to produce IFN-γ, TNF-α, and TNF-β (Table 1.1). [54,55,59-63] This leads to activation of macrophages and an internal autoregulatory loop to potentiate Th1 development and inhibit alternate T cell differentiation. Through this cycle, IFN-γ activates macrophages and enhances inflammatory cell recruitment through augmenting cytokine, chemokine, and adhesion molecule expression. [60,61] Macrophages then produce additional IL-12, which promotes further Th1 activation. [54,60] This potentiates a cycle of matrix destruction and enhanced aneurysm formation. Interestingly, the best data available is conflicting regarding the expression of IL-12 and its downstream transcription factor STAT4. IL-12 protein levels are decreased in AAA tissue compared to aortic occlusive disease tissue. [60] Conversely, STAT4 levels are upregulated in AAA compared to non-aneurysmal control. [64] This apparent inconsistency may be due to different controls used for each study. The decrease in IL-12 from AAA patients was in comparison to patients that have severe atherosclerosis, whereas the STAT4 increase from AAA patients was in comparison to organ donors who likely had minimal disease.

Galle et al. found human aneurysmal tissue expressed high levels of IFN-γ but not IL-4, a typical Th2 marker. [29] They also identified overexpression of T-bet, the intracellular signaling pathway for Th1 polarization, without significant Th2 signaling.

Table 1.1

Table 1.1. Th cell differentiation, function, and role in disease.

	Th1	Th2	Th17	T_{reg}
Stimulating Factors	IL-12	IL-4	IL-23, IL-1, IL-6	IL-2, TGF-β
Pathway	STAT4, T-bet	STAT6, GATA-3	RORγt, STAT3	STAT5, Foxp3
Secreted Products	IFN-γ	IL-4, IL-5, IL-10, IL-13	IL-17A & F	IL-10 & TGF-β
Role in Disease	Macrophage activation, ↑Inflammatory cell recruitment	Limit macrophage cytotoxicity, ↓MMPs & cytokines (IL-4/10), ↑MMPs (IL-13)	↑macrophage recruitment	↓T_{eff} proliferation, ↓TNF-α & IFN-γ secretion from T_{eff} and macrophages, remove autoreactive T cells

This suggests robust presence of the Th1 cell with minimal Th2 involvement in end stage human disease. Juvonen et al. found elevated serum levels of IFN-γ in humans with AAA, which correlated with an increased aneurysm growth rate. [36] We have previously demonstrated that mice deficient in $CD4^+$ T cells had attenuated MMP expression and no aneurysm formation in a murine model of AAA, where replacing IFN-γ alone reconstituted aneurysm formation. [34] This contrasts with work done in the $ApoE^{-/-}$ model of AAA, where Rag1 deficiency had no effect on reducing aneurysm size. [65] This was also true for IFN-γ and its downstream transcription factor STAT1 in the $ApoE^{-/-}$ model. [66,67] These data highlight differences in the models. The $CaCl_2$ model relies on an inflammatory response for aneurysm formation whereas the $ApoE^{-/-}$ model depends to a much greater extent on a combination of hemodynamics and hypercholesterolemia. Taken together, the animal models have failed to elucidate a clear role of lymphocytes and IFN-γ in AAA (Table 1.2).

Th2

The Th2 cell, along with its cytokine profile, is largely considered anti-inflammatory. Interestingly, the Th2 cell can also be associated with inflammatory processes including IgE-mediated antibody responses, allergy, and asthma. [54,61,63] IL-4 drives the differentiation of $CD4^+$ T cells into the Th2 phenotype. Through the STAT6 and GATA-3 pathway, the Th2 cell secretes IL-4, IL-5, IL-10, and IL-13 (Table 1). [54,55,60-63] IL-4 and IL-10 limit the cytotoxic potential of macrophages and decrease expression of pro-inflammatory mediators and MMPs. IL-13 enhances development of anti-inflammatory M2 macrophages but also increases MMP expression. [60,61]

The Th2 cell profile has been implicated as a culprit in aneurysmal disease in both human and murine studies. [68] Schonbeck et al. found increased levels of Th2 associated cytokines and low expression of Th1 related cytokines, particularly IFN-γ, in

Table 1.2.

Table 1.2. Th cell differentiation in human and experimental AAA.

	Th1	Th2	Th17	T_{reg}
Human AAA	Increased[23, 30]	Increased[54,56] Decreased[23]	Increased[29,65]	Decreased[69]
$ApoE^{-/-}$ AngII model	Increased[60]	Increased[62]	Increased[65,66]	Decreased[65,70]
$CaCl_2$ model	Increased[28]	Undefined	Undefined	Undefined
Elastase-perfusion model	Undefined	Undefined	Increased[29,65]	Undefined

human tissue.[60] They suggested that IL-4 overexpression prevents Th1 differentiation and that IL-4 and IL-5 induced chemoattraction of neutrophils contributes to excessive elastolytic activity. Shimizu et al. showed that in allografted mice aortas, AAA development was more severe in IFN-γ deficient mice while mice deficient in IL-4 were protected from AAA.[61] Contradictory to the murine data, IL-4 has been shown to stimulate production of ECM proteins in human fibroblasts and suppress MMP expression (MMP-1 and MMP-9) in human alveolar macrophages.[69,70] Chan et al. suggested an alternate source for the Th2 associated cytokines; another member of the T cell family, the natural killer (NK) T cell.[62] NK and NKT cells produce both IL-4 and IFN-γ and have a profile that is neither Th1 nor Th2; referred to as Th0. Unlike most immune cells whose function appears to decline with age, the NK and NKT cells increase in number and produce greater IL-4 with advancing age. The important role of the Th2 cell may be specific to the murine transplant model, as other murine models show Th1 predominance. The conflicting data between the Th1 and Th2 profiles may relate to technical differences in how measurements were made, differences in animal models, and the late disease state at which human aneurysm samples are obtained (Table 1.2).

Th17

A more recently identified distinct subclass of T helper cell, the Th17 cell, has generated interest with regard to its potential role in AAA. This cell type is unique from Th1 and Th2 cells based on both its cytokine profile and differentiation pathway.[59] The Th17 cell is stimulated by IL-23, IL-1, and IL-6, which primarily induce retinoic acid receptor–related orphan receptor γt (RORγt) and STAT3, leading to secretion of IL-17 (Table 1.1).[55,59,63,71] IL-17 has 6 known isoforms, A through F, of which Th17 cells secrete IL-17A and F. IL-17A, its primary cytokine, mediates many immune and

inflammatory diseases and is critical for vascular superoxide production.[72] The Th17 cell promotes macrophage recruitment to the vascular wall while deficiency of IL-17 appears to reduce aortic macrophages in murine models.[71,72]

Madhur et al. found aneurysm formation in the ApoE$^{-/-}$ murine model to be unchanged when comparing control mice to IL-17 knockout mice.[72] This suggested that IL-17 did not have a critical role in this murine model. In contrast, Sharma et al. showed that IL-23 and Il-17 expression was increased in human AAA.[35] Using an elastase-perfusion murine model, deletion of IL-17 or IL-23 attenuated aneurysm development and decreased pro-inflammatory cytokine production. Furthermore, mesenchymal stem cell treatment, at the time of aneurysm induction, decreased IL-17 production and reduced aortic dilation. Recently, Wei et al. showed that the T helper and IL-17 inflammatory response was diminished by administration of digoxin in a dose dependent manner.[71] This was associated with a decrease in AAA incidence and increased mouse survival in the ApoE$^{-/-}$ and elastase-perfusion murine models. Digoxin was found to antagonize RORyt, inhibit Th17, and augment T_{reg} cells. This growing body of evidence suggests an important role of the Th17 cell in promoting inflammation and enhancing aneurysmal disease.

T_{reg}

T_{reg} cells are a unique subclass of CD4^{+} T cells that function to counteract the pro-inflammatory effects of the T effector subclasses and are important in immune tolerance. IL-2 and transforming growth factor (TGF)-β stimulate T_{reg} cells, which produce IL-10 and TGF-β through the STAT5 and forkhead box P3 (Foxp3) pathway (Table 1.1).[55,63] The T_{reg} assumes the critical function of curtailing the inflammatory process, limiting collateral damage, and allowing matrix repair to begin. Known functions of T_{reg} cells include blocking further proliferation of T_{eff} cells,[63,73] inhibiting the

inflammatory cascade by blocking TNF-α and IFN-γ secretion from effector cells and invading macrophages,[48] and removal of autoreactive T cell clones generated in response to matrix degradation products.[74] Because one of the most important functions of the T_{reg} cells is to limit the proliferation of T_{eff} cells, a relative increase in T_{eff} cells indicates a loss of control of the inflammatory response. Yin et al. showed a reduction in the proportion of T_{reg} cells in AAA patients.[75] Increasing the T_{reg} population, by injection of splenic T_{reg} cells from a donor mouse, protected $ApoE^{-/-}$ mice from aneurysm formation.[76] An imbalance in the proportion of the T_{reg} cell population or dysfunction of the T_{reg} cell has been implicated in other chronic inflammatory processes, including COPD,[57,77] inflammatory bowel disease,[78,79] lupus,[58,80,81] scleroderma,[82,83] and organ rejection.[84,85] Importantly, matrix destruction, which leads to end stage disease in each of these processes, appears to represent collateral damage from an uncontrolled inflammatory response. Normally functioning T_{reg} cells have the potential to limit matrix damage by inhibiting T cell proliferation, blocking TNF-α and IFN-γ secretion, and removing autoreactive T cells.

In summary, the majority of $CD4^+$ cells are effector T cells whose specific role is largely confined to regulation of the acute inflammatory response as part of their central purpose in the adaptive immune system. With an acute insult, these cells are pivotal to the normal host defense. As part of this initial and aggressive response, the T_{eff} cells secrete and induce the secretion of proteases allowing the inflammatory cells to migrate into tissues to establish contact with the injurious agent. In normal conditions, the T_{reg} allows for resolution of this response once the threat has been curtailed. In chronic inflammatory processes such as AAA, this pro-inflammatory and proteolytic milieu is not adequately opposed by anti-inflammatory mechanisms. The result is significant and progressive destruction of the ECM.

Macrophage phenotypes: M1 and M2

Macrophages play crucial roles in the innate and adaptive immune responses and have been studied in various diseases since their discovery in the late 19th century by Élie Metchnikoff. Like other immune cells, macrophages respond to various stimuli in their microenvironmental milieu. These highly plastic cells play dual roles in initiation and resolution of inflammation. The macrophage population consists of two major phenotypes, M1 and M2. M1 macrophages respond to stimuli that enhance and sustain ongoing inflammation via production of proteolytic enzymes and pro-inflammatory mediators. Initial arterial injury leads to recruitment of M1 macrophages. Normally, these infiltrating macrophages would later convert to M2 macrophages, promoting tissue repair and wound healing. This M1/M2 balance is vital to proper wound repair and resolution of the inflammatory response. If the M1 phenotype continually predominates, chronic inflammation occurs. Conversely, if the M2 phenotype predominates, ongoing infection or poor wound healing may result. In certain cancers this M2 imbalance has been shown to be detrimental, actually leading to tumor growth. [86,87] Histologically, AAA tissue shows marked inflammatory cell infiltrates. Evidence suggests a chronic inflammatory milieu where the M1 phenotype is not adequately balanced by the M2 phenotype, consistent with progressive aneurysm expansion.

M1

M1 macrophages respond to environmental stimuli and sustain ongoing inflammation via production of proteolytic enzymes and pro-inflammatory mediators. The classical M1 macrophage phenotype can be activated *in vitro* by pro-inflammatory cytokines including IFN-γ and TNF-α. IFN-γ primes the macrophages for activation but is inadequate alone to produce the M1 phenotype. [88] A secondary signal, such as TNF-α or lipopolysaccharide (LPS), is required for the activation of toll-like receptor 4 (TLR4)

resulting in M1 macrophage polarization. [89] This phenotypic polarization triggers production of various M1 markers such as inducible nitric oxide synthase (iNOS), TNF-α, IL-1β, and other pro-inflammatory mediators (Table 1.3). Characteristic cell surface markers, including those associated with antigen presentation such as CD80 and CD86, can further identify these cells as M1 macrophages. The M1 macrophage products may produce a positive feedback loop resulting in chronic inflammation and significant tissue damage.

In AAAs, examination of these M1 markers in human tissues and in experimental animal models has yielded noteworthy results. Many studies have focused on the discovery of novel biomarkers in AAA patient serum. Through these studies, researchers have identified some potential targets, which are associated with the M1 phenotype. Although human studies of macrophages in AAA have been limited to examination of end stage disease tissue or circulating monocytes, key findings have emerged. Circulating monocytes from AAA patients displayed enhanced adhesive activity to the endothelial cell wall and increased MMP-9 production. [90] Although these monocytes were not studied specifically for M1 or M2 markers, their presence suggests a systemic inflammatory response, which would be expected due to the presence of high levels of MMP-9 resulting in tissue breakdown. Hance et al. demonstrated that monocyte chemotaxis to AAA tissue can be directly linked to breakdown of the ECM, specifically via a six-peptide sequence (VGVAPG) found mainly in elastin. [91] Experimental animal studies have shown that blocking the presence of the VGVAPG sequence with a monoclonal antibody reduces monocyte/macrophage recruitment limiting further ECM breakdown. [92-94] These ECM breakdown products act as pro-inflammatory mediators, further recruiting monocytes and promoting their differentiation into M1 macrophages. Once initiated, the resolution of this inflammatory response is unlikely.

Table 1.3

Table 1.3. Macrophage differentiation, function, and role in disease

	M1	M2
Stimulating Factors	TNF-α, IFN-γ, LPS	IL-4, IL-13, IL-10
Pathway	STAT1, AP-1, NF-κB	STAT6, PPAR-γ, CREB
Secreted Products	TNF-α, IL-6, IL-1β, iNOS, MCP-1	Arg1, Ym1, FIZZ1 (mouse only)
CD markers	CD80, CD86, CD16, CD14	CD206, CD163
Role in Disease	Pro-inflammatory, cytotoxicity, microbicidal activity, tumor suppression	Anti-inflammatory, matrix remodeling, tissue repair, tumor suppression

AP – activator protein, NF-κB – nuclear factor-κB, PPAR – peroxisome proliferator-activated receptor, CREB – cAMP response element-binding protein, Arg – arginase, Ym1 – Chi3l3 (Chitinase 3-like-3), FIZZ – found in inflammatory zone

Various cell surface markers are associated with M1 macrophage polarization. CD14 acts as a co-receptor with TLR4, which is required for M1 polarization through the IFN-γ and LPS activation pathway. [95] Recent studies showed that patients with AAAs have increased levels of $CD14^{+}CD16^{+}$ monocytes compared to control patients, suggesting these monocytes may be associated with the chronic inflammatory process of AAA. [96] CD16, a low affinity Fc receptor for IgG antibodies involved in antibody-dependent cytotoxicity, is also associated with an M1 macrophage polarization. [97] Experimental aneurysm models indicated that CD14 deletion reduced inflammatory cell infiltration therefore reducing AAA incidence. [98] With the increase in CD markers associated with increased pro-inflammatory processes, it is clear that the M1 phenotype plays a major role in AAAs, at least in the latter stages of disease when tissue samples are obtained.

Examination of pro-inflammatory cytokines in AAAs has been more extensive and has led to many treatment strategies focused on their antagonism. M1 associated pro-inflammatory cytokines TNF-α, IL-6, IL-1β, and IFN-γ were all increased in human aneurysmal tissue and serum (Table 1.4). [36,37] IFN-γ is one stimulus that activates M1 macrophage polarization, and deletion of IFN-γ in experimental mouse models inhibited aneurysm formation and macrophage infiltration. [34] Another M1 associated cytokine, TNF-α, stimulates M1 macrophage polarization resulting in further TNF-α production. Genetic deletion of TNF-α or antibody-mediated sequestration with Infliximab reduced macrophage infiltration and aneurysm formation in a murine model. [99] Similar deletion studies focused on M1 associated cytokines IL-6 and IL-1β have yielded comparable results. [100,101] Without these M1 polarizing cytokines, aneurysm formation is dramatically reduced and macrophage infiltration is minimized. These data are now being further investigated in a translational study using Canakinumab, an IL-1β neutralizing antibody,

Table 1.4

Table 1.4. Macrophage differentiation in human and experimental AAA.

	M1	M2
Human AAA	Increased[30,31,90]	Increased[101,102]
ApoE$^{-/-}$ AngII model	Increased[92]	Increased[103]
$CaCl_2$ model	Increased[28,93,94,95]	Undefined
Elastase-perfusion model	Increased[92]	Undefined

in patients with small AAAs with a goal of inhibiting aneurysm expansion (NCT02007252). [102]

M2

In contrast to classically activated M1 macrophages, alternatively activated M2 macrophages are associated with wound repair and inflammation resolution. M2 activation is achieved by IL-4 or IL-13, both antagonizing the actions of IFN-γ. IL-4 and IL-13, associated with Th2 cells, bind to the IL-4 receptor and signal M2 polarization through STAT6. [103,104] Polarization of macrophages to an anti-inflammatory M2 phenotype results in production of anti-inflammatory cytokines including IL-10 and TGF-β. The M2 macrophage is identified by markers such as mannose receptor (CD206), arginase I, and CD163 (Table 1.3). These anti-inflammatory markers have been identified in tumors, where tumor-associated M2 macrophages suppress the natural immune response to cancer cells. [105] However, in diseases associated with chronic inflammation such as AAA, enhancement of the M2 response could potentially limit the ongoing inflammatory response.

A few recent studies have examined one of the most common M2-linked markers, CD206. CD206 regulates the levels of glycoproteins released after inflammatory responses, aiding in wound resolution. [106] Examination of CD206 in human AAA tissue has revealed contrasting results. Boytard et al. demonstrated that $CD206^{+}$ macrophages are present in the intraluminal thrombus (ILT) but absent in the heavily damaged aortic adventitia. [107] Conversely, Dutertre et al. found $CD206^{+}$ macrophages to be present in the damaged aorta, potentially signaling wound resolution. [108] An experimental aneurysm model using $ApoE^{-/-}$ mice revealed increased CD206 staining in the more severely affected tissue. [109] These contradictory data indicate the further need for M2 phenotype clarification and examination of additional M2 markers. Despite the

conflicting results, targeting the M1/M2 imbalance may offer an interesting therapeutic aim in aneurysmal disease.

Neutrophils and mast cells

Neutrophils are quickly recruited to sites of injury and are characteristic of acute inflammation.[110] These cells are most commonly found in the ILT in AAAs.[111,112] While ILT are frequently found in human AAAs, animal models fail to recapitulate formation of an ILT.[113] However, examination of neutrophils in AAA has elucidated important findings. In an elastase-perfused model of aneurysm formation, depletion of polymophonuclear neutrophils reduced aortic dilation in a MMP-independent manner.[114] Human AAA studies revealed a negative correlation of neutrophil catalase activity and aortic size.[115] These studies indicate a role for neutrophils in aneurysm formation that may depend on regulation of reactive oxygen species.

Mast cells are inflammatory cells associated with immediate hypersensitivity and chronic allergic reactions.[116] These cells have been found in human AAA tissue, primarily residing in the media and adventitia.[117,118] Genetic deletion of mast cells protects against aneurysm formation in both the elastase-perfusion and $CaCl_2$ murine models of aneurysm formation.[119] MMP-2 and -9, as well as other ECM degrading enzymes, can be activated by mast cell secreted chymase, promoting aneurysm formation.[120,121] Although much of the focus on aneurysm formation has been on T cells and macrophages because they are the predominant inflammatory cells, interactions between these and other inflammatory cells also play a role in aneurysm formation.

Discussion

AAA is a complex disease where an improper balance of T cell or macrophage phenotypes may worsen the disease process. This imbalance that occurs with the

numerous cell types involved in AAAs enhances the chronic inflammatory aspect of the disease. $CD4^+$ T cells display many different phenotypes, most of which have been found in AAA tissue. Studies targeting the switch of T cells from a pro-inflammatory phenotype to an anti-inflammatory phenotype, such as upregulation of T_{reg} cells, create exciting new strategies for targeting AAA progression. Macrophage phenotype polarization is a promising new field that may prove beneficial in identifying key regulators of chronic inflammation in AAA. Whether macrophages in AAA tissue exhibit a stronger M1 or M2 phenotype and altering the M1/M2 balance are being explored. Understanding and addressing the imbalances in the immune system associated with AAA offer new and exciting translational strategies.

It is difficult to determine the cause of AAA in humans because of the chronicity of the disease and the problem of obtaining specimens at different stages of the disease Therefore, investigators have attempted to make use of animal models with similarities to the human disease. Validations of these animal models must be performed by correlating these studies with human tissueobtained from patients with end stage disease. Correlating data obtained from murine models to human AAA tissue has yet to yield useful therapeutic inflammation thus far. Therefore, development of humanized animal models may help to alleviate some of the differences seen in the human and mouse disease process. Opportunities to obtain human AAA tissue are becoming more limited due to the transition from open to endovascular aneurysm repair. Clinical trials must develop protocols to examine as many parameters of the disease as possible, including serially obtaining precise imaging and circulating biomarkers. By correlating biomarkers with changes in aneurysm shape and size, it may be possible to develop a greater understanding of which bioactive molecules and cell types promote aneurysm growth.

CHAPTER 2

Genetic differences in MMP levels influence AAA susceptibility

The following is a modified version of an article published in *Atherosclerosis* 2015 Dec; 243(2):621-9. This work was coauthored by Melissa K. Suh, Shijia Zhao, Trevor Meisinger, Linxia Gu, Vicki J. Swier, Devendra K. Agrawal, Timothy C. Greiner, Jeffrey S. Carson, B. Timothy Baxter, Wanfen Xiong, and myself.

Introduction

Abundant evidence has demonstrated the profound influence of genetic background on cardiovascular phenotypes. [122-125] Although a single gene mutation has not been found in association with most AAAs, a positive family history of AAA in a first degree relative is known to increase the risk of aortic aneurysm by up to a factor of ten. [126] Attempts to define the genetic component(s) underlying AAA have used a variety of strategies, including both linkage analysis and candidate gene approaches; [127] nonetheless, a consensus on the patterns of inheritance or specific linkages associated with AAA has yet to emerge.

A variety of different mouse strains have been used to assess aortic aneurysms. [109,128-131] The most widely used parent strains for the production of mutants in aneurysm research are C57Bl/6 and 129/SvEv mice. [25,26,132] In contrast to AAA, thoracic aortic aneurysms are associated with a number of known genetic mutations. Marfan syndrome (MFS) is caused by fibrillin-1 gene mutations that are responsible for thoracic aneurysm development. [133] Studies of animal models of MFS have shown that genetic background-related variations, C57Bl/6 or 129/SvEv, affect aneurysm formation, rupture, and lifespan of mice. [132,134] The 129/SvEv genetic background is associated with more rapid aneurysm progression in MFS mice when compared to the C57Bl/6 background. [132] As in AAA, higher MMP-2 expression in the aorta of Marfan syndrome mice plays an important role in aneurysm formation. [133] Therefore, the variance of thoracic aneurysm susceptibility in MFS could also be informative regarding the underlying genetic susceptibility to AAA. In reviewing our previous studies, we noted that 129/SvEv mice also developed larger AAAs compared to C57Bl/6 mice in response to $CaCl_2$-aneurysm induction. [25] Based on these observations, we hypothesized that the difference seen in

aneurysm susceptibility between the two genetic backgrounds is related to intrinsic differences in smooth muscle cell MMP-2 or macrophage MMP-9 expression.

Methods

Animal aneurysm model. All procedures and animal studies were approved by the University of Nebraska Medical Center IACUC. The experimental groups consisted of 24 eight weeks-old male C57Bl/6 mice (The Jackson Laboratory, Bar Harbor, Maine) and 20 eight weeks-old male 129/SvEv mice (Taconic, Germantown, New York). Mice were anesthetized and underwent laparotomy. The abdominal aorta between the renal arteries and bifurcation of the iliac arteries was isolated from the surrounding retroperitoneal structures. The diameter of the aorta was measured using a Leica Application System (Leica Microsystems Inc, Buffalo Grove, IL). After baseline measurements, 0.25 M $CaCl_2$ was applied to the aorta with care taken to avoid surrounding tissue. After 15 minutes the aorta was rinsed with 0.9 % sterile saline, the laparotomy incision was closed, and mice were returned to their cages after recovery. Six weeks later the mice underwent repeat laparotomy, dissection, and measurement of the aorta. Aortic diameter was measured at the point of maximal dilatation. The aorta tissue was collected for zymographic and Western blot analyses. For histological studies, the aorta was perfusion-fixed with 10% neutral buffered formalin. NaCl (0.9%) was substituted for $CaCl_2$ in sham controls.

Isolation and infusion of myelogeous cells. To evaluate the role of the myelogenous cells on aneurysm susceptibility, 6 week-old C57Bl/6 or 129/SvEv mice were irradiated (1200 rads) and transplanted with bone marrow from 129/SvEv (designated as $C57^{bkg}/SvEv^{bm}$ mice) or C57Bl/6 mice ($SvEv^{bkg}/C57^{bm}$ mice), respectively. As controls, we also transplanted bone marrow from C57Bl/6 or 129/SvEv mice into the irradiated, same back ground mice, C57Bl/6 (designated as $C57^{bkg}/C57^{bm}$) or 129/SvEv ($SvEv^{bkg}/SvEv^{bm}$), respectively. We have previously demonstrated that this radiation protocol results in bone marrow ablation and is fatal without rescue by bone marrow

transplantation. [135] Bone marrow cell suspensions were prepared from the femurs of C57Bl/6 or 129/SvEv mice, and 5 × 10^6 cells were infused via the lateral tail veins. Aneurysm induction followed 1 week after bone marrow transplantation.

Western blot analysis and gelatin zymography. Aortic proteins were extracted as previously described. [133] The protein concentration of aortic tissues was standardized with a Bio-Rad protein assay. Equal amounts (10 μg) of aortic extracts were loaded under reducing conditions onto a 10% SDS-polyacrylamide gel and transferred to a polyvinylidene difluoride (PVDF) membrane (Amersham Biosciences, Piscataway, NJ). The membranes were then incubated with rabbit anti-tropoelastin antibody (Elastin Products Company, Owensville, MO) or rabbit anti-collagen1a antibody (Cell Signaling, Danvers, MA). The bound primary antibody was detected with HRP-linked anti-rabbit IgG (Cell Signaling). Immunoreactive bands were visualized by autoradiography using ECL (Amersham Biosciences). Gelatin zymography for aortic tissue extracts was performed as described previously by Longo et al., with 0.8% gelatin in a 10% SDS-polyacrylamide gel.[7] (Longo 2002) The molecular sizes were determined using protein standards from Fermentas (Glen Burnie, MD). The intensity of each band was quantified by densitometry (Amersham Biosciences).

Microscopy. *1)Verhoeff-Van Gieson (VVG) connective tissue staining:* After perfusion-fixation with 10% neutral-buffered formalin, mouse abdominal aortic tissues were embedded in paraffin and cut into 4 μm sections. The slides were stained with Verhoeff's solution, ferric chloride, sodium thiosulfate, and Van Gieson's solution (Poly Scientific, Bay Shore, NY). Each staining cycle alternated between fixing and washing procedures. The slides were examined and photographed using light microscopy (Nikon). *2) Quantification of Elastin Disruption:* slides of both $CaCl_2$ treated C57Bl/6 and 129/SvEv

mice were examined under low power magnification. A semi-quantitative analysis was used to estimate the percentage of the total circumference that demonstrated elastin disruption. The analysis was performed by an observer blinded to mouse background. 3) *Immunohistochemistry:* Tissue sections on the slides were deparaffinized in xylene, rehydrated in ethanol, and rinsed in double-distilled water. The sections were incubated with a monoclonal rat anti-mouse Mac3 antibody (PharMingen, San Diego, CA) diluted 1:500 for 30 minutes at 37^{o}C. The sections were then briefly washed in citrate solution and subsequently incubated with the secondary antibody, which is a mouse-absorbed, biotin-conjugated rabbit anti-rat IgG. Macrophage staining was examined using light microscopy. Sections incubated with secondary antibody only showed no positive staining. Three samples in each mouse strain were stained and evaluated.

Elastic modulus measurement. Quasi-static nanoindentation tests were performed on mouse aortas using a commercial TriboScope nanoindenter with a light microscope mounted (Hysitron, Minneapolis, MN). A nonporous conospherical fluid cell probe (TI-0077) with a radius of curvature of R = 100 μm was chosen. A custom-built sample holder was used to hold sample and ensure its hydration during indentation test. The optical images obtained from the microscope will guide the movementt of the indenter and allow accurate control on the indentation positions.

A trapezoidal load-hold-unload profile, which was composed of a linear loading portion of 2 seconds, a dwell portion of 20 seconds at a predetermined peak load and a linear unloading portion of 2 seconds, was used for each indentation. All samples were tested at peak load of 5 μN during the dwell period. In total, 16 indentations in a 4×4 grid were conducted on each sample. The time interval between two indentations was 120 seconds. The distance between two indentation points was 200μm. After indentations,

the force-displacement data were collected. The elastic moduli of the specimens were obtained by fitting the force-displacement data to the Oliver-Pharr model.

Elastase activity assay. Elastase activity in the aortic extract (100 μg) from NaCl- and $CaCl_2$-treated C57Bl/6 and 129/SvEv mice were measured using an elastase assay kit (AnaSpec, Fremont, CA) with and without 10 mM EDTA according to manufacturer instructions. Neutrophil elastase gene expression in the aortic tissue of NaCl- and $CaCl_2$-treated C57Bl/6 and 129/SvEv mice were examined by RT-PCR as described previously.[24]

Statistical analysis. Measurements of aortic diameter, elastin levels, and elastic moduli were expressed as mean value ± S.D. ANOVA was used to compare aortic diameters. Student's *t* test was used to compare protein expression, MMP activity, and elastic moduli in different groups. Statistical significance was accepted at the $P < .05$ levels.

Results

Aneurysm size and histology. To test the hypothesis that genetic influences contribute to susceptibility of aneurysm formation, 129/SvEv and C57Bl/6 mice were subjected to $CaCl_2$-aneurysm induction. Six weeks after periaortic application of $CaCl_2$, 129/SvEv mice showed a larger increase in abdominal aortic diameter compared to C57Bl/6 mice (Fig. 1a, b-e and Table 1). The initial aortic diameter between two strains was not significantly different. At baseline, VVG staining of aortic sections from C57Bl/6 and 129/SvEv mice showed no difference (Fig. 1f, g, j, k) while both showed disruption and fragmentation of medial elastic lamellae after aneurysm induction (Fig. 1h, i, l, m). However, aortic elastic lamellae degradation appeared to be more severe in 129/SvEv mice (Fig. 1i & m) compared to C57Bl/6 mice (Fig. 1h & l). These observations are consistent with the larger aneurysms that develop in the 129/SvEv mice.

Aortic elastic moduli. The elastic lamella, which is comprised of elastic fibers, collagens, proteoglycans, and glycosaminoglycans, determines the biomechanical properties of the aorta. To test the hypothesis that baseline aortic mechanical properties of C57Bl/6 mice differed from 129/SvEv mice, quasi-static nanoindentation tests were performed on the aortas isolated from the two strains of mice. The elastic moduli of the specimens were obtained by fitting the force-displacement data to the Oliver-Pharr model. The elastic moduli of C57Bl/6 mice were significantly less than that of the 129/SvEv mice (Fig. 2). Thus, the aortic wall in 129/SvEv mice was stiffer or less compliant than in the C57Bl/6 mice.

Aortic tropoelastin content. Matrix synthesis is known to accompany the matrix degradation seen in AAA. Production of tropoelastin, the precursor molecule that becomes incorporated into mature elastin fibers, in the aneurysmal aortas was examined

Figure 1. Aortic changes after NaCl and $CaCl_2$ treatment in C57Bl/6 and 129/SvEv mice. Aortic diameters were measured before NaCl or $CaCl_2$ incubation and at sacrifice. Aortic diameter increases are shown in the bar graph (a). Bars represent the mean +/- SD of at least 6 mice per group. The diameter in the $CaCl_2$-treated groups was increased significantly at sacrifice in both C57Bl/6 and 129/SvEv mice compared to NaCl treated mice (* $P < .01$). The aortic dilatation in $CaCl_2$-treated 129/SvEv mice was significantly greater compared to $CaCl_2$-treated C57Bl/6 mice (# $P < .05$). Photographs (b-e) show the mouse aortas in C57Bl/6 and 129/SvEv mice with the dotted line indicating the outer border of the aortas before (b, c) and after (d, e) $CaCl_2$ aneurysm induction, respectively, (n = 6-10/group). VVG staining for elastic fibers (f-m). Aortic lamellae disruption (10× magnification) (h, i) and elastic fiber fragmentation (40× magnification) (l, m) were more severe in 129/SvEv (i. m) than in C57Bl/6 (h, l) mice (n = 3-5/group). n, percentage of aortic circumference showing elastin disruption in $CaCl_2$-treated C57Bl/6 and 129/SvEv mice (n = 3 aortas/group).

Figure 1

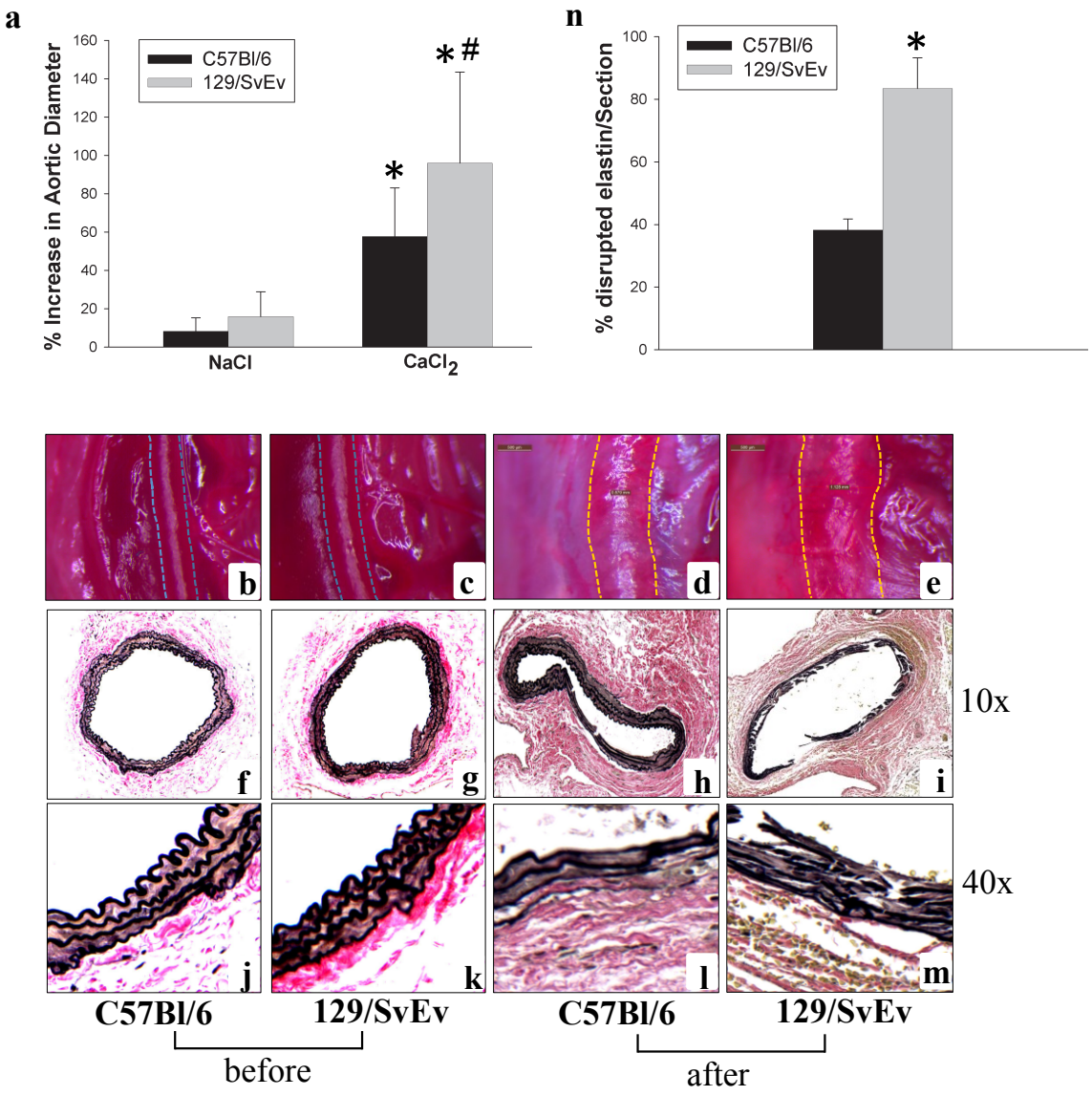
a
% Increase in Aortic Diameter
C57Bl/6
129/SvEv
NaCl
CaCl2
n
% disrupted elastin/Section
b
c
d
e
f
g
h
i
10x
j
k
l
m
40x
C57Bl/6
129/SvEv
C57Bl/6
129/SvEv
before
after

Table 1.

Table1. Changes in aortic diameter in C57Bl/6 and 129/SvEv mice after treatment of NaCl and $CaCl_2$

	C57Bl/6		**129/SvEv**	
Treatment	**NaCl**	**$CaCl_2$**	**NaCl**	**$CaCl_2$**
Number	8	16	6	12
Pre-treatment (μm)	520 ± 14	507 ± 7	544 ± 15	550 ± 17
Post-treatment (μm)	562 ± 17	797 ± 30 *	628 ± 18	1067 ± 67 *#
AAA development	0	56	0	83
Percent Increase (%)	8.3	57.8	15.9	96.3

Aortic diameters were measured before NaCl or $CaCl_2$ incubation (Pre) and at sacrifice (Post). Measurements of aortic diameter were expressed as mean ± SE. The percent of increase was represented as a percent compared with pre-treatment. The development of aneurysm was defined as at least a 50% increase relative to original aortic diameter. * P <.01, Student's t test, compared to pre-treatment; # P < .05 compared to $CaCl_2$-treated C57Bl/6.

Figure 2. Elastic modulus of aortic tissues from C57Bl/6 and 129/SvEv mice. Prior to aneurysm induction, quasi-static nanoindentation tests were performed on the aortas and the elastic modulus was determined (n = 3 per group, * $P < .05$).

Figure 2

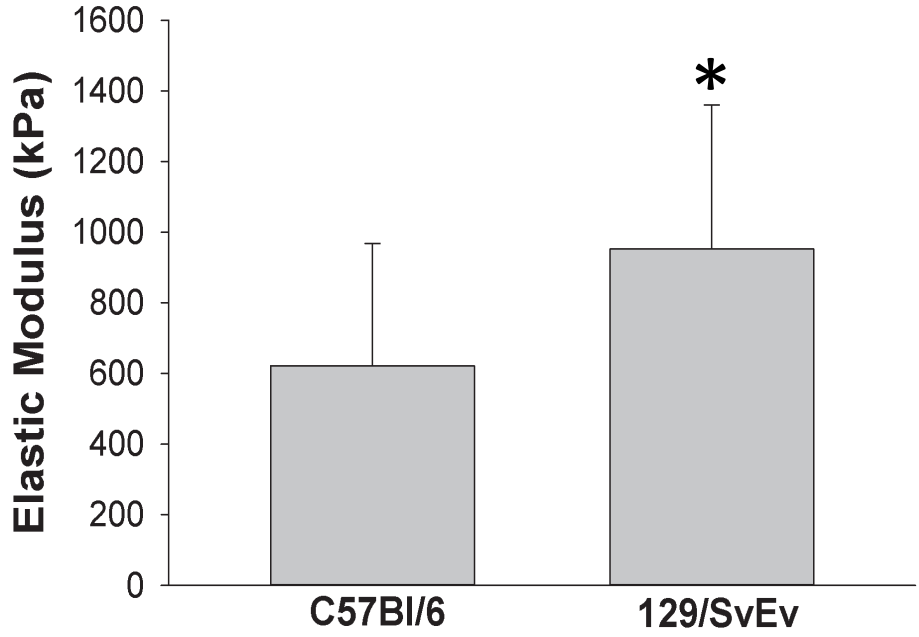
Elastic Modulus (kPa)
1600
1400
1200
1000
800
600
400
200
0
*
C57Bl/6
129/SvEv

by Western blot analysis. At baseline, there was no different in tropoelastin production between two strains (Fig. 3a). The tropoelastin levels in $CaCl_2$-treated aortas of 129/SvEv mice were decreased by one third compared to $CaCl_2$-treated aortas of C57Bl/6 mice (Fig. 3b). The procollagen 1α levels in the aortas were also examined by Western blot analysis. There was no difference in procollagen 1α content between the two strains of mice (data not shown). These data suggest that the 129/SvEv mice may be less able to repair elastin once it has been disrupted.

Aortic MMP-2 and MMP-9 expression. MMP-2 and MMP-9 are essential for the connective tissue degradation in the aortic wall leading to AAA.[25] Because the greater level of elastin degradation in the 129/SvEv mice suggests higher levels of MMP activity, we determined if the aortas from C57Bl/6 and 129/SvEv mice expressed different levels of MMP-2 and MMP-9 at baseline and after aneurysm induction. Aortic protein was analyzed by gelatin zymography. As shown in Figure 4a, latent MMP-2 expression in untreated 129/SvEv mice was significantly higher than in untreated C57Bl/6 mice. Furthermore, after aneurysm induction, active forms of MMP-2 and MMP-9 were higher in the aortas of 129/SvEv mice (Fig. 4b). These results demonstrated that 129/SvEv mice express higher levels of pro-MMP-2 intrinsically. Additionally, after aortic injury, there is greater activation of MMP-2 and MMP-9 in 129/SvEv mice.

Increased MMP-9 expression in aortic tissues after aneurysm induction may indicate higher levels of MMP-9 expression from macrophages or increased macrophage infiltration into the aortic tissue in 129/SvEv mice compared to C57Bl/6 in response to $CaCl_2$ treatment. Therefore, aortic tissues were examined for the presence of Mac3-positive macrophages. The images obtained suggested greater macrophage infiltration in the 129/SvEv mice aortas compared to C57Bl/6 mice (Fig. 4c). These

Figure 3. Aortic tropoelastin content. Western blot analysis was used to determine tropoelastin content from C57Bl/6 and 129/SvEv mice before (a) and after (b) AAA induction. Relative levels of tropoelastin content in mouse aortas were quantified as shown in bar graphs (* $P < .05$ compared to $CaCl_2$-treated C57Bl/6 mice) (n = 5-7/group).

Figure 3

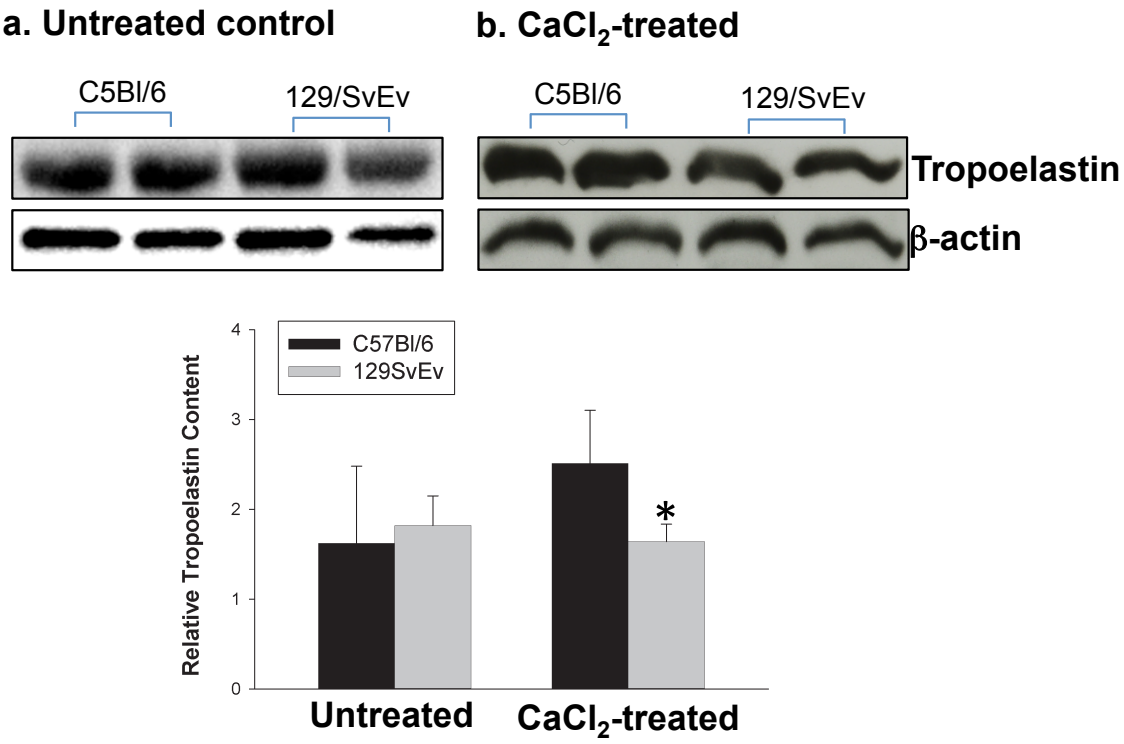
a. Untreated control
b. CaCl2-treated
C5Bl/6
129/SvEv
C5Bl/6
129/SvEv
Tropoelastin
β-actin
C57Bl/6
129SvEv
Relative Tropoelastin Content
0
1
2
3
4
*
Untreated
CaCl2-treated

Figure 4. Aortic MMP-2 and MMP-9 expression. Gelatin zymography analysis of MMP activities expressed in the aortas of C57Bl/6 and 129/SvEv mice, a) Untreated controls; b) $CaCl_2$-treated mice. Representative zymogram gels are shown in left panels. Relative levels of pro-MMP-9, MMP-9, pro-MMP-2, MMP-2 in mouse aortas were quantified and data shown in the bar graphs (* $P < .05$). c) Representative immunoperoxidase staining for macrophages of aneurysmal aortic tissues from C57Bl/6 and 129/SvEv mice. Mac3-positive cells are indicated by arrows. Macrophages in aortic tissue were evaluated and scored with values from 0-3 as previously described (7). Zero indicates that there were no Mac3-positive cells, 3 indicated many Mac3-positive cells in a limited area, and 1 and 2 were used to classify intermediate grades of Mac3 positive cells (n = 3/group).

Figure 4

a. Untreated control

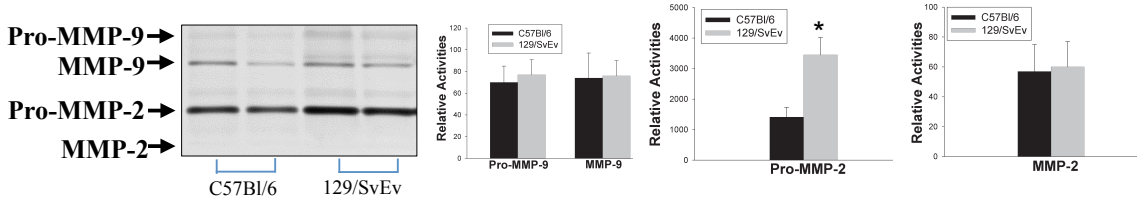

b. $CaCl_2$-treated

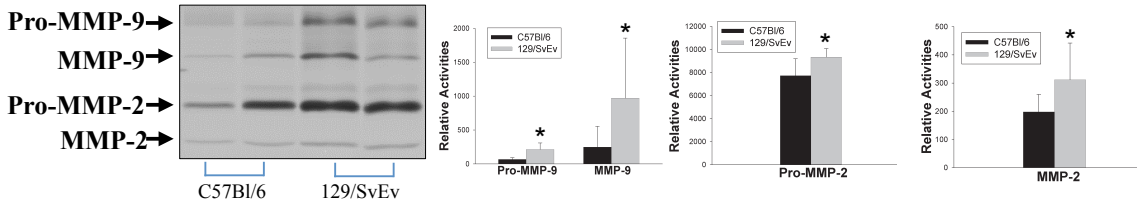

c

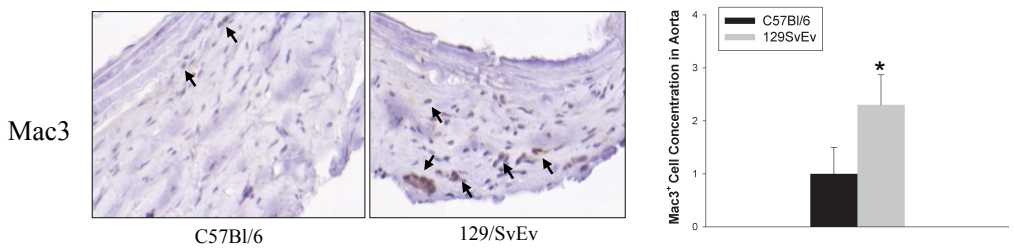

Table 2

Table 2. The concentration of macrophages in the $CaCl_2$-treated aorta of 129/SvEv and C57Bl/6 mice

Mouse Strain	Macrophages
129/SvEv	2.3 ± 0.6*
C57Bl/6	1.0 ± 0.5

Macrophages in aorta were evaluated and scored with values from 0 to 3. Zero means no $Mac3^+$ cells and 3 meanys many cells in a limited area, the values of 1 and 2 are used to classify intermediate grades of infiltration. The values reflect the mean ± SD. * *P* = 0.0390, Student's *t*-test. n = 3.

results suggest intrinsic differences in mesenchymal cell MMP-2 levels and also differences in response to injury.

Aortic elastase activity. In addition to MMP-2 and -9, other elastases could be responsible for the elastin degradation in AAA. We measured elastase activity in the aortic tissue from C57Bl/6 and 129/SvEv mice. Elastolytic activity was similar between NaCl-treated C57Bl/6 and 129/SvEv mice (Fig. 5a). However, elastase activity in $CaCl_2$-treated 129/SvEv and C57Bl/6 mice was significantly higher than NaCl-treated 129/SvEv or C57Bl/6, respectively (Fig. 5a). Furthermore, compared to $CaCl_2$-treated C57Bl/6 mice, elastolytic activity in $CaCl_2$-treated 129/SvEv was higher (Fig. 5a). Neutrophils play an important role in aneurysm formation.[114,136] We also tested neutrophil elastase gene expression using RT-PCR. We found that there were no significant differences between C57Bl/6 and 129/SvEv mice at baseline or in aneurysmal aortic tissue (Fig. 5b &c). In order to determine the contribution of MMPs, EDTA was used to block MMP activity prior to measuring total elastolytic activity (Fig. 5a). These data demonstrated that the majority of enhanced activity was due to increased elastin degradation by MMPs.

Role of myelogenous cells in AAA susceptibility. The known role of inflammatory cells in AAA and differences in the levels of active MMP-9 in the C57Bl/6 and the 129/SvEv mice suggested that there could be intrinsic differences in the myelogenous cells. In order to investigate this, C57Bl/6-derived bone marrow cells were infused into irradiated 129/SvEv ($SvEv^{bkg}/C57^{bm}$) mice and 129/SvEv-derived bone marrow cells were infused into irradiated C57Bl/6 ($C57^{bkg}/SvEv^{bm}$) mice. As controls, we also transplanted bone marrow from C57Bl/6 or 129/SvEv mice into the irradiated, same back ground mice, C57Bl/6 ($C57^{bkg}/C57^{bm}$) or 129/SvEv ($SvEv^{bkg}/SvEv^{bm}$), respectively. The

Figure 5. Aortic elastase activity and neutrophil elastase expression a) Elastase activity in aortic tissue extract from C57Bl/6 and 129/SvEv mice was measured, (* P < .05 compared to NaCl-treated control, # P < .05 compared to $CaCl_2$-treated C57Bl/6 mice) (n = 3/group). EDTA was used to block MMP activity. b) The neutrophil elastase expression in the aortas of C57Bl/6 and 129/SvEv mice was examined by RT-PCR; untreated controls (left panel) and $CaCl_2$-treated mice (right panel). c) The levels of neutrophil elastase mRNA relative to GAPDH in the aorta were quantified; data shown in the bar graphs (n = 3/group).

Figure 5

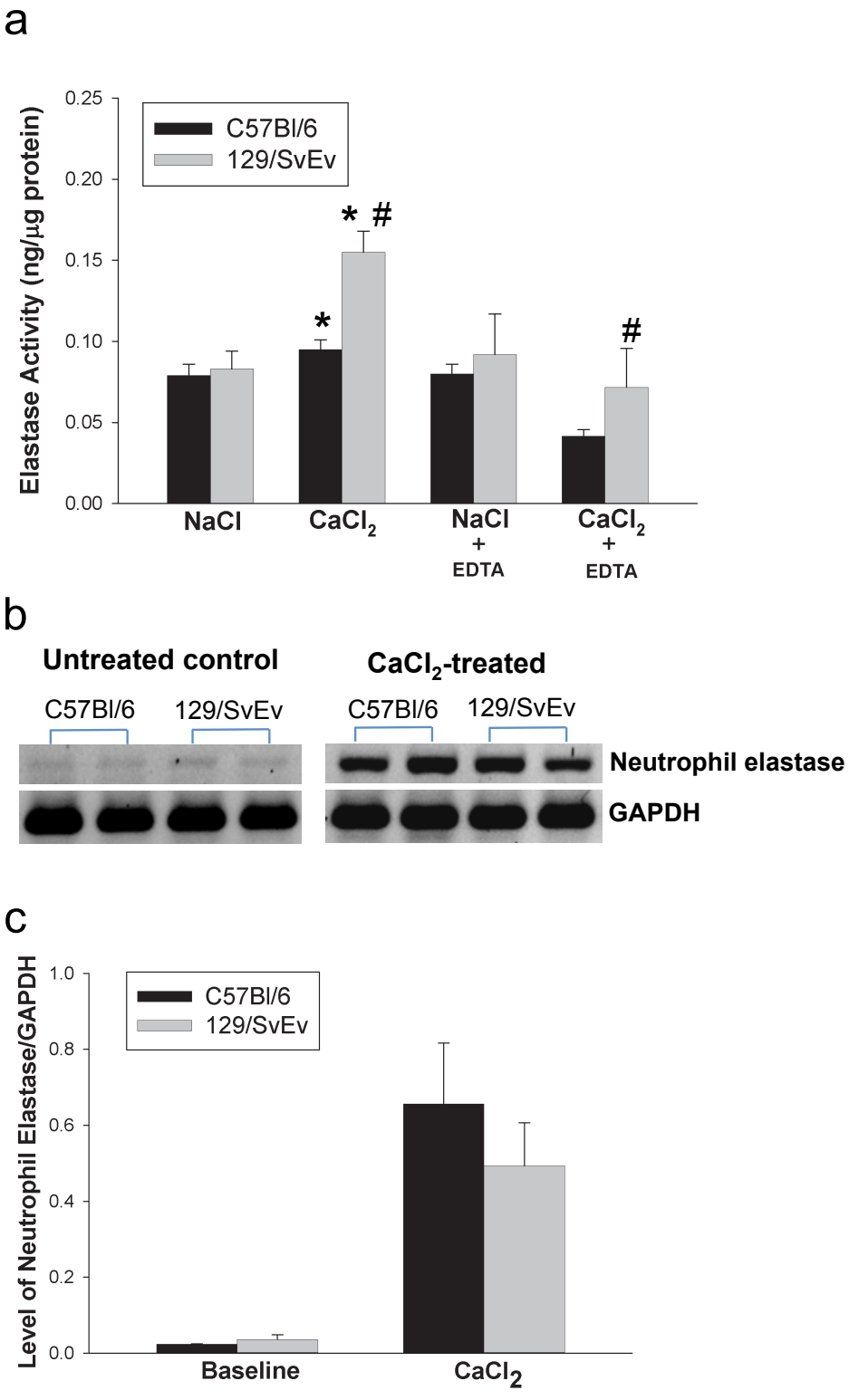
a
Elastase Activity (ng/μg protein)
0.25
0.20
0.15
0.10
0.05
0.00
C57Bl/6
129/SvEv
* #
*
#
NaCl
CaCl2
NaCl + EDTA
CaCl2 + EDTA
b
Untreated control
CaCl2-treated
C57Bl/6
129/SvEv
C57Bl/6
129/SvEv
Neutrophil elastase
GAPDH
c
Level of Neutrophil Elastase/GAPDH
1.0
0.8
0.6
0.4
0.2
0.0
C57Bl/6
129/SvEv
Baseline
CaCl2

chimeric mice were subjected to $CaCl_2$-aneurysm induction. Six weeks after aneurysm induction, $SvEv^{bkg}/C57^{bm}$ developed larger aneurysms than the $C57^{bkg}/SvEv^{bm}$ (Fig. 6a). Aortic diameter in the $SvEv^{bkg}/C57^{bm}$ increased by 85% ± 4, while the $C57^{bkg}/SvEv^{bm}$ increased by 56% ± 6 (Table 3). The aortic diameter changes in $C57^{bkg}/C57^{bm}$ and $SvEv^{bkg}/SvEv^{bm}$ were similar to $C57^{bkg}/SvEv^{bm}$ and $SvEv^{bkg}/C57^{bm}$, respectively. Furthermore, the disruption of the elastic lamellae of the aortic wall of $CaCl_2$-treated $C57^{bkg}/SvEv^{bm}$ was less severe than the $SvEv^{bkg}/C57^{bm}$ chimeric mice (Fig. 6b). Aortic MMP-2 and MMP-9 levels in $C57^{bkg}/SvEv^{bm}$ mice were lower than in $SvEv^{bkg}/C57^{bm}$ mice while it is similar between $C57^{bkg}/C57^{bm}$ and $C57^{bkg}/SvEv^{bm}$ and between $SvEv^{bkg}/SvEv^{bm}$ and $SvEv^{bkg}/C57^{bm}$(Fig. 6c). The changes in aortic diameter in the chimeric mice were very similar in magnitude to the differences noted when the background strains were compared. These data do not support the concept that differences in the white cell compartments account for differences in aneurysm susceptibility.

Figure 6. The role of myelogenous cells in AAA susceptibility. The chimeric mice, $C57^{bkg}/C57^{bm}$, $SvEv^{bkg}/SvEv^{bm}$, $C57^{bkg}/SvEv^{bm}$ and $SvEv^{bkg}/C57^{bm}$, were subjected to $CaCl_2$ aneurysm induction. Aortic diameter changes were shown in the bar graph (a) (* $P < 0.01$ compared to NaCl control; # $P < 0.05$ $C57^{bkg}/SvEv^{bm}$ vs. $SvEv^{bkg}/C57^{bm}$ and $C57^{bkg}/C57^{bm}$ vs. $SvEv^{bkg}/SvEv^{bm}$ after $CaCl_2$ treatment). Bars represent the mean ± SD of 6 mice per group. Representative VVG staining of elastic fibers after aneurysm induction (b). Gelatin zymography of aortic MMP-2 and -9 levels in $CaCl_2$-treated $C57^{bkg}/C57^{bm}$ (lane 1), $C57^{bkg}/SvEv^{bm}$ (lane 2), $SvEv^{bkg}/SvEv^{bm}$ (lane 3), and $SvEv^{bkg}/C57^{bm}$ (lane 4) (c).

Figure 6

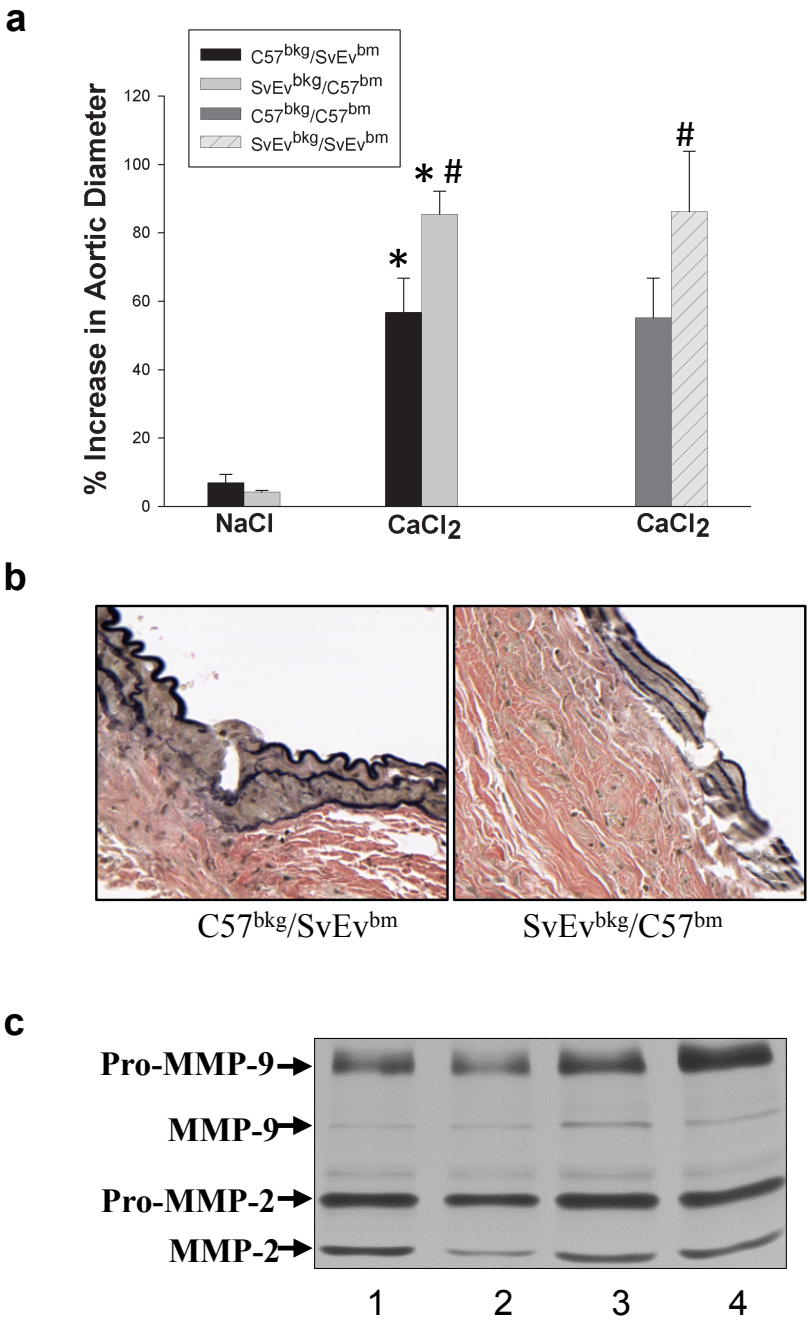
a
C57bkg/SvEvbm
SvEvbkg/C57bm
C57bkg/C57bm
SvEvbkg/SvEvbm
% Increase in Aortic Diameter
120
100
80
60
40
20
0
*
* #
#
NaCl
CaCl2
CaCl2
b
C57bkg/SvEvbm
SvEvbkg/C57bm
c
Pro-MMP-9
MMP-9
Pro-MMP-2
MMP-2
1
2
3
4

Table 3 Changes in aortic diameter in chimeric mice after treatment of NaCl and $CaCl_2$

	$C57^{bkg}/SvEv^{bm}$		**$SvEv^{bkg}/C57^{bm}$**		**$C57^{bkg}/C57^{bm}$**	**$SvEv^{bkg}/SvEv^{bm}$**
Treatment	**NaCl**	**$CaCl_2$**	**NaCl**	**$CaCl_2$**	**$CaCl_2$**	**$CaCl_2$**
Number	5	5	5	5	4	5
Pre-Treatment (μm)	505 ± 11	534 ± 12	509 ± 7	510 ± 28	502 ± 20	517 ± 23
Post-Treatment (μm)	540 ± 21	837 ± 48*	531 ± 6	945 ± 71*,#	779 ± 48	960 ±77 ł
AAA development (%)	0	60	0	100	50	100
Percent increase (%)	7	57	4	85	55	86

Aortic diameters were measured before NaCl (or $CaCl_2$) incubation (Pre) and at sacrifice (Post). Measurements of aortic diameter were expressed as mean ± SD. The percent of increase was represented as a percent compared with pre-treatment. The development of aneurysm was defined as at least 50% increase relative to original diameter of aortic diameter. * $p < .01$, student's *t* test, compared to pre-treatment; # $p < .05$ compared to $CaCl_2$-treated $C57^{bkg}/SvEv^{bm}$; ł $p < .05$ compared to $CaCl_2$-treated $C57^{bkg}/C57^{bm}$.

Discussion

The majority of genomic studies used to identify susceptibility pathways involved in disease pathologies have been performed in the mouse. [137-139] The mouse provides a suitable model for the study of human genetics because more than 95% of the genome is identical. The mouse genome is easy to manipulate allowing diseases to be modeled in transgenic animals once the target genes have been determined. Mice are also easy to breed with a short generation time and a short lifespan allowing direct study of disease development. Abundant evidence, however, demonstrates the profound influence of genetic background on the course and severity of many diseases. [140-142] Strain variability has been shown to influence aneurysm formation, progression, and even lifespan in MFS mouse models. Lima et al. demonstrated the effect of genetic background on the severity of the MFS phenotype by backcrossing the mgΔ allele, in which fibrillin-1 expression is reduced to 10% of normal levels, in 129/SvEv and C57Bl/6 mouse strains. [132] The 129/SvEv background was more susceptible to aneurysm formation and earlier aortic rupture. Increased susceptibility to aneurysm formation in the 129/SvEv background when compared to the C57Bl/6 background was also present in the least severe model of MFS ($Fbn1^{C1039G/+}$; 50% normal fibrillin-1 expression levels). Clearly, the genetic differences between the two strains are relevant to thoracic aortic aneurysm pathogenesis. To determine whether the development of AAA is dependent on mouse genetic background, we induced aneurysms in two widely used mouse strains, C57Bl/6 and 129/SvEv. Mice from both genetic backgrounds displayed increased aortic diameters and developed aneurysms in response to $CaCl_2$ induction, but the aneurysms formed in 129/SvEv mice were significantly larger compared to C57Bl/6 mice. Compared to our previous study, [25] the difference in $CaCl_2$-treated aortic diameter between two strains was bigger in the present study. In previous study, the aneurysms in the two strains were not induced concurrently. In the present study, the

aneurysms in two strains were induced simultaneously with one operator. We believe this better represents the differences between the two strains. In NaCl-treated controls of 129/SvEv mice, the average increase in aortic diameter was larger than previous reported. [25] In the present study, we have used a camera having higher resolution to define the aortic borders. We believe this primarily reflects growth of the aorta between 7 to 14 weeks. Consistent with these differences in aneurysm size, aortic elastic lamellar disruption and degradation in 129/SvEv mice were more severe compared to C57Bl/6 mice. Age and gender are also important factors in aneurysm development in patients with AAA. Mice of the same age and gender were used to exclude these as possible confounding factors.

Our current results, based on determination of the elastic modulus, demonstrate that the abdominal aortas of 129/SvEv mice were stiffer at baseline than those of C57Bl/6 mice. There is indirect evidence that patients with AAAs may have a systemic increase in arterial stiffness. Dijk et al. have shown that the carotid artery is stiffer in AAA patients compared to control patients without AAA. [143] In order to determine if the differences in mechanical properties were related to intrinsic differences in gene expression, we examined aortic elastin and collagen precursor levels prior to aneurysm induction. C57Bl/6 and 129/SvEv mice express similar levels of tropoelastin and procollagen (data not shown). There is evidence that the elasticity of arterial wall may impact susceptibility to arterial diseases. Studies have shown that aortic elastin haploinsufficiency leads to high blood pressure and progressive aortic valve malformation. [144,145] We did not measure tail cuff blood pressure in the current study but other studies have demonstrated that 129/SvEv mice have higher basal blood pressure than C57Bl/6 mice and 129/SvEv mice are more likely to develop hypertension and renal damage than C57Bl/6 mice in response to deoxycorticosterone acetate. [146,147] These results could occur because of baseline differences in mechanical properties or be the

result of differences in response to exogenous stimuli. Currently, the association between hypertension and AAA remains unclear. It has been reported that in angiotensin II (Ang II) infused apoE null mice, AAA formation is independent of blood pressure elevation. [148-150] We have previously demonstrated that there is an ongoing repair mechanism in patients with AAA as evidenced by high levels of collagen gene expression. [151] Six weeks after $CaCl_2$-induction, tropoelastin levels in 129/SvEv mice were significantly lower than C57Bl/6 mice. Procollagen levels did not differ between the two strains after aneurysm induction (data not shown). Aneurysm susceptibility may be related to baseline differences in tissue properties. This difference would be exacerbated in the 129/SvEv because of the reduced ability to produce equivalent amounts of tropoelastin as is produced by C57Bl/6.

Matrix metalloproteinases, especially MMP-2 and -9, play important roles in aneurysm formation. Interestingly, 129/SvEv mice intrinsically produce higher amounts of latent MMP-2 in the aorta compared to C57Bl/6 mice. This results in higher levels of active MMP-2 in 129/SvEv after $CaCl_2$-treatment compared to C57Bl/6. MMP-2 is primarily a product of resident aortic smooth muscle cells and fibroblasts. Initial degradation of elastin by MMP-2 may produce elastin fragments, which are known to induce monocyte chemotaxis. [92,152] This may account for the increased macrophage infiltrates seen in the aortas of 129/SvEv mice compared to C57Bl/6 mice. Baseline levels of active and latent MMP-9 were similar between the two mouse strains. This is not unexpected since macrophages are the main source of MMP-9 in aneurysm tissue but are not present in normal aortic tissue. [153] Levels of both latent and active MMP-9 were higher in 129/SvEv aortas than in C57Bl/6 aortas in response to $CaCl_2$-treatment. In addition to MMP-2 and -9, other proteases such as MMP-12, MMP-7, MT1-MMP, neutrophil elastase, and cysteine proteases may contribute to elastin degradation and aneurysm formation. [114,135,154-156] We tested neutrophil elastase expression in the mouse

aorta and found no difference between the two mouse strains (Fig. 5b). Using EDTA to block MMP activity, it is evident that the majority of the increased elastolytic activity is due to MMPs. These data suggest three possible mechanisms for the increased aneurysm susceptibility in 129/SvEv. First, the larger reservoir of latent MMP-2 could result in more elastin fragmentation with resultant recruitment of inflammatory cells to the aorta. Second, the differences in aneurysm sizes could be related to inherent differences in tissue mechanical properties. Finally, the myelogenous cells of the 129/SvEv may produce a more vigorous response to injury, greater elastin degradation, and aortic expansion.

It is known that inflammatory infiltrates play a pivotal role in aneurysm formation. [21,24,34,157] We investigated whether the myelogenous cell differences between the two strains of mice contribute to aneurysm susceptibility. Two chimeric mice were created, $C57^{bkg}/SvEv^{bm}$ mice, hematopoietic tissue ablated C57Bl/6 mice transplanted with 129/SvEv mouse myelogenous cells, and $SvEv^{bkg}/C57^{bm}$ mice, hematopoietic tissue ablated 129/SvEv mice transplanted with C57Bl/6 mouse bone marrow cells. Six weeks after $CaCl_2$-aneurysm induction, both chimeric mice produced aneurysms. However, the aneurysm sizes and pathological changes were similar to mice of their genetic background. These results demonstrate that myelogenous cells are not responsible for the background specific differences in aneurysm size between the two mouse strains. Thus, the difference in aneurysm susceptibility is related to tissue properties, MMP expression, or some combination of both.

A genetic predisposition to AAA formation is well-documented. [158,159] However, the genetic basis for this predisposition is unknown. Although animal models may not perfectly recapitulate human diseases, they can provide mechanistic insight toward understanding human pathology. The $CaCl_2$-induced murine aneurysm model reproduces many features that have been clinically described in human AAA tissue,

including macrophage and T cell recruitment, MMP up-regulation, and elastin fragmentation. Studies have demonstrated that manipulation of MMP-2 and MMP-9 levels have profound impacts on experimental aneurysm formation. [25,26] The current studies extend the previous work in demonstrating that even small differences in baseline or stimulated expression of MMP-2 and MMP-9 affect aneurysm size. Future studies examining factors regulating MMP gene expression will not only provide a greater understanding of the pathophysiology, but also may provide potential targets for therapeutic intervention.

CHAPTER 3

Elastin-derived peptides enhance M1 macrophage polarization

The following is a modified version of an article published in *Journal of Immunology* 2016
This work was coauthored by Wanfen Xiong, Jeffrey S. Carson, Melissa K. Suh, Trevor M. Meisinger, George P. Casale, B. Timothy Baxter, and myself.

Introduction

A key feature associated with aneurysm formation is loss of ECM and the destruction of the aortic wall. ECM degradation leads to proteolysis of elastin, the predominant ECM protein in the aortic wall. [160] Elastin proteolysis releases elastin-derived peptides (EDPs), including peptides with the xGxxPG motif, a commonly repeated sequence in elastin. [161] Of those EDPs released by elastin degradation, the VGVAPG repeat sequence in the human tropoelastin molecule has been shown to have the highest affinity for elastin-binding protein. [161-164] EDPs are upregulated in the serum of patients with AAA, and an increase in their level is predictive of AAA expansion. [36,165,166] Previous reports have demonstrated that EDPs recruit inflammatory cells to sites of ECM damage and neutralizing their effect with BA4, a monoclonal antibody that binds to VGVAPG and other xGxxPG motifs, prevents elastin damage. [92,93,167,168] The precise mechanism through which EDPs affect macrophages and subsequently lead to enhanced tissue damage has not been fully elucidated.

Macrophages play critical roles in the innate immune system, responding to various stimuli in their microenvironment. They can exist in a pro-inflammatory M1 phenotype as well as an anti-inflammatory M2 phenotype. [169] M1 macrophages are characteristically described by their release of pro-inflammatory cytokines, such as TNF-α and IL-1β. TNF-α, has been shown to be required for experimental aneurysm formation in mice. [170] Previous studies have demonstrated an increase in M1 macrophages in human AAA tissue. [36,37] In contrast, M2 macrophages are considered anti-inflammatory, aiding in the healing process by release of IL-10 and profibrotic factors such as TGF-β. [171] Their role in AAA formation and progression is less well known. The chronic inflammatory process in AAA promotes aneurysm expansion by active ECM degradation and pro-inflammatory cell recruitment to areas of tissue damage, potentially caused by an abnormally high ratio of M1/M2 macrophages. Thus,

altering the M1/M2 ratio may play an important role in slowing or preventing AAA expansion.

The purpose of this study was to evaluate the role of the M1/M2 ratio in AAA and the effect of EDPs on macrophage polarization. These studies were performed by three different methods. First, EDPs were used to examine whether they polarize macrophages to a pro-inflammatory M1 or anti-inflammatory M2 phenotype *in vitro*. Next, M1 or M2 macrophages were injected into mice in order to directly alter the M1/M2 ratio in the $CaCl_2$ AAA model. Finally, the effect of direct inhibition of EDPs on AAA and macrophage polarization was examined by administration of BA4 after aneurysm induction.

Methods

Reagents

Monoclonal anti-elastin antibody BA4, IgG, soluble elastin, and LPS were purchased from Sigma-Aldrich (St. Louis, MO, USA). VGVAPG peptide was purchased from Elastin Products Company (Owensville, MO, USA). Mouse IFN-γ and IL-4 were purchased from R&D systems (Minneapolis, MN, USA).

Mouse aneurysm induction model

The Institutional Animal Care and Use Committee (IACUC) approved all animal procedures. Male C57BL/6 mice at 8 weeks of age were obtained from The Jackson Laboratory (Bar Harbor, ME, USA). Mice underwent surgery as described previously.[172] To induce AAA, mice were anesthetized with tribromethanol (250 mg/kg; Sigma Aldrich) and underwent laparotomy. The abdominal aorta between the iliac artery bifurcation and renal arteries was isolated from the surrounding retroperitoneal structures. Next, the external diameter of the abdominal aorta was measured in triplicate midway between the renal arteries and iliac artery bifurcation. After baseline measurements, periaortic application of 0.25 M $CaCl_2$ was administered for 15 minutes followed by two washes with 0.9% sterile saline. Sterile saline (0.9% NaCl) replaced 0.25 M $CaCl_2$ in sham control mice. The laparotomy incision was closed followed immediately by subcutaneous injections of buprenorphine (0.15 mg/ml) for analgesic after surgery.

Anti-EDP antibody injections

After aortic exposure, application of $CaCl_2$, and closure of the laparotomy incision, antibody treatment was administered by intraperitoneal injection of BA4 (10

mg/kg) or IgG (10 mg/kg) in $CaCl_2$-treated mice. NaCl-treated mice received no treatment after laparotomy. Weekly injections of BA4 or IgG continued for six weeks after initial injection. One week or six weeks after surgery, mice underwent laparotomy and isolation of the infrarenal aorta. Tissue from BA4-treated mice were harvested one week after aneurysm induction in order to allow one injection of the antibody to have its potential full effect based on previous work showing that 10 mg/kg of BA4 is still detectable in the serum one week after i.p. injection.[94] Measurements were repeated in triplicate at the same locations as baseline measurements. Mice were sacrificed and the entire infrarenal aorta was removed for protein or mRNA isolation or histological studies. For histological studies, aortic tissue was perfusion-fixed with 10% neutral buffered formalin.

Bone marrow-derived macrophage isolation

Bone marrow-derived macrophages (BMDMs) were isolated from C57Bl/6 or C57Bl/6J-Tg(UBC-GFP)30Scha/J (GFP) mice as described previously.[173] Briefly, mice were euthanized by cervical dislocation. The femur and tibia were isolated from the surrounding muscle tissue and sterilized in 70% ethanol for 15 seconds then washed in PBS (1x). The ends of each femur and tibia were removed and the bone marrow was flushed out with Dulbecco's modified eagle medium (DMEM) supplemented with 1% fetal bovine serum (FBS) using a 25-gauge needle. Bone marrow cells were then passed through a cell strainer, washed with 1x PBS after centrifugation, then plated in a T75 dish at $1x10^7$ cells per 10 ml of BMDM media. BMDM media is defined as DMEM supplemented with 10% FBS, 20% conditioned medium from L929 cells (a source of M-CSF), 1% Penicillin/Streptomycin, and 1% glutamine. BMDMs were grown at 37^{o}C for seven days and media was removed and replaced with fresh BMDM media every two days. Flow cytometric analysis was used to determine purity of F4/80 positive

macrophages (98.6%). After seven days of growth, cells were treated for 24 hours with one of the five following treatments: No Tx (no treatment), M1 [IFN-γ (20 ng/ml) and LPS (100 ng/ml)], M2 [IL-4 (20 ng/ml)], EDP (1 μg/ml), or VGVAPG (1 μg/ml). Cell media was collected and RNA was isolated from the cells using TriZol according to manufacturer's instructions. RNA levels were examined using qPCR analysis with SYBR Green (BioRad). GAPDH was used as an internal control.

Bone marrow-derived macrophage polarization and injection

Bone marrow cells were isolated and differentiated into macrophages as described above. After differentiation, BMDMs were treated with IFN-γ and LPS (M1) or IL-4 (M2). After polarization, $5x10^6$ M1 or M2 BMDMs were injected into the mouse circulation via the tail vein. Mice were subjected to $CaCl_2$-induced aneurysm induction 24 hours after M1 or M2 injection. As a control, a group of mice received no M1 or M2 macrophages prior to $CaCl_2$ treatment. Mice were monitored for three days or six weeks. The three day-time point was chosen based on data presented in Supplemenatry Figure 1, where expression of M1 and M2 associated markers are highest in the aortic tissue after application of $CaCl_2$. Mice were sacrificed and the infrarenal aortic tissue was collected for histological, flow cytometry, RNA, or protein analysis.

Histology and microscopy

After perfusion-fixation with 10% neutral buffered formalin, aortic tissue samples were embedded in paraffin and sectioned into 4 μm sections. For Verhoeff-Van Gieson (VVG) staining, sections were stained with Verhoeff's solution, ferric chloride, sodium thiosulfate, and Van Gieson's solution. After each staining cycle, a fixing and washing procedure followed. Slides were then examined and photographed using light microscopy (40×; Nikon). Four sections were viewed per mouse.

Supplementary Figure 1. Aortic tissue mRNA levels of Ym1, CD206, and iNOS after aneurysm induction with $CaCl_2$. Levels were examined at day zero, three days (D3), one week (D7), two weeks (D14), four weeks (D28), and six weeks (D42) after aneurysm induction (n = 3-4 aortas per group). GAPDH used as internal control. Data expressed as mean ± SEM.

Figure 1

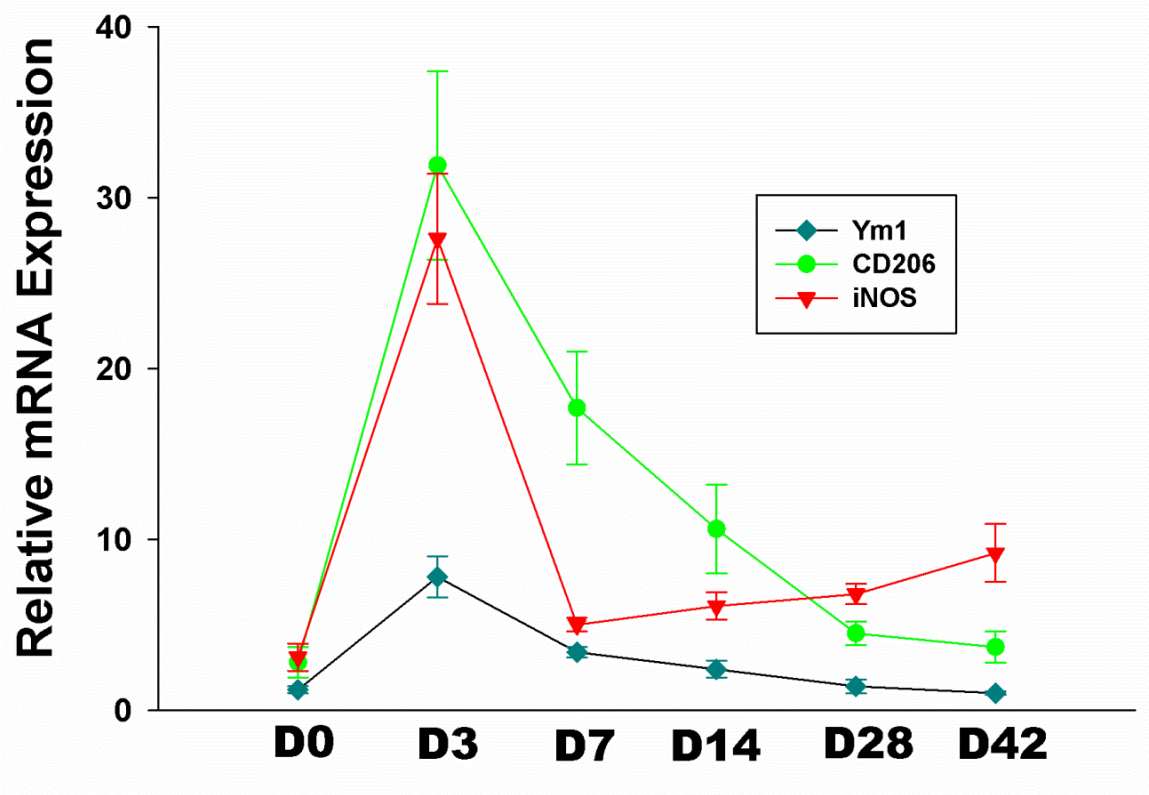
Relative mRNA Expression
40
30
20
10
0
D0
D3
D7
D14
D28
D42
Ym1
CD206
iNOS

Flow Cytometry

Aortic tissue from mice was isolated and digested for one hour at 37^{o}C with collagenase and elastase in RPMI with 1% FBS. [174] In order to isolate cells, the suspension from the digested tissue was filtered through a 40 μm filter. Cells were then pelleted by centrifugation and resuspended in flow cytometry staining buffer (1× PBS with 1% FBS). Cells were blocked with anti-mouse CD16/32 (1 μg/ml; BD Biosciences, San Diego, CA, USA) before surface labeling with the following antibodies: AlexaFluor 700-labeled CD86 (BioLegend, San Diego, CA, USA) APC-labeled F4/80 (BioLegend) and RPE-labeled CD206 (Bio-Rad Laboratories, Hercules, CA, USA). Flow cytometry data were analyzed using BD FACSDIVA software.

Detection of TNF-α concentration

Bone marrow-derived macrophages were isolated as described above. Media was collected from cells after incubation with increasing doses of EDP (0.01, 0.1, 1.0, 10, 100 μg/ml), VGVAPG (1 μg/ml), IFN-γ (20 ng/ml) and LPS (100 ng/ml), or IL-4 (20 ng/ml) for 24 hours. Cell media was used in a TNF-α ELISA from R&D Systems (Minneapolis, MN, USA) according to manufacturer's instructions.

Immunofluorescence

Mice that were injected with M1 or M2 macrophages were sacrificed at three days after aneurysm induction for macrophage staining performed on paraffin-embedded 4 μm aortic sections. After deparaffinizing the sections, antigen retrieval was performed using Proteinase K (Viagen Biotech, Los Angeles, CA, USA; 20 μg/ml in TE buffer pH 8.0). Sections were incubated in the Proteinase K working solution for three minutes at

room temperature. Sections were then washed and blocked with 10% normal goat serum. Rat monoclonal anti-F4/80 (ab6640, Abcam, Cambridge, MA, USA) diluted 1:400 was applied to the sections and incubated at room temperature for one hour. Sections were then washed and incubated with AlexaFlour 488 goat anti-rat IgG (A-11006, Life Technologies, Grand Island, NY, USA) diluted 1:200 for one hour at room temperature. Slides were then mounted with ProLong gold antifade mountant with DAPI (P-36931, Life Technologies). Fluorescence images were captured with a Leica epifluorescence widefield microscope (DMRXA2) and CCD camera (Orca C4742; Hamamatsu Photonics, Bridgewater, NJ, USA), with Hamamatsu software (HCImage 4.0).

Immunohistochemistry

Mice underwent AAA induction according to the method described above. Three to four mice from the NaCl, $CaCl_2$-IgG, $CaCl_2$-BA4 were sacrificed six weeks after aneurysm induction. Paraffin-embedded aortic sections were stained for CD206 (M2) and CD86 (M1). Sections were incubated with monoclonal rabbit anti-mouse CD86 (Abcam) diluted 1/500 or monoclonal rabbit anti-mannose receptor (CD206; Abcam) diluted 1/100 for 30 minutes at 37^{o}C. The sections were then briefly washed in citrate solution followed by incubation with a biotin-conjugated rat anti-rabbit IgG. CD206 and CD86 stained sections were examined by light microscopy (40×). The number of CD206 or CD86 positive cells per high powered field were counted and displayed in a bar graph. Four separate sections from each aorta were stained and evaluated.

Gelatin zymography

Aortic tissue protein was extracted as previously described and protein concentration was measured using the Bio-Rad protein assay (Bio-Rad Laboratories, Hercules, CA, USA).[175] Gelatin zymography was performed as previously described.[172] Standardized protein samples (5 μg) were resolved by nondenaturing electrophoresis with 0.8% gelatin in a 10% SDS-polyacrylamide gel. Molecular sizes of gelatinolytic activity were determined using protein standards (Bio-Rad). Signal intensities were quantified using ImageJ version 1.38x software (NIH, Bethesda, MD, USA).

Statistical analysis

The change in external aortic diameter over the course of aneurysm development was compared to baseline for each animal, and results for each group were expressed as mean ± SEM. ANOVA and post-hoc *t*-test with Bonferroni's correction were used to compare multiple groups. Statistical significance was accepted at a *P*-value < .05.

Results

Elastin-derived peptides promoted a pro-inflammatory M1 phenotype

To determine the role that EDPs have on macrophage phenotype, bone marrow cells were isolated and differentiated into BMDMs. To establish control M1 or M2 cells, BMDMs were treated with IFN-γ and LPS (M1), IL-4 (M2), or left untreated (No Tx) for 24 hours (Fig. 1A). To examine the effect of elastin fragments on macrophage polarization, BMDMs were treated with 1 μg/ml of EDPs or VGVAPG for 24 hours. EDP and VGVAPG treatment induced mRNA expression of M1 associated markers, such as TNF-α and IL-1β (Fig. 1A). In contrast, mRNA expression of M2 markers, CD206 and Ym1, was not affected by EDP or VGVAPG treatment (Fig. 1A). MMP-9 mRNA expression was also increased by EDP or VGVAPG treatment (Fig. 1A). To determine if the EDP-mediated M1 polarization was concentration dependent, BMDMs were treated with increasing doses of EDPs. An ELISA demonstrated a stepwise increase in TNF-α levels in the media with increasing doses of EDPs (Fig. 1B).

M2 macrophages reduced aortic dilation in an experimental AAA model

To determine the *in vivo* effects of influencing the M1/M2 ratio in an experimental AAA model, macrophages polarized to the M1 or M2 phenotype were injected intravenously into mice 24 hours prior to aneurysm induction. Cells were sampled from each treatment group prior to injection and M1 or M2 polarization was confirmed by protein expression of M1 (iNOS) and M2 (Ym1) markers (Fig. 2B). A control group of mice underwent aneurysm induction without injection of macrophages (Control). Aortic diameters were measured six weeks after aneurysm induction. Three of the eight mice that received M1 macrophages were sacrificed prior to the six-week time point due to severe systemic illness; necropsy revealed severe aortic damage in these mice. All of the mice that received M2 macrophages (9/9) survived to the six-week time point.

Figure 1. Elastin-derived peptides polarize macrophages to a pro-inflammatory M1 phenotype. A) qPCR analysis of M1 and M2 phenotype markers after treatment of macrophages with IFN-γ and LPS (M1), IL-4 (M2), VGVAPG (1 μg/ml), or EDP (1 μg/ml) for 24 hours. GAPDH was used as an internal control. B) ELISA measurement of TNF-α levels from EDP- or VGVAPG-treated macrophage media. Statistics performed using ANOVA and Student's *t*-tests. Data expressed as mean ± SEM. *, $P < .05$; **, $P < .01$ versus no treatment (No Tx).

Figure 1

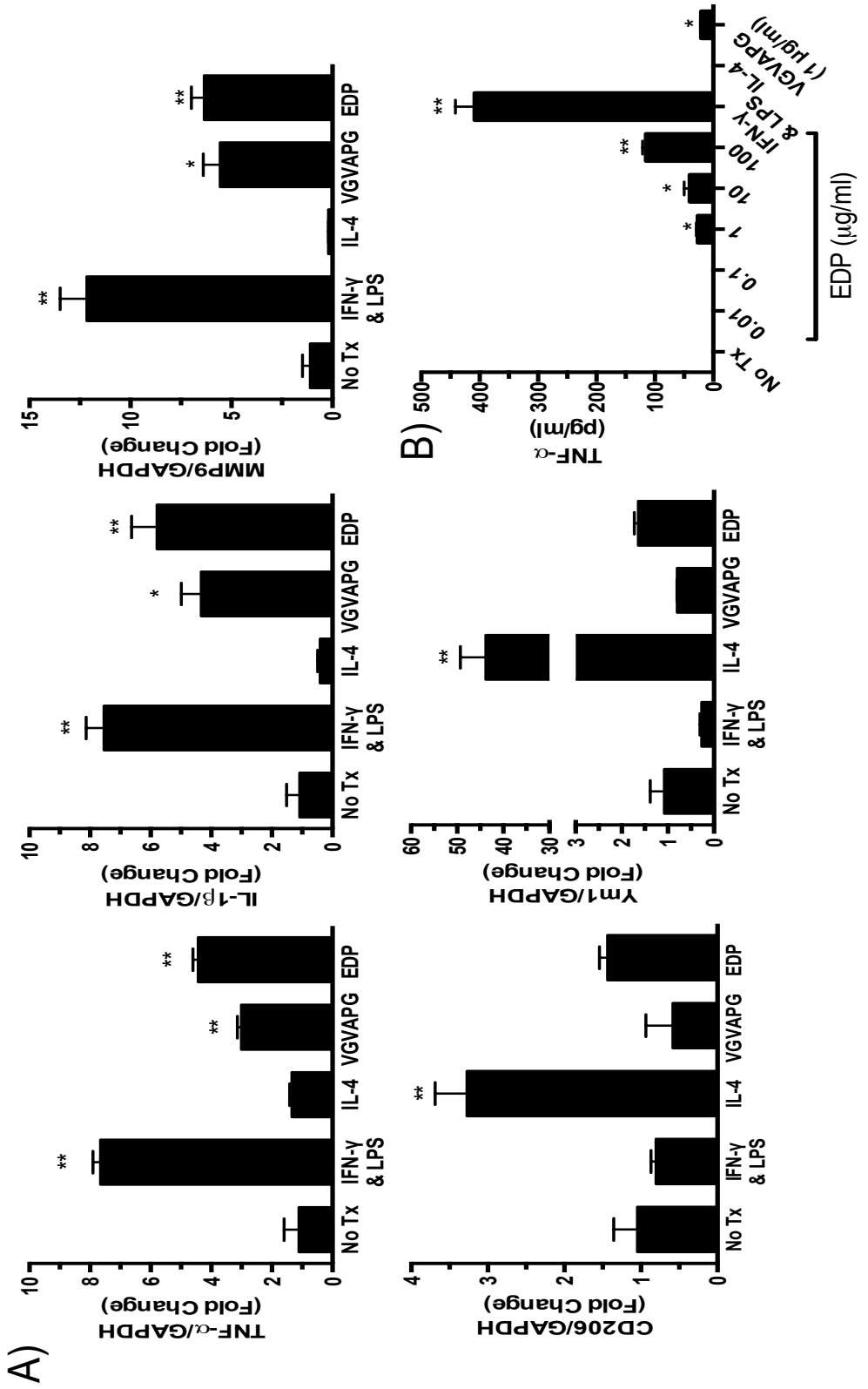
A)
TNF-α/GAPDH (Fold Change)
IL-1β/GAPDH (Fold Change)
MMP9/GAPDH (Fold Change)
CD206/GAPDH (Fold Change)
Ym1/GAPDH (Fold Change)
No Tx
IFN-γ & LPS
IL-4
VGVAPG
EDP
B)
TNF-α (pg/ml)
No Tx
0.01
0.1
1
10
100
IFN-γ & LPS
IL-4
VGVAPG (1 μg/ml)
EDP (μg/ml)

Figure 2. M1 and M2 macrophage influence on aortic size six weeks after aneurysm induction. A) Schematic representation of method of BMDM isolation, injection, and aortic aneurysm induction. B) Representative image of protein expression of M1 (iNOS) or M2 (Ym1) markers of macrophages treated with IFN-γ (20 ng/ml) and LPS (100 ng/ml) or IL-4 (20 ng/ml) prior to injection. C) Aortic diameter percent increase six weeks after aneurysm induction with M1 or M2 macrophage injection (n = 5-9 per group). Statistics performed using ANOVA and Student's *t*-tests. Data expressed as mean ± SEM. *, $P < .05$; **, $P < .01$. D) Representative VVG images of aortas six weeks after aneurysm induction with injection of M1, M2, or no macrophages (Control) (n = 3-4 per group). VVG image of aorta from a mouse that required sacrifice within one week after aneurysm induction. Arrows indicate sites of elastin fragmentation.

Figure 2

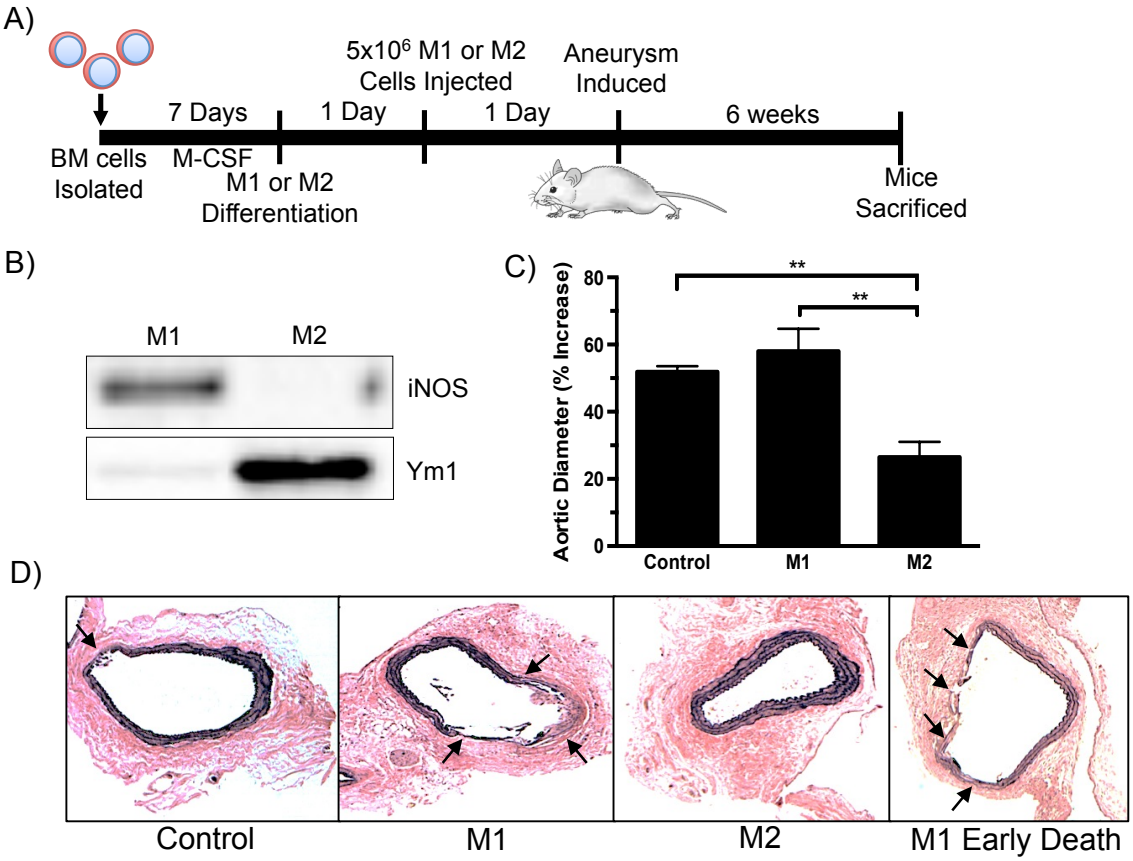
A)
5x10^6 M1 or M2
Cells Injected
Aneurysm
Induced
7 Days
1 Day
1 Day
6 weeks
BM cells
Isolated
M-CSF
M1 or M2
Differentiation
Mice
Sacrificed
B)
M1
M2
iNOS
Ym1
C)
Aortic Diameter (% Increase)
80
60
40
20
0
**
**
Control
M1
M2
D)
Control
M1
M2
M1 Early Death

Comparing survival (5/8 vs. 9/9) between the two groups by Fisher's exact test demonstrated a *P*-value of 0.08. While M1 macrophage injection did not show a statistically significant increase in aortic diameter, the trend toward larger aneurysms may have been attenuated by the three mice that required sacrifice prior to six weeks. The aortic diameters from mice injected with M2 macrophages were significantly smaller than $CaCl_2$-treated control mice or mice injected with M1 macrophages (Fig. 2C). Connective tissue staining indicated robust elastin degradation in aortas from the M1 injected mice compared to $CaCl_2$-treated control mice. The most severe elastin degradation was seen in mice sacrificed prior to the six-week time point (Fig. 2D). Aortas from M2-injected mice displayed overall elastin preservation six weeks after aneurysm induction (Fig. 2D). The elastin preservation seen in these animals coincided with a decrease in levels of both MMP-9 and MMP-2 in M2-injected mice compared to M1-injected mice (Fig. 3). No differences in MMP levels were seen between Control and M1-injected mice.

Infleunce of M1 and M2 macrophages at three days

To determine the effect of M1 or M2 macrophages on early aortic aneurysm formation, $CaCl_2$- or NaCl-treated mice that had undergone M1 or M2 injection were sacrificed three days after aneurysm induction. The effect of the M2 macrophages observed at six weeks was also seen at the earlier three-day time point (Fig. 4B). In contrast to the six-week time point, M1 macrophage injection did show a significant increase in aortic diameter compared to $CaCl_2$-treated control mice. M1 or M2 injection had no effect on aortic diameter in NaCl-treated mice (Fig. 4B). In order to assess that the injection of M1 or M2 cells were having a local effect on the macrophage population in the aortic tissue, cells were isolated from the aorta by enzymatic digestion three days after aneurysm induction. Cells were analyzed by flow cytometry to determine the ratio

Figure 3. Active MMP-2 and MMP-9 levels are decreased in mice injected with M2 macrophages. Signal intensities of ProMMP-9 MMP-9, ProMMP-2, and MMP-2 were quantified using ImageJ software. Statistics performed using ANOVA and Student's *t*-tests. Data are presented as mean ± SEM (n = 4-5 aortas per group). *, $P < .05$.

Figure 3

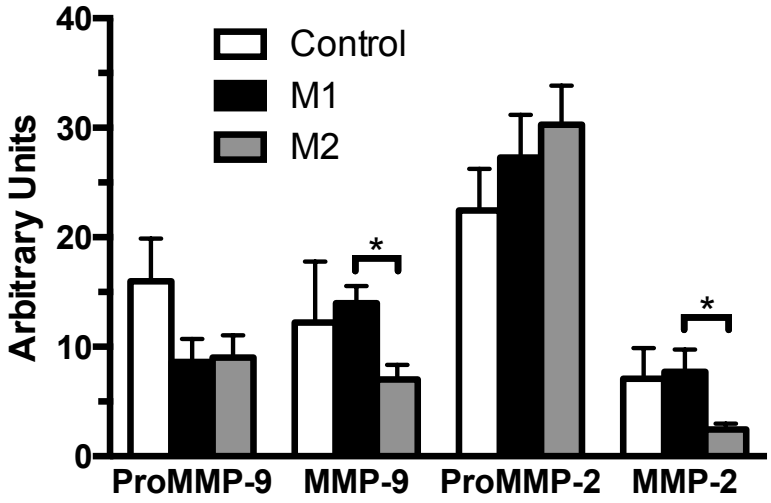
40
30
20
10
0
Arbitrary Units
Control
M1
M2
*
*
ProMMP-9
MMP-9
ProMMP-2
MMP-2

Figure 4. M1 and M2 macrophage influence on aortic size three days after aneurysm induction. A) Schematic representation of methods three days after aneurysm induction and macrophage injection. B) Aortic diameter percent increase three days after aneurysm induction with injection of M1, M2, or no macrophages (Control) (n = 5-6 per group). NaCl was used as sham control. C) Bar graph on left represents M1/M2 ratio of M1 (CD86) to M2 (CD206) positive macrophages (F4/80) from flow cytometry (n = 5-6 per group). Right bar graph shows proportion of $F4/80^{+}$ macrophages found in tissue. D) Representative immunofluorescence and VVG stained images of aortas three days after surgery and M1 or M2 macrophage injection (n = 3 per group). Top panel shows aortas stained with a rat anti-mouse F4/80 antibody (red), cell nuclei stained with DAPI (blue); bottom panel shows VVG stained aortas. Arrows indicate sites of elastin fragmentation or abnormal structure. Statistics performed using ANOVA and Student's *t*-tests. Data expressed as mean ± SEM. *, $P < .05$; **, $P < .01$.

Figure 4

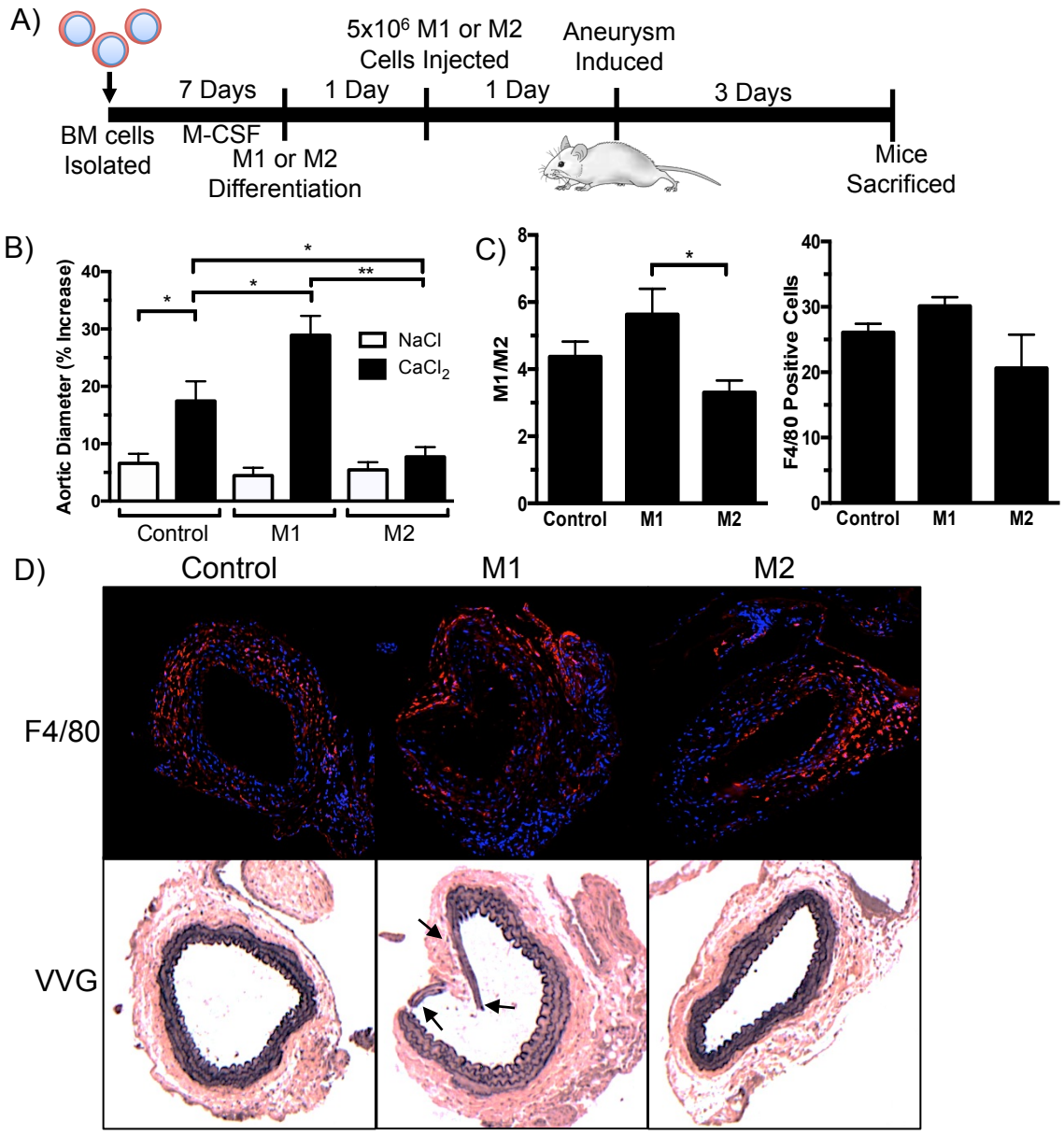
A)
5x10⁶ M1 or M2
Cells Injected
Aneurysm
Induced
7 Days
1 Day
1 Day
3 Days
BM cells
Isolated
M-CSF
M1 or M2
Differentiation
Mice
Sacrificed
B)
Aortic Diameter (% Increase)
NaCl
CaCl2
Control
M1
M2
C)
M1/M2
F4/80 Positive Cells
Control
M1
M2
D)
Control
M1
M2
F4/80
VVG

of M1 to M2 polarized cells (Fig 4C). These data demonstrated a higher M1/M2 ratio in the aortas of M1-injected mice and a decreased ratio in M2-injected mice. By immunofluorescence staining, there did not appear to be a difference in the total number macrophages in aortic tissue when comparing M1- to M2-injected mice (Fig. 4D). This was consistent with flow cytometry data showing no difference in the percentage of $F4/80^+$ macrophages in the aortic tissue. Connective tissue staining revealed that M1 macrophage injection resulted in severe elastin fragmentation three days after aneurysm induction; the corresponding immunofluorescence studies indicated a high concentration of macrophages adjacent to the sites of marked elastin damage (Fig. 4D). Aortas from M2-injected mice showed preserved elastin architecture.

In order to determine whether injected macrophages migrated to the aorta, GFP^+ BMDMs were incubated with IFN-γ and LPS (M1) and IL-4 (M2). After polarization, GFP^+ M1 or GFP^+ M2 cells were injected intravenously into mice 24 hours prior to aneurysm induction. Aortic tissue was harvested three days after aneurysm induction, digested, and a single cell suspension was analyzed by flow cytometry. GFP^+ cells were found in aortas of 6/7 mice injected with M1 cells and 5/6 mice injected with M2 cells. Further analysis revealed that 1.18% ± 0.22 of the total M1 cells detected in the M1-injected mice were GFP^+ and that 9.25% ± 2.74 of the total M2 cells detected in the M2-injected mice were GFP^+.

BA4 reduced aortic diameter and elastin degradation

BA4 is a monoclonal antibody that specifically binds xGxxPG motifs, particularly VGVAPG, which is a common motif repeated in elastin. Previous studies have shown that BA4 reduces monocyte/macrophage chemotaxis in diseases associated with elastin fragmentation, such as Marfan syndrome and emphysema. [92,94] To determine if BA4 can reduce aortic dilation in AAA, mice were treated with weekly i.p. injections of BA4 (10

Figure 5. BA4 attenuates aortic dilation and elastin degradation. A) Schematic representation of methods for weekly anti-EDP treatment. B) Percent increase in aortic diameter six weeks after aneurysm induction and treatment with IgG or BA4 (n = 7-8 mice per group). C) Representative gelatin zymogram of mouse aortic tissue six weeks after aneurysm induction. Signal intensities of MMP-2, ProMMP-2, and MMP-9 were quantified using ImageJ software. Statistics performed using ANOVA and Student's *t*-tests. Data are presented as mean ± SEM (n = 4-5 aortas per group). *, $P < .05$; **, $P < .01$. C) Representative VVG staining of aortic tissue sections from NaCl, $CaCl_2$ IgG, and $CaCl_2$ BA4 treated mice (n = 3-4 aortas per group). Arrows indicate sites of elastin damage.

Figure 5

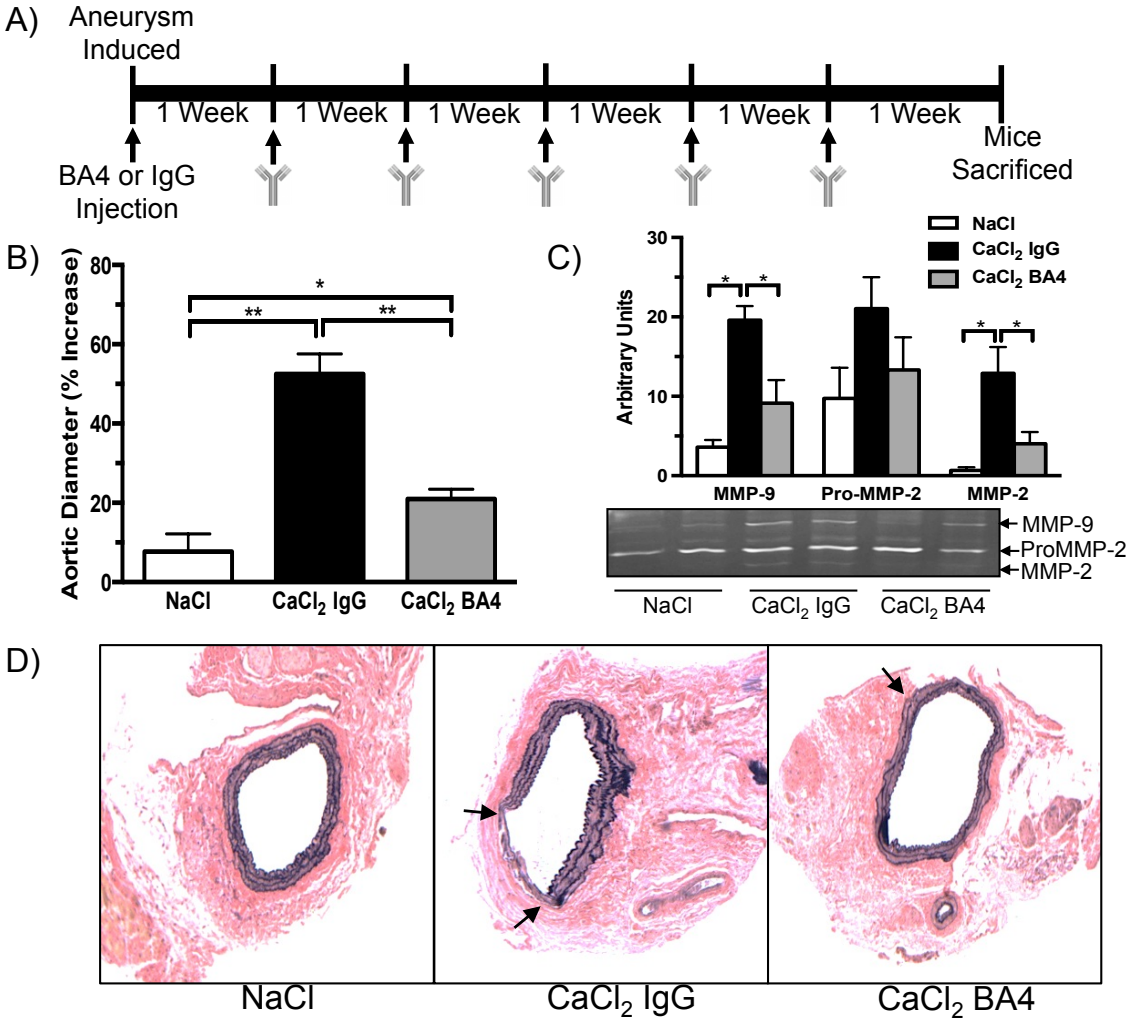
A)
Aneurysm Induced
1 Week
1 Week
1 Week
1 Week
1 Week
1 Week
Mice Sacrificed
BA4 or IgG Injection
B)
Aortic Diameter (% Increase)
NaCl
CaCl2 IgG
CaCl2 BA4
C)
Arbitrary Units
MMP-9
Pro-MMP-2
MMP-2
ProMMP-2
D)
NaCl
CaCl2 IgG
CaCl2 BA4

mg/kg) after $CaCl_2$ aneurysm induction. A control group of mice received weekly injections of non-specific IgG (10 mg/kg). Six weeks after aneurysm induction, mice were sacrificed and aortas harvested for analysis. BA4 reduced aortic dilation compared to IgG treatment (Fig. 5B). Active forms of both MMP-9 and MMP-2 in aortic tissue were also decreased in BA4-treated mice, whereas the inactive form of MMP-2 was not significantly reduced (Fig. 5C). Connective tissue staining revealed general elastin preservation in aortas from BA4-treated mice (Fig. 5D). Treatment with NaCl had no effect on elastin fragmentation. Immunohistochemical staining revealed an increase in CD206 positive cells (M2 macrophage marker) in aortic tissue from BA4-treated mice compared to NaCl and IgG-treated mice (Supplementary Fig. 2). The number of CD86 positive cells was higher in aortas from IgG-treated mice but not significantly different from NaCl or BA4-treated mice.

In order to better understand the early pathogenesis of aneurysm formation, the effects of EDP neutralization were evaluated one week after aneurysm induction. Aortic diameter was increased in both BA4-treated and IgG-treated mice; however, IgG-treated mice exhibited a markedly greater increase in diameter (Fig. 6A). A previous study showed that monocyte/macrophage chemotaxis in response to human AAA explants was reduced by preincubation of the tissue with BA4. [167] In this present study, BA4's ability to reduce macrophage migration *in vivo* was assessed by flow cytometry. As expected, migration of $F4/80^+$ macrophages to aortic tissue was increased after $CaCl_2$-IgG treatment compared to NaCl treatment (Fig. 6B). BA4 reduced the frequency of macrophage migration to the baseline levels seen in NaCl-treated aortas. Gelatin zymography demonstrated that BA4 treatment reduced the active forms of both MMP-2 and MMP-9 in aortic tissue at one week (Fig. 6C). M1 or M2 polarization was assessed in aortic tissue after $CaCl_2$ treatment. Quantitative PCR revealed downregulation of M1 associated genes (TNF-α, CD86) and upregulation of M2 associated genes (CD206,

Supplementary Figure 2. BA4 increases CD206^{+} macrophages in aortic tissue. Representative immunohistochemisty of CD206 or CD86 positive cells in aortic tissue six weeks after aneurysm induction. Bar graph represents number of CD206 or CD86 positive cells per high powered field (HPF). The anti-CD86 antibody demonstrated some nonspecific binding to connective tissue. Arrows indicate representative CD206 or CD86 positive cells. Statistics performed using ANOVA and Student's *t*-tests. Data are presented as mean ± SEM (n = 4-5 aortas per group). *, $P < .05$; **, $P < .01$.

Supplementary Figure 2

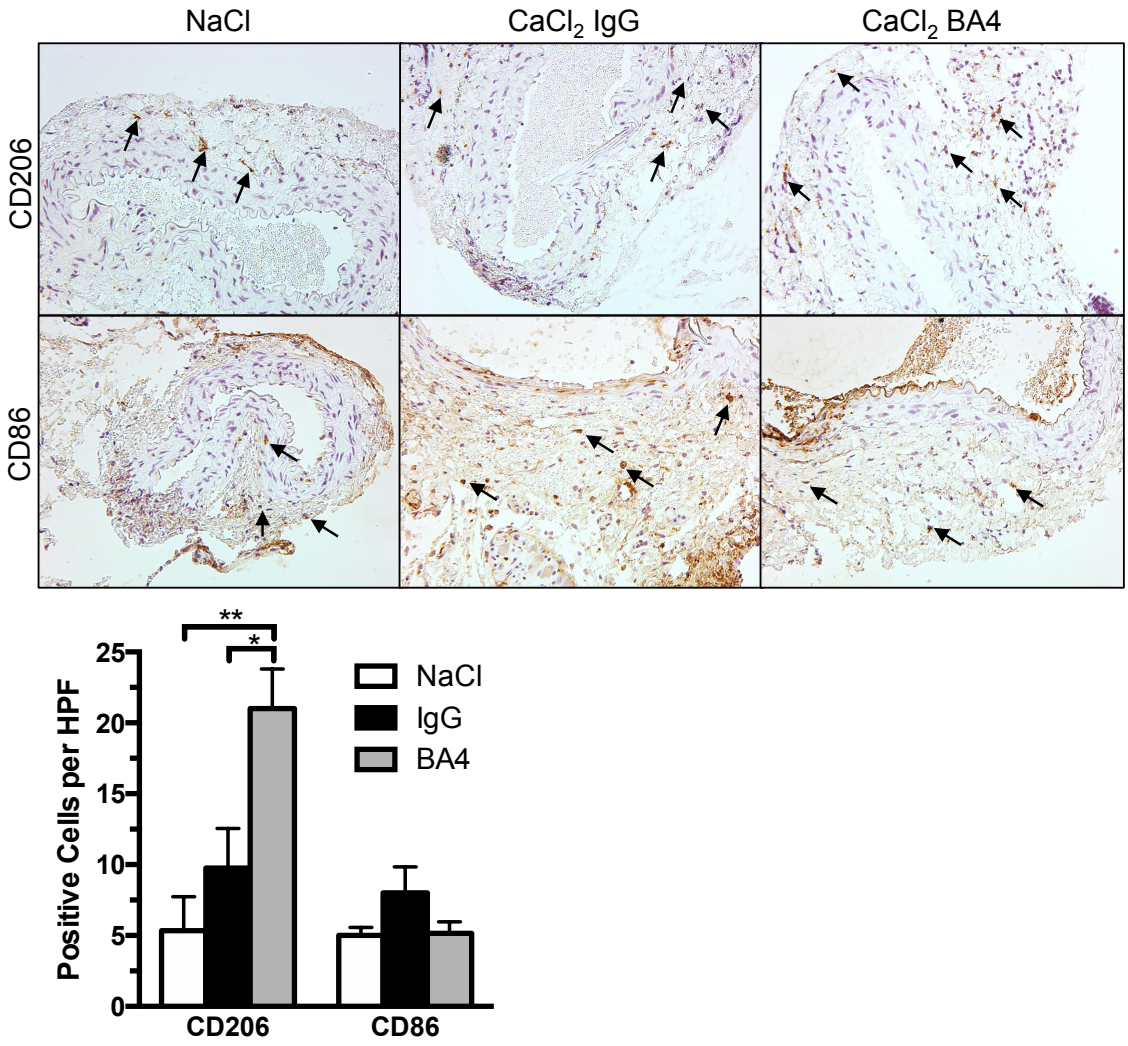

Figure 6. BA4 reduced macrophage migration, MMP production, and the ratio of M1/M2 markers in aortic tissue one week after aneurysm induction. A) Percent increase aortic diameter one week after aneurysm induction (n = 8-10 per group). B) Number of F4/80 positive cells in NaCl, $CaCl_2$-IgG, and $CaCl_2$-BA4 treated aortas (n = 7-8 per group). C) Representative gelatin zymogram of aortic tissue one week after aneurysm induction. Bar graphs represent signal intensities of ProMMP-9, MMP-9, ProMMP-2, and MMP-2 by quantification with ImageJ software (n = 3-4 per group). Data expressed as mean ± SEM. *, $P < .05$; **, $P < .01$. D) Fold change in mRNA expression of M1 and M2 associated markers from aortic tissue of mice treated with $CaCl_2$-IgG or $CaCl_2$-BA4 compared to NaCl-treated mice one week after aneurysm induction (n = 4 per group). GAPDH was used as internal control. Dashed line indicates NaCl control (fold change = 1). Statistics performed using ANOVA and Student's *t*-tests. Data expressed as mean ± SEM. *, $P < .05$; **, $P < .01$ versus NaCl. †, $P < .05$; ††, $P < .01$ versus $CaCl_2$-IgG treatment.

Figure 6

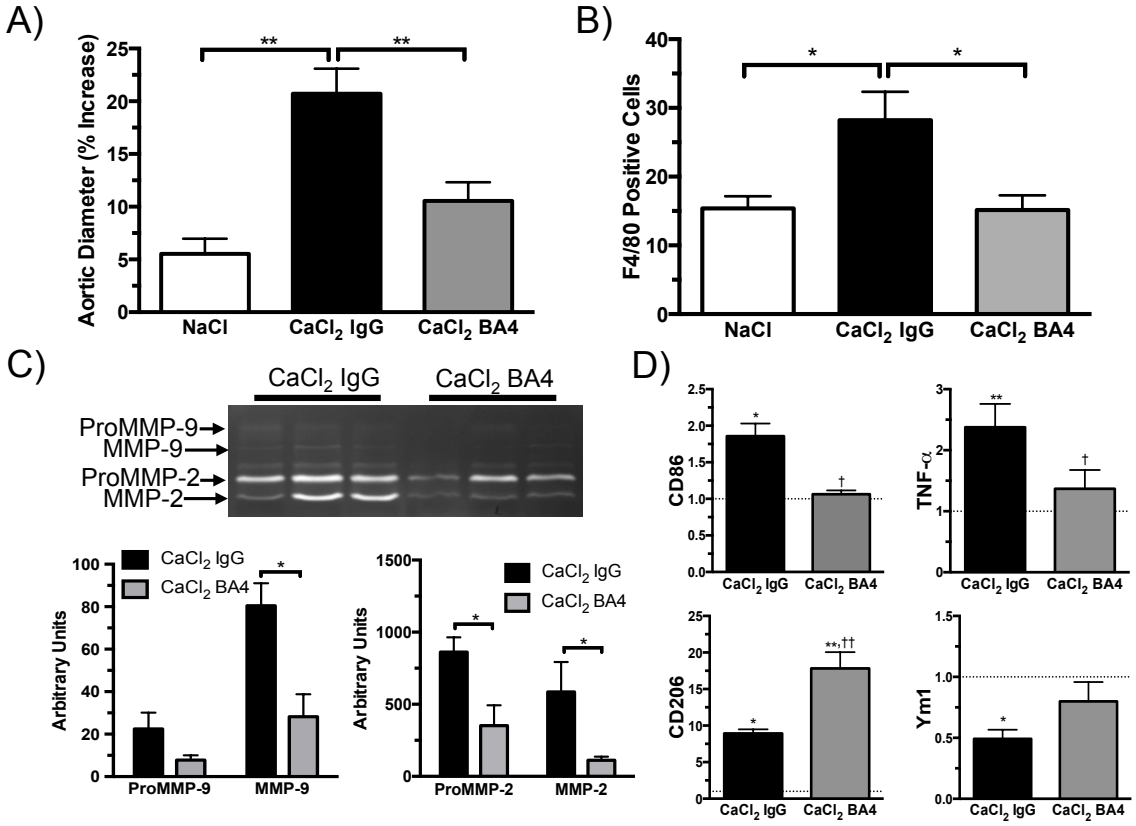
A)
Aortic Diameter (% Increase)
NaCl
CaCl2 IgG
CaCl2 BA4
B)
F4/80 Positive Cells
C)
ProMMP-9
MMP-9
ProMMP-2
MMP-2
Arbitrary Units
D)
CD86
TNF-α
CD206
Ym1

Ym1) with BA4 treatment (Fig. 6D). Many typical pro-inflammatory markers identified in aneurysm tissue were decreased by BA4 treatment (Supplementary Fig. 3A) while anti-inflammatory markers were increased (Supplementary Fig. 3B). By Western blot analysis, the M2-associated marker Ym1 was increased in BA4-treated aortic tissue compared to IgG treatment (Supplementary Fig. 4).

Supplementary Figure 3. BA4 treatment promotes an anti-inflammatory environment in aortic tissue one week after aneurysm induction. A) Bar graphs represent fold change in mRNA expression levels of pro-inflammatory and M1 associated markers from aortic tissue relative to NaCl controls (dashed line) one week after surgery. B) Bar graphs represent fold change in mRNA expression levels of anti-inflammatory and M2 associated markers from aortic tissue relative to NaCl controls (dashed line) one week after aneurysm induction (n = 4 per group). GAPDH was used as internal control. Statistics perfumed using ANOVA and Student's *t*-tests. Data expressed as mean ± SEM. *, $P < .05$; **, $P < .01$ versus NaCl. †, $P < .05$; ††, $P < .01$ versus $CaCl_2$-IgG treatment.

Supplemental Figure 3

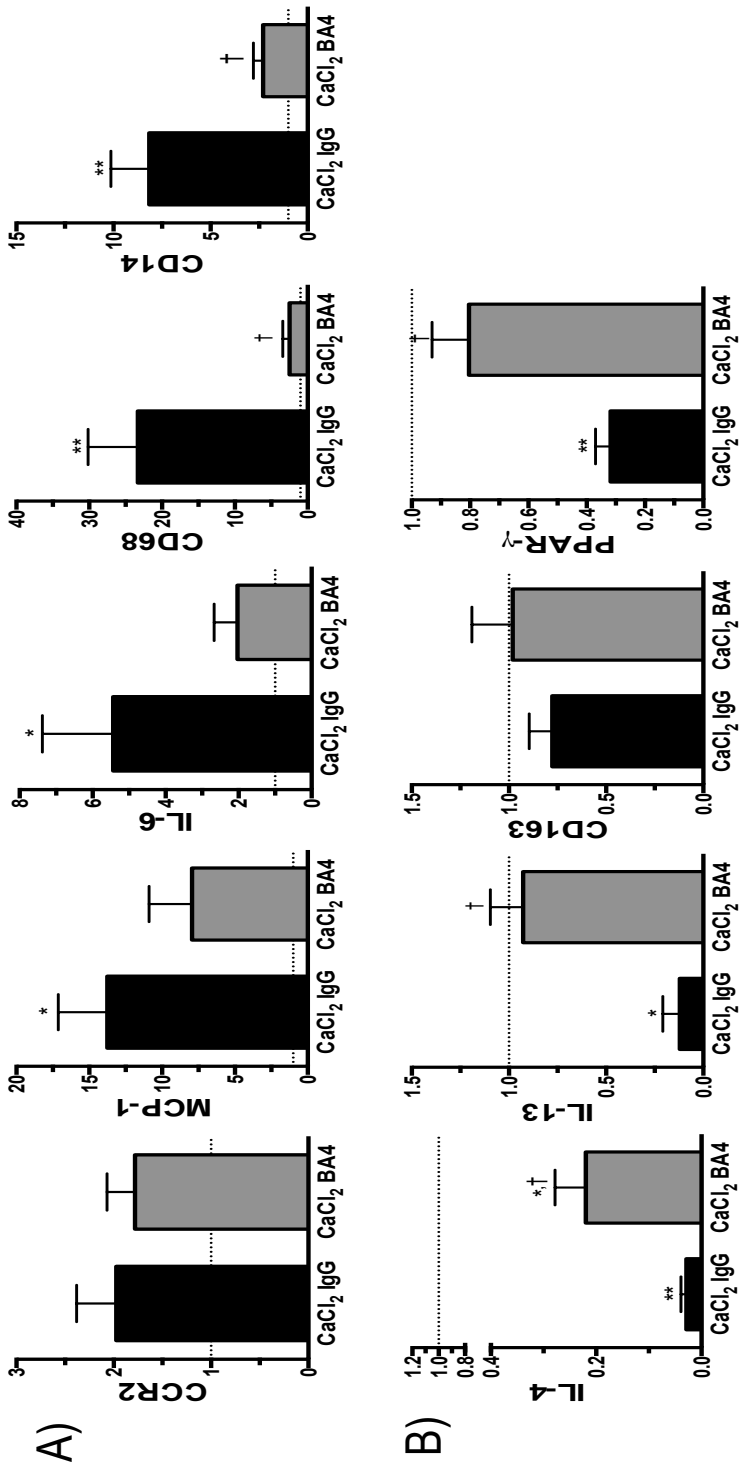

Supplementary Figure 4. Aortic tissue protein levels of Ym1 one week after BA4 treatment. Bar graph represents relative protein expression levels of Ym1 one week after aneurysm induction and IgG or BA4 treatment (n = 4 aortas per group). GAPDH used as internal control. Statistics perfumed using ANOVA and Student's *t*-tests. Data expressed as mean ± SEM. *, $P < .05$.

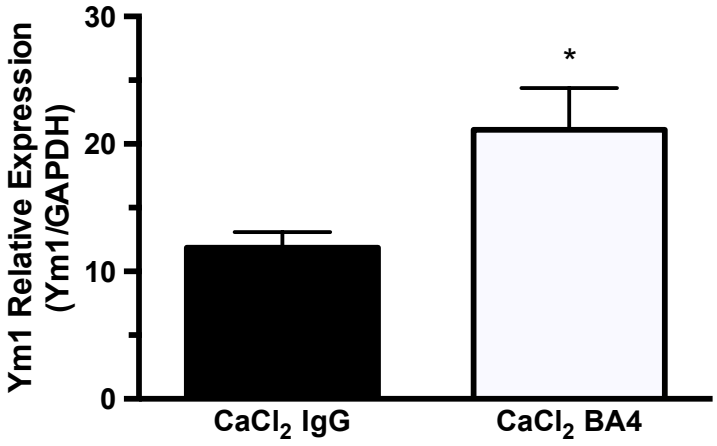
Ym1 Relative Expression
(Ym1/GAPDH)
30
20
10
0
*
CaCl2 IgG
CaCl2 BA4

Discussion

Using a murine model of AAA, we found that M1 macrophages strongly promoted aneurysm formation. This effect was seen as early as three days after aneurysm induction; aortic diameters were larger in the M1-infused group. This increase was not significant compared to $CaCl_2$-treated control at six weeks. This may be explained, however, by the fact that three of the eight mice treated with M1 macrophages required sacrifice within one week of aneurysm induction due to severe systemic illness. Post-mortem examination of the aortic tissue from these three mice demonstrated severe elastin damage not typically seen until six weeks. This early morbidity is atypical for this model and was not seen in any of the M2-treated mice, suggesting that an excess number of M1 macrophages may be toxic. Conversely, M2 macrophage infusion was highly protective against elastin degradation and aneurysm formation. Furthermore, EDPs, systemic levels of which are elevated in AAA patients, [176] promoted polarization of macrophages to a pro-inflammatory M1 phenotype. EDPs also enhanced the transcription of MMP-9, which has previously been shown to be required for AAA development. [172,177] *In vitro* studies showed that EDPs or the VGVAPG peptide did not upregulate expression of M2-associated genes. Administration of the antibody BA4, which binds the repeated elastin motif VGVAPG, dramatically reduced aortic dilation, elastin fragmentation, and MMP production. BA4 lowered M1 and raised M2 markers early after aneurysm induction, leading to a reduction in aneurysm formation at six weeks.

EDPs are created as a result of breakdown of elastin, a key extracellular matrix protein that is present in the skin, lungs, arteries, and other structures. Elastin makes up 50% of the aortic wall proteins by weight. [178] Once elastin is incorporated into the tissue structure, there is little to no turnover except under pathological conditions. [92,179-181] Previous studies have shown that EDPs are increased in the serum of patients with

AAAs.[165,166,176] EDPs have been shown to have inflammatory properties by examination of their effects on lymphocytes and MMP expression; they increase Th1 associated cytokines and MMP-9 synthesis.[182] This polarization of lymphocytes appears to be mediated through a receptor for specific EDPs, since it can be blocked by neutralization of the elastin receptor or with lactose, which causes shedding of the receptor from the cell membrane.[161] Similar treatment inhibited monocyte migration when monocytes were exposed to human AAA tissue extract.[167] A previous study has suggested that EDPs may have an anti-inflammatory effect on macrophages under specific conditions.[183] In contrast, the present study indicated that EDPs had a profound pro-inflammatory effect. Furthermore, we demonstrated that this effect was mediated by promoting M1 macrophage polarization.

Chronic inflammation occurs in the aortic tissue of patients with AAA; the predominate cell types found in this infiltrate are T lymphocytes and macrophages.[30,184] Inflammation induced by ablumenal application of $CaCl_2$ in a model of AAA recapitulates many features seen in human AAA tissue including macrophage and lymphocyte infiltration, MMP upregulation, elastin degradation, and aortic dilation.[31,155,172,185] Pro-inflammatory M1-associated cytokines such as TNF-α, IL-6, and IFN-γ are increased in both human and experimental AAAs.[36,37] Deletion or neutralization of these M1-associated cytokines resulted in reduced aortic dilation or complete aneurysm inhibition.[100,101,170,175] M1 or M2 macrophage polarization can have a significant role in regulating chronic inflammatory processes; little is known about the role of M1 or M2 macrophage polarization in aortic aneurysms. We demonstrated that the pro-inflammatory state induced by $CaCl_2$ was enhanced by supplementation with M1-polarized macrophages. M2 macrophage injection rescued the aorta from expansion and elastin disruption. The pathogenesis of aneurysm development was altered early in its course by M2 macrophages, where the impact on aortic dilation and elastin fragmentation could be

seen as early as three days after aneurysm induction. Taken together, these data demonstrate that the M1/M2 ratio plays a fundamental role in aneurysm development, and could prove an important therapeutic target.

By using flow cytometry, we were able to determine that injected macrophages are able to migrate to the damaged aorta. This small proportion of injected cells found in the aorta three days after aneurysm induction may not completely account for how these cells induce the distinct aortic phenotypes observed. It is known that small populations of cells, such as T regulatory cells, can have a major effect on inflammatory processes in both human and murine AAAs.[76,186] These injected M1 or M2 cells may also be acting systemically by increasing circulating levels of cytokines levels vital to aneurysm formation. Injection of M1 macrophages led to early mortality in three mice within a week of aneurysm induction suggesting a profound systemic inflammatory response not seen in M2-injected mice. These injected M1 or M2 cells may also be influencing other cell types important in aneurysm formation such as T regulatory cells.[187] In the case of injected M2 cells, they may be creating a positive feedback loop by enhancing other anti-inflammatory cell populations. These populations may further enhance the M2 phenotype leading to decreased damage to the aortic wall and preservation of elastin. Previous studies have shown that macrophages are not terminally differentiated and have the ability to change phenotypes over time.[188-190] Future studies will focus on better understanding these mechanisms and, particularly, the potential benefit of injecting macrophages polarized to the M2 phenotype.

The elastin-binding protein is assumed to have a role in normal elastin assembly by secreting the elastin precursor, tropoelastin, into the ECM.[191] This protein is found on many cell types, including cells that don't normally produce elastin.[192] This study suggests that the elastin-binding protein, through its interaction with EDPs, contributes to disease pathogenesis when present on inflammatory cells such as macrophages.

Previous studies have shown that the peptide sequence predominantly recognized by the elastin-binding protein is VGVAPG. Other peptides of this motif, xGxxPG, have a lower affinity for the elastin-binding protein. [193] These particular motifs are found primarily in elastin, but are also present to a lesser extent in other connective tissue proteins. Binding of the BA4 antibody to elastin fragments with the xGxxPG motif reduces or inhibits cellular activation in response to the presence of EDPs. [92-94,167, 194] In this study, we demonstrate this critical role of EDPs in potentiating aneurysm formation, in part, through the elastin-binding protein on macrophages. The *in vitro* studies indicated that the mechanism for this effect is mediated by altering macrophage polarization. As expected, BA4 reduced macrophage migration to the site of aortic injury. Importantly, the BA4 treatment also influenced production of M1 and M2 related proteins, reducing the pro-inflammatory microenvironment caused by EDPs. Since M2 macrophages are known to play a role in healing, the effects seen with BA4 may represent attempted tissue repair.

In conclusion, this study demonstrated that EDPs have an important role in promoting aneurysm expansion by altering the macrophage phenotype. This increase in M1/M2 ratio would be expected to create a positive feedback loop by further degradation of the elastin matrix and continued release of EDPs. The profound inhibitory effects of the M2 macrophages suggest a key role in preventing small aneurysm expansion. All current treatments for aortic aneurysms rely on mechanical intervention. Yet, when most AAAs are detected, they are below the threshold for repair leading to a significant observation period during which there is currently no medical therapy to prevent or slow aneurysm growth. The results presented herein suggest that decreasing the M1/M2 ratio, either by neutralization of pro-inflammatory EDPs or enhancing the anti-inflammatory environment created by M2 macrophages, could prove a useful therapeutic target for small aortic aneurysms.

DISSERTATION DISCUSSION

The course of human AAA is a long, complex, and multifactorial process. Most patients are asymptomatic until the AAA ruptures, which 90% of the time results in death. [195] Of those patients that have been diagnosed and are aware of their aneurysm, a period of cautious waiting occurs until the aneurysm is dilated enough to need surgical intervention. While advances in surgical techniques have reduced the immediate complications after open aneurysm repair, [196] the game of waiting for this ticking time bomb to rupture needs to become obsolete. Therefore, the need for pharmacological intervention is critical in order to prevent the progression or stimulate the regression of established AAAs. Clinical trials are underway in order to identify a therapeutic alternative to mechanical AAA intervention.

Studies on human AAA tissue focus on the end stage of disease since the tissue is obtained most often at the time of open aneurysm repair when the aorta is significantly enlarged and damaged. In addition, the ability to obtain human AAA tissue is decreasing as endovascular AAA repair increases. Therefore, in order to study AAA pathogenesis, animal models must be used. The three most commonly used murine AAA models are the $ApoE^{-/-}$ angiotensin-II infusion model, elastase perfusion, and $CaCl_2$ topical application. The $CaCl_2$ model is able to recapitulate many characteristics similar to human AAA such as elastin degradation, inflammatory cell infiltration, and MMP upregulation. This model and the elastase perfusion model are less widely used due to their technical challenges compared to the $ApoE^{-/-}$ angiotensin-II infusion model. Regardless of the AAA model used, these murine models are considered to be acute models that cannot completely capture the chronic inflammatory disease process occurring in human AAAs.

By using the $CaCl_2$ aneurysm model on two different strains of mice, C57Bl/6 and 129/SvEv, the dissimilarities seen in aortic growth, MMP production, and inflammatory cell infiltration can mimic the heterogeneity seen between patients with AAAs. These important findings show that baseline and activated MMP differences seen between the 129/SvEv and C57Bl/6 mice have a vital role in the aortic growth rate. These data can help to explain why one patient's aneurysm may grow at a faster rate than another's. Aortic diameter can provide important information as to how susceptible the patient may be to aortic rupture. Being able to produce larger aneurysms in the 129/SvEv mouse could help to recreate the characteristics observed in tissue taken from large human AAAs obtained at the time of surgery. These larger aneurysms could also recapitulate the pathological processes occurring in human patients at the time of aneurysm rupture since a large aneurysm diameter is predictive of the susceptibility to rupture.

Specific genetic linkages are known for thoracic aortic aneurysms, such the fibrillin-1 mutation in MFS or the TGF-β receptor 1 mutation in Loeys-Dietz syndrome. Heredity influences AAA susceptibility, however, a specific genetic linkage for the susceptibility to AAA formation has not yet been discovered. Moreover, it is not yet known why male siblings of known patients have a greater risk of developing AAAs. [197] Recent studies have identified mutations in kallikrein 1, a serine protease, or MMP-3 as genetic loci associated with AAA formation. [198,199] The increased levels of Pro-MMP-2 at baseline and six weeks after aneurysm induction in mice indicate that these proteases are vital to the growth rate of aneurysm formation. The differences seen in aneurysm size between the 129/SvEv and C57Bl/6 mice may not simply be due to a mutation in MMP-2, as implied by the kallikrein 1 and MMP-3 mutations identified in human AAA, but also due to the pathways involved in MMP-2 activation. Since the activated levels of MMP-2 in 129/SvEv mice were no different from C57Bl/6 mice prior to aneurysm induction but significantly increased six weeks after application of $CaCl_2$, these data

imply a difference in the activation pathway associated with MMP-2. Previous studies demonstrate that membrane-type 1 MMP cleaves Pro-MMP-2 to active MMP-2 and that membrane- type 1 MMP levels were elevated in human AAA tissue.[200] Mice deficient in membrane-type 1 MMP were unable to form aneurysms.[135] The results presented herein indicate that future directions should be focused not just on inactivation of MMPs, but also on pathways leading to MMP activation.

Knowledge of pathways and proteases associated with ECM degradation is critical to understand the destruction process associated with AAA formation. Investigation of the reparative process is equally as important in developing therapeutic targets. Stopping the aortic wall degradation process is important in preventing aneurysms from growing large enough to rupture, but this does not fix the damaged structural integrity of the aortic wall. Focus should also be directed to promoting pathways associated with aortic repair, where restoration of a healthy aortic diameter is the objective. The differences in tropoelastin observed between C57Bl/6 mice and 129/SvEv mice demonstrate unequal reparative processes. C57Bl/6 mice express higher levels of tropoelastin, which may answer why these mice develop smaller aneurysms and exhibit reduced elastin degradation compared to 129/SvEv mice that underwent the same treatment. While baseline levels of tropoelastin indicate no difference in protein expression between C57Bl/6 and 129/SvEv mice, increased levels of tropoelastin are seen in the C57Bl/6 mice six weeks after aneurysm induction. These data demonstrate that pathways associated with ECM deposition, specifically elastin deposition, are increased. Human AAA tissue expresses lower levels of tropoelastin than human tissue from an atheromatous plaque, indicating that an inability to properly repair the damaged aorta may be leading to outward remodeling and aneurysm formation.[201]

The genetic differences seen between these two strains of mice imply that the reason why some patients develop AAA while others develop atherosclerotic plaques

may not only be due to differences in proteolytic process but also due to differences in reparative processes. Therapeutic targets enhancing proper tissue repair is vital to correcting the abnormal aortic dilation. This process will undoubtedly be quite difficult considering the formation of mature elastin is complex. Many proteins, such as fibrillin-1, fibronectin, and lysyl oxidase are involved in the proper formation of mature elastin while specific timing associated with their expression is critical. [202] Recreating the complex temporal, spatial, and structural interactions for proper elastin fiber assembly will be challenging. If all of the proteins are not deposited in the proper quantities and proper order, the repaired aorta will likely be prone to aneurysm formation as evidenced in MFS where fibrillin-1 deficiency results in ascending aortic aneurysm formation. Producing enough elastin to combat the proteolytic process produced by MMPs is essential, but producing too much elastin may create complications as evidenced by the release of EDPs.

Elastin is the major ECM protein responsible for maintaining an artery's elastic properties. These mechanical properties are important for small to medium sized arteries ability to maintain blood pressure. Elastin in larger arteries, such as the aorta, has a role in load bearing in relation to tension in the aortic wall. [203] As seen in the data presented herein, breakdown of elastin in these larger arteries results in release of EDPs, which promote pro-inflammatory M1 macrophage polarization. Serum from patients with AAAs has higher levels of EDPs when compared to serum from patients with other vascular diseases such as atherosclerosis. The initial damage to the aortic wall likely results in release of EDPs into the blood stream, creating a pro-inflammatory environment and enhancing the chronic inflammation associated with AAAs. Whether AAA is caused by genetics, patient lifestyle, or some traumatic event, release of these EDPs most certainly exacerbates disease progression. Targeting these free floating or exposed elastin fragments could prove to be a useful therapeutic target in slowing the rate of aneurysmal

growth or even stimulating aneurysm regression. Stopping these EDPs from creating a pro-inflammatory environment or directly altering the ratio of pro-inflammatory M1 cells to anti-inflammatory M2 cells are exciting new prospects in understanding the disease process. The data presented demonstrates that blocking EDPs could be a therapeutic target. Not only does neutralization of EDPs with BA4 reduce MMP activity, but it also limits the recruitment of macrophages to the aortic wall. Of those macrophages that were able to infiltrate the mouse aortic wall, a higher number of alternatively activated M2 cells were present in BA4-treated mice than classically activated M1 cells. The pro-inflammatory environment commonly found in the aortic wall of this animal model had switched to an anti-inflammatory environment by neutralization of EDPs, potentially promoting tissue repair. Further investigation into how neutralization of EDPs affects already established mouse aneurysms is needed. This scenario would better recapitulate the stage of the disease typically found in patients diagnosed with AAAs. Determining what effect EDP neutralization has on other cell types in the aortic wall is also important, since the phenotype of T cells or SMCs have also been found to play a role in AAA formation and repair.

While AAAs have a complex and multifactorial disease process, studies have been able to identify common inflammatory cells found in the aneurysmal wall. $CD4^+$ T cells can exist in many different phenotypes ranging from the pro-inflammatory Th1 or Th17 cells to the anti-inflammatory Th2 or T_{reg} cells. Serum samples from patients with AAA have demonstrated a deficiency in the anti-inflammatory T_{reg} population when compared to age- and sex-matched controls.[76] Furthermore, animal studies have demonstrated that the deletion or expansion of T_{reg} cells can have harmful or beneficial effects on aneurysm formation, respectively. [204,205] The same could be true for macrophages. Whether there is a deficiency in anti-inflammatory M2 macrophages circulating in serum from AAA patients or in AAA tissue compared to disease-matched

patients has yet to be determined. Conflicting data exists concerning the phenotype of macrophages found in human AAA tissue. By using the $CaCl_2$ AAA model, we demonstrated that macrophages are pro-inflammatory after the initial insult, and then may progress to a more anti-inflammatory phenotype over time. The proportion of M1/M2 cells is vital at various time points along the course of the disease progression. By directly altering that M1/M2 phenotype ratio through tail vein injection of M1 or M2 cells, we were able to change the course of the disease. This M1/M2 balance is likely very delicate. Further studies are needed to elucidate the direct mechanism of how injection of M2 cells was able to minimize aortic dilation. Furthermore, manipulation of the M1/M2 phenotypes in established aneurysms needs to be investigated to properly capture the AAA clinical scenario. Whether the goal should be to enhance the M2 phenotype or decrease the M1 phenotype has yet to be determined. Taken together, targeting the M1/M2 ratio by either direct injection of M2 macrophages or pharmacological manipulation of the M1/M2 ratio may provide an important therapeutic target.

AAA is a genetic, inflammatory, and life-threatening disease. As of yet, only surgical intervention and smoking cessation have been shown to be effective treatment strategies. No medical therapy currently exists. Until we are able to understand more about factors that exacerbate aneurysmal growth or the genetic predisposition of some patients developing AAA, mechanical intervention is the only solution. One of the difficulties is obtaining human AAA tissue. This difficulty is increasing due to the less invasive surgical techniques employed today. Finding tissue that is not toward the end stage of the disease and close to aneurysmal rupture is rare. Therefore, we must turn to animal models of disease. Animal models do well at recapitulating many of the features associated with human AAAs, but in the end they are just models, and each have their

pitfalls. However, the data obtained from animal models is necessary and can provide much needed insight into many of the pathways and processes associated with AAAs.

In summary, genetic differences observed between C57Bl/6 and 129/SvEv indicate that baseline and activated levels of MMP-2 are vital to aneurysm formation and explain the differences in aneurysm susceptibility between the two models. With the decreased tropoelastin production and increased elastase activity seen in the 129/SvEv mice after aneurysm induction, there is high probability that pathways associated with elastin breakdown and formation are significant in the pathogenesis of AAAs. Elastin breakdown releases pro-inflammatory EDPs which polarize macrophages to an M1 phenotype. Neutralization of these EDPs *in vivo* with BA4 minimized aortic dilation by reducing MMP-2 and MMP-9 activity, reducing macrophage infiltration, and altering the pro-inflammatory environment created by M1 macrophages. The effect of these M1 macrophages can be altered by directly injecting anti-inflammatory M2 cells, thereby decreasing the M1/M2 ratio and promoting tissue repair rather than creating chronic inflammation. These insights can help identify genetic linkages in AAA and lead to prospective new strategies for medical therapy.

BIBLIOGRAPHY

1. Thom T, Haase N, Rosamond W, et al. Heart disease and stroke statistics--2006 update: a report from the American Heart Association Statistics Committee and Stroke Statistics Subcommittee. Circulation. 2006;113:e85-151.

2. LeFevre ML, U.S. Preventive Services Task Force. Screening for abdominal aortic aneurysm: u.s. Preventive services task force recommendation statement. Ann Intern Med. 2014;161:281-290.

3. Pande RL, Beckman JA. Abdominal aortic aneurysm: populations at risk and how to screen. J Vasc Interv Radiol. 2008;19:S2-8.

4. Lederle FA, Johnson GR, Wilson SE, Gordon IL, Chute EP, Littooy FN, Krupski WC, Bandyk D, Barone GW, Graham LM, Hye RJ, Reinke DB. Relationship of age, gender, race, and body size to infrarenal aortic diameter. The Aneurysm Detection and Management (ADAM) Veterans Affairs Cooperative Study Investigators. J Vasc Surg. 1997;26:595-601.

5. Powell JT, Greenhalgh RM. Clinical practice. Small abdominal aortic aneurysms. N Engl J Med. 2003;348:1895-1901.

6. Lederle FA, Johnson GR, Wilson SE, Chute EP, Littooy FN, Bandyk D, Krupski WC, Barone GW, Acher CW, Ballard DJ. Prevalence and associations of abdominal aortic aneurysm detected through screening. Aneurysm Detection and Management (ADAM) Veterans Affairs Cooperative Study Group. Ann Intern Med. 1997;126:441-449.

7. Lederle FA, Johnson GR, Wilson SE, Chute EP, Hye RJ, Makaroun MS, Barone GW, Bandyk D, Moneta GL, Makhoul RG. The aneurysm detection and management study

screening program: validation cohort and final results. Aneurysm Detection and Management Veterans Affairs Cooperative Study Investigators. Arch Intern Med. 2000;160:1425-1430.

8. Salem MK, Rayt HS, Hussey G, Rafelt S, Nelson CP, Sayers RD, Naylor AR, Nasim A. Should Asian men be included in abdominal aortic aneurysm screening programmes? Eur J Vasc Endovasc Surg. 2009;38:748-749.

9. Blanchard JF, Armenian HK, Friesen PP. Risk factors for abdominal aortic aneurysm: results of a case-control study. Am J Epidemiol. 2000;151:575-583.

10. Steinmetz EF, Buckley C, Shames ML, Ennis TL, Vanvickle-Chavez SJ, Mao D, Goeddel LA, Hawkins CJ, Thompson RW. Treatment with simvastatin suppresses the development of experimental abdominal aortic aneurysms in normal and hypercholesterolemic mice. Ann Surg. 2005;241:92-101.

11. Nagashima H, Aoka Y, Sakomura Y, Sakuta A, Aomi S, Ishizuka N, Hagiwara N, Kawana M, Kasanuki H. A 3-hydroxy-3-methylglutaryl coenzyme A reductase inhibitor, cerivastatin, suppresses production of matrix metalloproteinase-9 in human abdominal aortic aneurysm wall. J Vasc Surg. 2002;36:158-163.

12. Boucek RJ, Gunja-Smith Z, Noble NL, Simpson CF. Modulation by propranolol of the lysyl cross-links in aortic elastin and collagen of the aneurysm-prone turkey. Biochem Pharmacol. 1983;32:275-280.

13. Brophy CM, Tilson JE, Tilson MD. Propranolol stimulates the crosslinking of matrix components in skin from the aneurysm-prone blotchy mouse. J Surg Res. 1989;46:330-332.

14. Yamamoto D, Takai S, Jin D, Inagaki S, Tanaka K, Miyazaki M. Molecular mechanism of imidapril for cardiovascular protection via inhibition of MMP-9. J Mol Cell Cardiol. 2007;43:670-676.

15. Rizzoni D, Rodella L, Porteri E, Rezzani R, Sleiman I, Paiardi S, Guelfi D, De Ciuceis C, Boari GE, Bianchi R, Agabiti-Rosei E. Effects of losartan and enalapril at different doses on cardiac and renal interstitial matrix in spontaneously hypertensive rats. Clin Exp Hypertens. 2003;25:427-441.

16. Petrinec D, Liao S, Holmes DR, Reilly JM, Parks WC, Thompson RW. Doxycycline inhibition of aneurysmal degeneration in an elastase-induced rat model of abdominal aortic aneurysm: preservation of aortic elastin associated with suppressed production of 92 kD gelatinase. J Vasc Surg. 1996;23:336-346.

17. Prall AK, Longo GM, Mayhan WG, Waltke EA, Fleckten B, Thompson RW, Baxter BT. Doxycycline in patients with abdominal aortic aneurysms and in mice: comparison of serum levels and effect on aneurysm growth in mice. J Vasc Surg. 2002;35:923-929.

18. Shimizu K, Mitchell RN, Libby P. Inflammation and cellular immune responses in abdominal aortic aneurysms. Arterioscler Thromb Vasc Biol. 2006;26:987-994.

19. Carson JS, Xiong W, Dale M, Yu F, Duryee MJ, Anderson DR, Thiele GM, Baxter BT. Antibodies against malondialdehyde-acetaldehyde adducts can help identify patients with abdominal aortic aneurysm. J Vasc Surg. 2015;.

20. Duftner C, Seiler R, Dejaco C, Chemelli-Steingruber I, Schennach H, Klotz W, Rieger M, Herold M, Falkensammer J, Fraedrich G, Schirmer M. Antiphospholipid

antibodies predict progression of abdominal aortic aneurysms. PLoS One. 2014;9:e99302.

21. Michineau S, Franck G, Wagner-Ballon O, Dai J, Allaire E, Gervais M. Chemokine (C-X-C motif) receptor 4 blockade by AMD3100 inhibits experimental abdominal aortic aneurysm expansion through anti-inflammatory effects. Arterioscler Thromb Vasc Biol. 2014;34:1747-1755.

22. Qin Y, Cao X, Guo J, Zhang Y, Pan L, Zhang H, Li H, Tang C, Du J, Shi GP. Deficiency of cathepsin S attenuates angiotensin II-induced abdominal aortic aneurysm formation in apolipoprotein E-deficient mice. Cardiovasc Res. 2012;96:401-410.

23. Xiong W, Zhao Y, Prall A, Greiner TC, Baxter BT. Key roles of CD4+ T cells and IFN-gamma in the development of abdominal aortic aneurysms in a murine model. J Immunol. 2004;172:2607-2612.

24. Xiong W, MacTaggart J, Knispel R, Worth J, Persidsky Y, Baxter BT. Blocking TNF-alpha attenuates aneurysm formation in a murine model. J Immunol. 2009;183:2741-2746.

25. Longo GM, Xiong W, Greiner TC, Zhao Y, Fiotti N, Baxter BT. Matrix metalloproteinases 2 and 9 work in concert to produce aortic aneurysms. J Clin Invest. 2002;110:625-632.

26. Pyo R, Lee JK, Shipley JM, Curci JA, Mao D, Ziporin SJ, Ennis TL, Shapiro SD, Senior RM, Thompson RW. Targeted gene disruption of matrix metalloproteinase-9 (gelatinase B) suppresses development of experimental abdominal aortic aneurysms. J Clin Invest. 2000;105:1641-1649.

27. Travis J. . Origins. On the origin of the immune system. Science. 2009;324:580-582.

28. Curci JA, Liao S, Huffman MD, Shapiro SD, Thompson RW. Expression and localization of macrophage elastase (matrix metalloproteinase-12) in abdominal aortic aneurysms. J Clin Invest. 1998;102:1900-1910.

29. Galle C, Schandene L, Stordeur P, Peignois Y, Ferreira J, Wautrecht JC, Dereume JP, Goldman M. Predominance of type 1 CD4+ T cells in human abdominal aortic aneurysm. Clin Exp Immunol. 2005;142:519-527.

30. Koch AE, Haines GK, Rizzo RJ, Radosevich JA, Pope RM, Robinson PG, Pearce WH. Human abdominal aortic aneurysms. Immunophenotypic analysis suggesting an immune-mediated response. Am J Pathol. 1990;137:1199-1213.

31. Tsuruda T, Kato J, Hatakeyama K, Kojima K, Yano M, Yano Y, Nakamura K, Nakamura-Uchiyama F, Matsushima Y, Imamura T, Onitsuka T, Asada Y, Nawa Y, Eto T, Kitamura K. Adventitial mast cells contribute to pathogenesis in the progression of abdominal aortic aneurysm. Circ Res. 2008;102:1368-1377.

32. Ocana E, Bohorquez JC, Perez-Requena J, Brieva JA, Rodriguez C. Characterisation of T and B lymphocytes infiltrating abdominal aortic aneurysms. Atherosclerosis. 2003;170:39-48.

33. Forester ND, Cruickshank SM, Scott DJ, Carding SR. Increased natural killer cell activity in patients with an abdominal aortic aneurysm. Br J Surg. 2006;93:46-54.

34. Xiong W, Zhao Y, Prall A, Greiner TC, Baxter BT. Key roles of CD4+ T cells and IFN-gamma in the development of abdominal aortic aneurysms in a murine model. J Immunol. 2004;172:2607-2612.

35. Sharma AK, Lu G, Jester A, Johnston WF, Zhao Y, Hajzus VA, Saadatzadeh MR, Su G, Bhamidipati CM, Mehta GS, Kron IL, Laubach VE, Murphy MP, Ailawadi G, Upchurch GR,Jr. Experimental abdominal aortic aneurysm formation is mediated by IL-17 and attenuated by mesenchymal stem cell treatment. Circulation. 2012;126:S38-45.

36. Juvonen J, Surcel HM, Satta J, Teppo AM, Bloigu A, Syrjala H, Airaksinen J, Leinonen M, Saikku P, Juvonen T. Elevated circulating levels of inflammatory cytokines in patients with abdominal aortic aneurysm. Arterioscler Thromb Vasc Biol. 1997;17:2843-2847.

37. Karlsson L, Bergqvist D, Lindback J, Parsson H. Expansion of small-diameter abdominal aortic aneurysms is not reflected by the release of inflammatory mediators IL-6, MMP-9 and CRP in plasma. Eur J Vasc Endovasc Surg. 2009;37:420-424.

38. Koch AE, Kunkel SL, Pearce WH, Shah MR, Parikh D, Evanoff HL, Haines GK, Burdick MD, Strieter RM. Enhanced production of the chemotactic cytokines interleukin-8 and monocyte chemoattractant protein-1 in human abdominal aortic aneurysms. Am J Pathol. 1993;142:1423-1431.

39. Szekanecz Z, Shah MR, Harlow LA, Pearce WH, Koch AE. Interleukin-8 and tumor necrosis factor-alpha are involved in human aortic endothelial cell migration. The possible role of these cytokines in human aortic aneurysmal blood vessel growth. Pathobiology. 1994;62:134-139.

40. Satoh H, Nakamura M, Satoh M, Nakajima T, Izumoto H, Maesawa C, Kawazoe K, Masuda T, Hiramori K. Expression and localization of tumour necrosis factor-alpha and its converting enzyme in human abdominal aortic aneurysm. Clin Sci (Lond). 2004;106:301-306.

41. Galkina E, Ley K. Immune and inflammatory mechanisms of atherosclerosis (*). Annu Rev Immunol. 2009;27:165-197.

42. Glagov S, Weisenberg E, Zarins CK, Stankunavicius R, Kolettis GJ. Compensatory enlargement of human atherosclerotic coronary arteries. N Engl J Med. 1987;316:1371-1375.

43. Alexander MR, Moehle CW, Johnson JL, Yang Z, Lee JK, Jackson CL, Owens GK. Genetic inactivation of IL-1 signaling enhances atherosclerotic plaque instability and reduces outward vessel remodeling in advanced atherosclerosis in mice. J Clin Invest. 2012;122:70-79.

44. Galis ZS, Sukhova GK, Lark MW, Libby P. Increased expression of matrix metalloproteinases and matrix degrading activity in vulnerable regions of human atherosclerotic plaques. J Clin Invest. 1994;94:2493-2503.

45. Galis ZS, Muszynski M, Sukhova GK, Simon-Morrissey E, Unemori EN, Lark MW, Amento E, Libby P. Cytokine-stimulated human vascular smooth muscle cells synthesize a complement of enzymes required for extracellular matrix digestion. Circ Res. 1994;75:181-189.

46. Ward MR, Pasterkamp G, Yeung AC, Borst C. Arterial remodeling. Mechanisms and clinical implications. Circulation. 2000;102:1186-1191.

47. Basta G, Schmidt AM, De Caterina R. Advanced glycation end products and vascular inflammation: implications for accelerated atherosclerosis in diabetes. Cardiovasc Res. 2004;63:582-592.

48. Vlassara H, Brownlee M, Cerami A. Specific macrophage receptor activity for advanced glycosylation end products inversely correlates with insulin levels in vivo. Diabetes. 1988;37:456-461.

49. Kirstein M, Brett J, Radoff S, Ogawa S, Stern D, Vlassara H. Advanced protein glycosylation induces transendothelial human monocyte chemotaxis and secretion of platelet-derived growth factor: role in vascular disease of diabetes and aging. Proc Natl Acad Sci U S A. 1990;87:9010-9014.

50. Kirstein M, Aston C, Hintz R, Vlassara H. Receptor-specific induction of insulin-like growth factor I in human monocytes by advanced glycosylation end product-modified proteins. J Clin Invest. 1992;90:439-446.

51. Pleumeekers HJ, Hoes AW, van der Does E, van Urk H, Hofman A, de Jong PT, Grobbee DE. Aneurysms of the abdominal aorta in older adults. The Rotterdam Study. Am J Epidemiol. 1995;142:1291-1299.

52. Golledge J, Karan M, Moran CS, Muller J, Clancy P, Dear AE, Norman PE. Reduced expansion rate of abdominal aortic aneurysms in patients with diabetes may be related to aberrant monocyte-matrix interactions. Eur Heart J. 2008;29:665-672.

53. Wijdeven RH, Bakker JM, Paul P, Neefjes J. Exploring genome-wide datasets of MHC class II antigen presentation. Mol Immunol. 2013;55:172-174.

54. Abbas AK, Murphy KM, Sher A. Functional diversity of helper T lymphocytes. Nature. 1996;383:787-793.

55. Zhu J, Paul WE. CD4 T cells: fates, functions, and faults. Blood. 2008;112:1557-1569.

56. Berner B, Akca D, Jung T, Muller GA, Reuss-Borst MA. Analysis of Th1 and Th2 cytokines expressing CD4+ and CD8+ T cells in rheumatoid arthritis by flow cytometry. J Rheumatol. 2000;27:1128-1135.

57. Lee SH, Goswami S, Grudo A, Song LZ, Bandi V, Goodnight-White S, Green L, Hacken-Bitar J, Huh J, Bakaeen F, Coxson HO, Cogswell S, Storness-Bliss C, Corry DB, Kheradmand F. Antielastin autoimmunity in tobacco smoking-induced emphysema. Nat Med. 2007;13:567-569.

58. Blair PA, Chavez-Rueda KA, Evans JG, Shlomchik MJ, Eddaoudi A, Isenberg DA, Ehrenstein MR, Mauri C. Selective targeting of B cells with agonistic anti-CD40 is an efficacious strategy for the generation of induced regulatory T2-like B cells and for the suppression of lupus in MRL/lpr mice. J Immunol. 2009;182:3492-3502.

59. Harrington LE, Hatton RD, Mangan PR, Turner H, Murphy TL, Murphy KM, Weaver CT. Interleukin 17-producing CD4+ effector T cells develop via a lineage distinct from the T helper type 1 and 2 lineages. Nat Immunol. 2005;6:1123-1132.

60. Schonbeck U, Sukhova GK, Gerdes N, Libby P. T(H)2 predominant immune responses prevail in human abdominal aortic aneurysm. Am J Pathol. 2002;161:499-506.

61. Shimizu K, Shichiri M, Libby P, Lee RT, Mitchell RN. Th2-predominant inflammation and blockade of IFN-gamma signaling induce aneurysms in allografted aortas. J Clin Invest. 2004;114:300-308.

62. Chan WL, Pejnovic N, Liew TV, Hamilton H. Predominance of Th2 response in human abdominal aortic aneurysm: mistaken identity for IL-4-producing NK and NKT cells? Cell Immunol. 2005;233:109-114.

63. Wan YY, Flavell RA. How diverse--CD4 effector T cells and their functions. J Mol Cell Biol. 2009;1:20-36.

64. Liao M, Xu J, Clair AJ, Ehrman B, Graham LM, Eagleton MJ. Local and systemic alterations in signal transducers and activators of transcription (STAT) associated with human abdominal aortic aneurysms. J Surg Res. 2012;176:321-328.

65. Uchida HA, Kristo F, Rateri DL, Lu H, Charnigo R, Cassis LA, Daugherty A. Total lymphocyte deficiency attenuates AngII-induced atherosclerosis in males but not abdominal aortic aneurysms in apoE deficient mice. Atherosclerosis. 2010;211:399-403.

66. King VL, Lin AY, Kristo F, Anderson TJ, Ahluwalia N, Hardy GJ, Owens AP,3rd, Howatt DA, Shen D, Tager AM, Luster AD, Daugherty A, Gerszten RE. Interferon-gamma and the interferon-inducible chemokine CXCL10 protect against aneurysm formation and rupture. Circulation. 2009;119:426-435.

67. Eagleton MJ, Xu J, Liao M, Parine B, Chisolm GM, Graham LM. Loss of STAT1 is associated with increased aortic rupture in an experimental model of aortic dissection and aneurysm formation. J Vasc Surg. 2010;51:951-61; discussion 961.

68. Xu J, Ehrman B, Graham LM, Eagleton MJ. Interleukin-5 is a potential mediator of angiotensin II-induced aneurysm formation in apolipoprotein E knockout mice. J Surg Res. 2012;178:512-518.

69. Postlethwaite AE, Holness MA, Katai H, Raghow R. Human fibroblasts synthesize elevated levels of extracellular matrix proteins in response to interleukin 4. J Clin Invest. 1992;90:1479-1485.

70. Lacraz S, Nicod L, Galve-de Rochemonteix B, Baumberger C, Dayer JM, Welgus HG. Suppression of metalloproteinase biosynthesis in human alveolar macrophages by interleukin-4. J Clin Invest. 1992;90:382-388.

71. Wei Z, Wang Y, Zhang K, Liao Y, Ye P, Wu J, Wang Y, Li F, Yao Y, Zhou Y, Liu J. Inhibiting the Th17/IL-17A-Related Inflammatory Responses With Digoxin Confers Protection Against Experimental Abdominal Aortic Aneurysm. Arterioscler Thromb Vasc Biol. 2014;34:2429-2438.

72. Madhur MS, Funt SA, Li L, Vinh A, Chen W, Lob HE, Iwakura Y, Blinder Y, Rahman A, Quyyumi AA, Harrison DG. Role of interleukin 17 in inflammation, atherosclerosis, and vascular function in apolipoprotein e-deficient mice. Arterioscler Thromb Vasc Biol. 2011;31:1565-1572.

73. Shafiani S, Tucker-Heard G, Kariyone A, Takatsu K, Urdahl KB. Pathogen-specific regulatory T cells delay the arrival of effector T cells in the lung during early tuberculosis. J Exp Med. 2010;207:1409-1420.

74. Ehrenstein MR, Evans JG, Singh A, Moore S, Warnes G, Isenberg DA, Mauri C. Compromised function of regulatory T cells in rheumatoid arthritis and reversal by anti-TNFalpha therapy. J Exp Med. 2004;200:277-285.

75. Yin M, Zhang J, Wang Y, Wang S, Bockler D, Duan Z, Xin S. Deficient CD4+CD25+ T regulatory cell function in patients with abdominal aortic aneurysms. Arterioscler Thromb Vasc Biol. 2010;30:1825-1831.

76. Zhou Y, Wu W, Lindholt JS, Sukhova GK, Libby P, Yu X, Shi GP. Regulatory T cells in human and angiotensin II-induced mouse abdominal aortic aneurysms. Cardiovasc Res. 2015;.

77. Smyth LJ, Starkey C, Vestbo J, Singh D. CD4-regulatory cells in COPD patients. Chest. 2007;132:156-163.

78. Uhlig HH, Coombes J, Mottet C, Izcue A, Thompson C, Fanger A, Tannapfel A, Fontenot JD, Ramsdell F, Powrie F. Characterization of Foxp3+CD4+CD25+ and IL-10-secreting CD4+CD25+ T cells during cure of colitis. J Immunol. 2006;177:5852-5860.

79. Boschetti G, Nancey S, Sardi F, Roblin X, Flourie B, Kaiserlian D. Therapy with anti-TNFalpha antibody enhances number and function of Foxp3(+) regulatory T cells in inflammatory bowel diseases. Inflamm Bowel Dis. 2011;17:160-170.

80. Venigalla RK, Tretter T, Krienke S, Max R, Eckstein V, Blank N, Fiehn C, Ho AD, Lorenz HM. Reduced CD4+,CD25- T cell sensitivity to the suppressive function of CD4+,CD25high,CD127 -/low regulatory T cells in patients with active systemic lupus erythematosus. Arthritis Rheum. 2008;58:2120-2130.

81. Wan S, Xia C, Morel L. IL-6 produced by dendritic cells from lupus-prone mice inhibits CD4+CD25+ T cell regulatory functions. J Immunol. 2007;178:271-279.

82. Keystone EC, Lau C, Gladman DD, Wilkinson S, Lee P, Shore A. Immunoregulatory T cell subpopulations in patients with scleroderma using monoclonal antibodies. Clin Exp Immunol. 1982;48:443-448.

83. Deleuran B, Abraham DJ. Possible implication of the effector CD4+ T-cell subpopulation TH17 in the pathogenesis of systemic scleroderma. Nat Clin Pract Rheumatol. 2007;3:682-683.

84. Kisielewicz A, Schaier M, Schmitt E, Hug F, Haensch GM, Meuer S, Zeier M, Sohn C, Steinborn A. A distinct subset of HLA-DR+-regulatory T cells is involved in the induction of preterm labor during pregnancy and in the induction of organ rejection after transplantation. Clin Immunol. 2010;137:209-220.

85. Sumpter TL, Wilkes DS. Role of autoimmunity in organ allograft rejection: a focus on immunity to type V collagen in the pathogenesis of lung transplant rejection. Am J Physiol Lung Cell Mol Physiol. 2004;286:L1129-39.

86. Martinez FO, Sica A, Mantovani A, Locati M. Macrophage activation and polarization. Front Biosci. 2008;13:453-461.

87. Sica A, Larghi P, Mancino A, Rubino L, Porta C, Totaro MG, Rimoldi M, Biswas SK, Allavena P, Mantovani A. Macrophage polarization in tumour progression. Semin Cancer Biol. 2008;18:349-355.

88. Nathan C. . Mechanisms and modulation of macrophage activation. Behring Inst Mitt. 1991;(88):200-207.

89. Chow JC, Young DW, Golenbock DT, Christ WJ, Gusovsky F. Toll-like receptor-4 mediates lipopolysaccharide-induced signal transduction. J Biol Chem. 1999;274:10689-10692.

90. Samadzadeh KM, Chun KC, Nguyen AT, Baker PM, Bains S, Lee ES. Monocyte activity is linked with abdominal aortic aneurysm diameter. J Surg Res. 2014;190:328-334.

91. Hance KA, Tataria M, Ziporin SJ, Lee JK, Thompson RW. Monocyte chemotactic activity in human abdominal aortic aneurysms: role of elastin degradation peptides and the 67-kD cell surface elastin receptor. J Vasc Surg. 2002;35:254-261.

92. Houghton AM, Quintero PA, Perkins DL, Kobayashi DK, Kelley DG, Marconcini LA, Mecham RP, Senior RM, Shapiro SD. Elastin fragments drive disease progression in a murine model of emphysema. J Clin Invest. 2006;116:753-759.

93. Guo G, Booms P, Halushka M, Dietz HC, Ney A, Stricker S, Hecht J, Mundlos S, Robinson PN. Induction of macrophage chemotaxis by aortic extracts of the mgR Marfan mouse model and a GxxPG-containing fibrillin-1 fragment. Circulation. 2006;114:1855-1862.

94. Guo G, Munoz-Garcia B, Ott CE, Grunhagen J, Mousa SA, Pletschacher A, von Kodolitsch Y, Knaus P, Robinson PN. Antagonism of GxxPG fragments ameliorates manifestations of aortic disease in Marfan syndrome mice. Hum Mol Genet. 2012;.

95. Kitchens RL. . Role of CD14 in cellular recognition of bacterial lipopolysaccharides. Chem Immunol. 2000;74:61-82.

96. Ghigliotti G, Barisione C, Garibaldi S, Brunelli C, Palmieri D, Spinella G, Pane B, Spallarossa P, Altieri P, Fabbi P, Sambuceti G, Palombo D. CD16(+) monocyte subsets are increased in large abdominal aortic aneurysms and are differentially related with

circulating and cell-associated biochemical and inflammatory biomarkers. Dis Markers. 2013;34:131-142.

97. Aguilar-Ruiz SR, Torres-Aguilar H, Gonzalez-Dominguez E, Narvaez J, Gonzalez-Perez G, Vargas-Ayala G, Meraz-Rios MA, Garcia-Zepeda EA, Sanchez-Torres C. Human CD16+ and CD16- monocyte subsets display unique effector properties in inflammatory conditions in vivo. J Leukoc Biol. 2011;90:1119-1131.

98. Blomkalns AL, Gavrila D, Thomas M, et al. CD14 directs adventitial macrophage precursor recruitment: role in early abdominal aortic aneurysm formation. J Am Heart Assoc. 2013;2:e000065.

99. Xiong W, MacTaggart J, Knispel R, Worth J, Persidsky Y, Baxter BT. Blocking TNF-alpha attenuates aneurysm formation in a murine model. J Immunol. 2009;183:2741-2746.

100. Johnston WF, Salmon M, Pope NH, Meher A, Su G, Stone ML, Lu G, Owens GK, Upchurch GR,Jr, Ailawadi G. Inhibition of interleukin-1beta decreases aneurysm formation and progression in a novel model of thoracic aortic aneurysms. Circulation. 2014;130:S51-9.

101. Tieu BC, Lee C, Sun H, Lejeune W, Recinos A,3rd, Ju X, Spratt H, Guo DC, Milewicz D, Tilton RG, Brasier AR. An adventitial IL-6/MCP1 amplification loop accelerates macrophage-mediated vascular inflammation leading to aortic dissection in mice. J Clin Invest. 2009;119:3637-3651.

102. A Randomized, Double-blind, Placebo-controlled, Multiple Dose Study of Subcutaneous ACZ885 for the Treatment of Abdominal Aortic Aneurysm.

103. Takeda K, Tanaka T, Shi W, Matsumoto M, Minami M, Kashiwamura S, Nakanishi K, Yoshida N, Kishimoto T, Akira S. Essential role of Stat6 in IL-4 signalling. Nature. 1996;380:627-630.

104. Brunn A, Mihelcic M, Carstov M, Hummel L, Geier F, Schmidt A, Saupe L, Utermohlen O, Deckert M. IL-10, IL-4, and STAT6 promote an M2 milieu required for termination of P0(106-125)-induced murine experimental autoimmune neuritis. Am J Pathol. 2014;184:2627-2640.

105. Galdiero MR, Garlanda C, Jaillon S, Marone G, Mantovani A. Tumor associated macrophages and neutrophils in tumor progression. J Cell Physiol. 2013;228:1404-1412.

106. Gazi U, Martinez-Pomares L. Influence of the mannose receptor in host immune responses. Immunobiology. 2009;214:554-561.

107. Boytard L, Spear R, Chinetti-Gbaguidi G, Acosta-Martin AE, Vanhoutte J, Lamblin N, Staels B, Amouyel P, Haulon S, Pinet F. Role of proinflammatory CD68(+) mannose receptor(-) macrophages in peroxiredoxin-1 expression and in abdominal aortic aneurysms in humans. Arterioscler Thromb Vasc Biol. 2013;33:431-438.

108. Dutertre CA, Clement M, Morvan M, Schakel K, Castier Y, Alsac JM, Michel JB, Nicoletti A. Deciphering the stromal and hematopoietic cell network of the adventitia from non-aneurysmal and aneurysmal human aorta. PLoS One. 2014;9:e89983.

109. Rateri DL, Howatt DA, Moorleghen JJ, Charnigo R, Cassis LA, Daugherty A. Prolonged infusion of angiotensin II in apoE(-/-) mice promotes macrophage recruitment with continued expansion of abdominal aortic aneurysm. Am J Pathol. 2011;179:1542-1548.

110. Witko-Sarsat V, Rieu P, Descamps-Latscha B, Lesavre P, Halbwachs-Mecarelli L. Neutrophils: molecules, functions and pathophysiological aspects. Lab Invest. 2000;80:617-653.

111. Folkesson M, Kazi M, Zhu C, Silveira A, Hemdahl AL, Hamsten A, Hedin U, Swedenborg J, Eriksson P. Presence of NGAL/MMP-9 complexes in human abdominal aortic aneurysms. Thromb Haemost. 2007;98:427-433.

112. Houard X, Rouzet F, Touat Z, Philippe M, Dominguez M, Fontaine V, Sarda-Mantel L, Meulemans A, Le Guludec D, Meilhac O, Michel JB. Topology of the fibrinolytic system within the mural thrombus of human abdominal aortic aneurysms. J Pathol. 2007;212:20-28.

113. Houard X, Touat Z, Ollivier V, Louedec L, Philippe M, Sebbag U, Meilhac O, Rossignol P, Michel JB. Mediators of neutrophil recruitment in human abdominal aortic aneurysms. Cardiovasc Res. 2009;82:532-541.

114. Eliason JL, Hannawa KK, Ailawadi G, Sinha I, Ford JW, Deogracias MP, Roelofs KJ, Woodrum DT, Ennis TL, Henke PK, Stanley JC, Thompson RW, Upchurch GR,Jr. Neutrophil depletion inhibits experimental abdominal aortic aneurysm formation. Circulation. 2005;112:232-240.

115. Ramos-Mozo P, Madrigal-Matute J, Martinez-Pinna R, Blanco-Colio LM, Lopez JA, Camafeita E, Meilhac O, Michel JB, Aparicio C, Vega de Ceniga M, Egido J, Martin-Ventura JL. Proteomic analysis of polymorphonuclear neutrophils identifies catalase as a novel biomarker of abdominal aortic aneurysm: potential implication of oxidative stress in abdominal aortic aneurysm progression. Arterioscler Thromb Vasc Biol. 2011;31:3011-3019.

116. Gurish MF, Boyce JA. Mast cells: ontogeny, homing, and recruitment of a unique innate effector cell. J Allergy Clin Immunol. 2006;117:1285-1291.

117. Ihara M, Urata H, Kinoshita A, Suzumiya J, Sasaguri M, Kikuchi M, Ideishi M, Arakawa K. Increased chymase-dependent angiotensin II formation in human atherosclerotic aorta. Hypertension. 1999;33:1399-1405.

118. Mayranpaa MI, Trosien JA, Fontaine V, Folkesson M, Kazi M, Eriksson P, Swedenborg J, Hedin U. Mast cells associate with neovessels in the media and adventitia of abdominal aortic aneurysms. J Vasc Surg. 2009;50:388-95; discussion 395-6.

119. Sun J, Sukhova GK, Yang M, Wolters PJ, MacFarlane LA, Libby P, Sun C, Zhang Y, Liu J, Ennis TL, Knispel R, Xiong W, Thompson RW, Baxter BT, Shi GP. Mast cells modulate the pathogenesis of elastase-induced abdominal aortic aneurysms in mice. J Clin Invest. 2007;117:3359-3368.

120. Tchougounova E, Lundequist A, Fajardo I, Winberg JO, Abrink M, Pejler G. A key role for mast cell chymase in the activation of pro-matrix metalloprotease-9 and pro-matrix metalloprotease-2. J Biol Chem. 2005;280:9291-9296.

121. Furubayashi K, Takai S, Jin D, Miyazaki M, Katsumata T, Inagaki S, Kimura M, Tanaka K, Nishimoto M, Fukumoto H. Chymase activates promatrix metalloproteinase-9 in human abdominal aortic aneurysm. Clin Chim Acta. 2008;388:214-216.

122. Kozel BA, Knutsen RH, Ye L, Ciliberto CH, Broekelmann TJ, Mecham RP. Genetic modifiers of cardiovascular phenotype caused by elastin haploinsufficiency act by extrinsic noncomplementation. J Biol Chem. 2011;286:44926-44936.

123. Gauguier D, Behmoaras J, Argoud K, Wilder SP, Pradines C, Bihoreau MT, Osborne-Pellegrin M, Jacob MP. Chromosomal mapping of quantitative trait loci controlling elastin content in rat aorta. Hypertension. 2005;45:460-466.

124. Feng M, Deerhake ME, Keating R, Thaisz J, Xu L, Tsaih SW, Smith R, Ishige T, Sugiyama F, Churchill GA, DiPetrillo K. Genetic analysis of blood pressure in 8 mouse intercross populations. Hypertension. 2009;54:802-809.

125. Yuan Z, Pei H, Roberts DJ, Zhang Z, Rowlan JS, Matsumoto AH, Shi W. Quantitative trait locus analysis of neointimal formation in an intercross between C57BL/6 and C3H/HeJ apolipoprotein E-deficient mice. Circ Cardiovasc Genet. 2009;2:220-228.

126. Johansen K, Koepsell T. Familial tendency for abdominal aortic aneurysms. JAMA. 1986;256:1934-1936.

127. Kuivaniemi H, Ryer EJ, Elmore JR, Hinterseher I, Smelser DT, Tromp G. Update on abdominal aortic aneurysm research: from clinical to genetic studies. Scientifica (Cairo). 2014;2014:564734.

128. Liu S, Xie Z, Daugherty A, Cassis LA, Pearson KJ, Gong MC, Guo Z. Mineralocorticoid receptor agonists induce mouse aortic aneurysm formation and rupture in the presence of high salt. Arterioscler Thromb Vasc Biol. 2013;33:1568-1579.

129. Owens AP,3rd, Rateri DL, Howatt DA, Moore KJ, Tobias PS, Curtiss LK, Lu H, Cassis LA, Daugherty A. MyD88 deficiency attenuates angiotensin II-induced abdominal aortic aneurysm formation independent of signaling through Toll-like receptors 2 and 4. Arterioscler Thromb Vasc Biol. 2011;31:2813-2819.

130. Daugherty A, Manning MW, Cassis LA. Angiotensin II promotes atherosclerotic lesions and aneurysms in apolipoprotein E-deficient mice. J Clin Invest. 2000;105:1605-1612.

131. Daugherty A, Cassis LA. Mouse models of abdominal aortic aneurysms. Arterioscler Thromb Vasc Biol. 2004;24:429-434.

132. Lima BL, Santos EJ, Fernandes GR, Merkel C, Mello MR, Gomes JP, Soukoyan M, Kerkis A, Massironi SM, Visintin JA, Pereira LV. A new mouse model for marfan syndrome presents phenotypic variability associated with the genetic background and overall levels of Fbn1 expression. PLoS One. 2010;5:e14136.

133. Xiong W, Meisinger T, Knispel R, Worth JM, Baxter BT. MMP-2 regulates Erk1/2 phosphorylation and aortic dilatation in Marfan syndrome. Circ Res. 2012;110:e92-e101.

134. Xiong W, Knispel RA, Dietz HC, Ramirez F, Baxter BT. Doxycycline delays aneurysm rupture in a mouse model of Marfan syndrome. J Vasc Surg. 2008;47:166-72; discussion 172.

135. Xiong W, Knispel R, MacTaggart J, Greiner TC, Weiss SJ, Baxter BT. Membrane-type 1 matrix metalloproteinase regulates macrophage-dependent elastolytic activity and aneurysm formation in vivo. J Biol Chem. 2009;284:1765-1771.

136. Kurihara T, Shimizu-Hirota R, Shimoda M, Adachi T, Shimizu H, Weiss SJ, Itoh H, Hori S, Aikawa N, Okada Y. Neutrophil-derived matrix metalloproteinase 9 triggers acute aortic dissection. Circulation. 2012;126:3070-3080.

137. Rivera J, Tessarollo L. Genetic background and the dilemma of translating mouse studies to humans. Immunity. 2008;28:1-4.

138. Demant P. . Cancer susceptibility in the mouse: genetics, biology and implications for human cancer. Nat Rev Genet. 2003;4:721-734.

139. Ruivenkamp CA, Csikos T, Klous AM, van Wezel T, Demant P. Five new mouse susceptibility to colon cancer loci, Scc11-Scc15. Oncogene. 2003;22:7258-7260.

140. Maxwell MJ, Duan M, Armes JE, Anderson GP, Tarlinton DM, Hibbs ML. Genetic segregation of inflammatory lung disease and autoimmune disease severity in SHIP-1-/- mice. J Immunol. 2011;186:7164-7175.

141. Walkin L, Herrick SE, Summers A, Brenchley PE, Hoff CM, Korstanje R, Margetts PJ. The role of mouse strain differences in the susceptibility to fibrosis: a systematic review. Fibrogenesis Tissue Repair. 2013;6:18-1536-6-18.

142. McKhann GM,2nd, Wenzel HJ, Robbins CA, Sosunov AA, Schwartzkroin PA. Mouse strain differences in kainic acid sensitivity, seizure behavior, mortality, and hippocampal pathology. Neuroscience. 2003;122:551-561.

143. Dijk JM, van der Graaf Y, Grobbee DE, Banga JD, Bots ML, SMART Study Group. Increased arterial stiffness is independently related to cerebrovascular disease and aneurysms of the abdominal aorta: the Second Manifestations of Arterial Disease (SMART) Study. Stroke. 2004;35:1642-1646.

144. Pezet M, Jacob MP, Escoubet B, Gheduzzi D, Tillet E, Perret P, Huber P, Quaglino D, Vranckx R, Li DY, Starcher B, Boyle WA, Mecham RP, Faury G. Elastin haploinsufficiency induces alternative aging processes in the aorta. Rejuvenation Res. 2008;11:97-112.

145. Hinton RB, Adelman-Brown J, Witt S, Krishnamurthy VK, Osinska H, Sakthivel B, James JF, Li DY, Narmoneva DA, Mecham RP, Benson DW. Elastin haploinsufficiency results in progressive aortic valve malformation and latent valve disease in a mouse model. Circ Res. 2010;107:549-557.

146. Lum C, Shesely EG, Potter DL, Beierwaltes WH. Cardiovascular and renal phenotype in mice with one or two renin genes. Hypertension. 2004;43:79-86.

147. Hartner A, Cordasic N, Klanke B, Veelken R, Hilgers KF. Strain differences in the development of hypertension and glomerular lesions induced by deoxycorticosterone acetate salt in mice. Nephrol Dial Transplant. 2003;18:1999-2004.

148. Cassis LA, Gupte M, Thayer S, Zhang X, Charnigo R, Howatt DA, Rateri DL, Daugherty A. ANG II infusion promotes abdominal aortic aneurysms independent of increased blood pressure in hypercholesterolemic mice. Am J Physiol Heart Circ Physiol. 2009;296:H1660-5.

149. Trivedi DB, Loftin CD, Clark J, Myers P, DeGraff LM, Cheng J, Zeldin DC, Langenbach R. beta-Arrestin-2 deficiency attenuates abdominal aortic aneurysm formation in mice. Circ Res. 2013;112:1219-1229.

150. Miao XN, Siu KL, Cai H. Nifedipine attenuation of abdominal aortic aneurysm in hypertensive and non-hypertensive mice: Mechanisms and implications. J Mol Cell Cardiol. 2015;87:152-159.

151. Minion DJ, Davis VA, Nejezchleb PA, Wang Y, McManus BM, Baxter BT. Elastin is increased in abdominal aortic aneurysms. J Surg Res. 1994;57:443-446.

152. Kunitomo M, Jay M. Elastin fragment-induced monocyte chemotaxis. The role of desmosines. Inflammation. 1985;9:183-188.

153. Davis V, Persidskaia R, Baca-Regen L, Itoh Y, Nagase H, Persidsky Y, Ghorpade A, Baxter BT. Matrix metalloproteinase-2 production and its binding to the matrix are increased in abdominal aortic aneurysms. Arterioscler Thromb Vasc Biol. 1998;18:1625-1633.

154. Curci JA, Liao S, Huffman MD, Shapiro SD, Thompson RW. Expression and localization of macrophage elastase (matrix metalloproteinase-12) in abdominal aortic aneurysms. J Clin Invest. 1998;102:1900-1910.

155. Longo GM, Buda SJ, Fiotta N, Xiong W, Griener T, Shapiro S, Baxter BT. MMP-12 has a role in abdominal aortic aneurysms in mice. Surgery. 2005;137:457-462.

156. Woessner JF,Jr. . Matrilysin. Methods Enzymol. 1995;248:485-495.

157. Abdul-Hussien H, Hanemaaijer R, Kleemann R, Verhaaren BF, van Bockel JH, Lindeman JH. The pathophysiology of abdominal aortic aneurysm growth: corresponding and discordant inflammatory and proteolytic processes in abdominal aortic and popliteal artery aneurysms. J Vasc Surg. 2010;51:1479-1487.

158. Armani C, Curcio M, Barsotti MC, Santoni T, Di Stefano R, Dell'omodarme M, Brandi ML, Ferrari M, Scatena F, Carpi A, Balbarini A. Polymorphic analysis of the matrix metalloproteinase-9 gene and susceptibility to sporadic abdominal aortic aneurysm. Biomed Pharmacother. 2007;61:268-271.

159. Sandford RM, Bown MJ, London NJ, Sayers RD. The genetic basis of abdominal aortic aneurysms: a review. Eur J Vasc Endovasc Surg. 2007;33:381-390.

160. Botnar RM, Wiethoff AJ, Ebersberger U, Lacerda S, Blume U, Warley A, Jansen CH, Onthank DC, Cesati RR, Razavi R, Marber MS, Hamm B, Schaeffter T, Robinson SP, Makowski MR. In vivo assessment of aortic aneurysm wall integrity using elastin-specific molecular magnetic resonance imaging. Circ Cardiovasc Imaging. 2014;7:679-689.

161. Blanchevoye C, Floquet N, Scandolera A, Baud S, Maurice P, Bocquet O, Blaise S, Ghoneim C, Cantarelli B, Delacoux F, Dauchez M, Efremov RG, Martiny L, Duca L, Debelle L. Interaction between the elastin peptide VGVAPG and human elastin binding protein. J Biol Chem. 2013;288:1317-1328.

162. Duca L, Floquet N, Alix AJ, Haye B, Debelle L. Elastin as a matrikine. Crit Rev Oncol Hematol. 2004;49:235-244.

163. Mochizuki S, Brassart B, Hinek A. Signaling pathways transduced through the elastin receptor facilitate proliferation of arterial smooth muscle cells. J Biol Chem. 2002;277:44854-44863.

164. Senior RM, Griffin GL, Mecham RP, Wrenn DS, Prasad KU, Urry DW. Val-Gly-Val-Ala-Pro-Gly, a repeating peptide in elastin, is chemotactic for fibroblasts and monocytes. J Cell Biol. 1984;99:870-874.

165. Lindholt JS, Heickendorff L, Henneberg EW, Fasting H. Serum-elastin-peptides as a predictor of expansion of small abdominal aortic aneurysms. Eur J Vasc Endovasc Surg. 1997;14:12-16.

166. Lindholt JS, Ashton HA, Heickendorff L, Scott RA. Serum elastin peptides in the preoperative evaluation of abdominal aortic aneurysms. Eur J Vasc Endovasc Surg. 2001;22:546-550.

167. Hance KA, Tataria M, Ziporin SJ, Lee JK, Thompson RW. Monocyte chemotactic activity in human abdominal aortic aneurysms: role of elastin degradation peptides and the 67-kD cell surface elastin receptor. J Vasc Surg. 2002;35:254-261.

168. Hunninghake GW, Davidson JM, Rennard S, Szapiel S, Gadek JE, Crystal RG. Elastin fragments attract macrophage precursors to diseased sites in pulmonary emphysema. Science. 1981;212:925-927.

169. Murray PJ, Wynn TA. Protective and pathogenic functions of macrophage subsets. Nat Rev Immunol. 2011;11:723-737.

170. Xiong W, MacTaggart J, Knispel R, Worth J, Persidsky Y, Baxter BT. Blocking TNF-alpha attenuates aneurysm formation in a murine model. J Immunol. 2009;183:2741-2746.

171. Koh TJ, DiPietro LA. Inflammation and wound healing: the role of the macrophage. Expert Rev Mol Med. 2011;13:e23.

172. Longo GM, Xiong W, Greiner TC, Zhao Y, Fiotti N, Baxter BT. Matrix metalloproteinases 2 and 9 work in concert to produce aortic aneurysms. J Clin Invest. 2002;110:625-632.

173. Weischenfeldt J, Porse B. Bone Marrow-Derived Macrophages (BMM): Isolation and Applications. CSH Protoc. 2008;2008:pdb.prot5080.

174. Sharma AK, Lu G, Jester A, Johnston WF, Zhao Y, Hajzus VA, Saadatzadeh MR, Su G, Bhamidipati CM, Mehta GS, Kron IL, Laubach VE, Murphy MP, Ailawadi G, Upchurch GR,Jr. Experimental abdominal aortic aneurysm formation is mediated by IL-17 and attenuated by mesenchymal stem cell treatment. Circulation. 2012;126:S38-45.

175. Xiong W, Zhao Y, Prall A, Greiner TC, Baxter BT. Key roles of CD4+ T cells and IFN-gamma in the development of abdominal aortic aneurysms in a murine model. J Immunol. 2004;172:2607-2612.

176. Petersen E, Wagberg F, Angquist KA. Serum concentrations of elastin-derived peptides in patients with specific manifestations of atherosclerotic disease. Eur J Vasc Endovasc Surg. 2002;24:440-444.

177. Thompson RW, Curci JA, Ennis TL, Mao D, Pagano MB, Pham CT. Pathophysiology of abdominal aortic aneurysms: insights from the elastase-induced model in mice with different genetic backgrounds. Ann N Y Acad Sci. 2006;1085:59-73.

178. D'Armiento J. . Decreased elastin in vessel walls puts the pressure on. J Clin Invest. 2003;112:1308-1310.

179. Hornebeck W, Emonard H, Monboisse JC, Bellon G. Matrix-directed regulation of pericellular proteolysis and tumor progression. Semin Cancer Biol. 2002;12:231-241.

180. Shapiro SD, Endicott SK, Province MA, Pierce JA, Campbell EJ. Marked longevity of human lung parenchymal elastic fibers deduced from prevalence of D-aspartate and nuclear weapons-related radiocarbon. J Clin Invest. 1991;87:1828-1834.

181. Shinohara T, Suzuki K, Okada M, Shiigai M, Shimizu M, Maehara T, Ohsuzu F. Soluble elastin fragments in serum are elevated in acute aortic dissection. Arterioscler Thromb Vasc Biol. 2003;23:1839-1844.

182. Debret R, Antonicelli F, Theill A, Hornebeck W, Bernard P, Guenounou M, Le Naour R. Elastin-derived peptides induce a T-helper type 1 polarization of human blood lymphocytes. Arterioscler Thromb Vasc Biol. 2005;25:1353-1358.

183. Baranek T, Debret R, Antonicelli F, Lamkhioued B, Belaaouaj A, Hornebeck W, Bernard P, Guenounou M, Le Naour R. Elastin receptor (spliced galactosidase) occupancy by elastin peptides counteracts proinflammatory cytokine expression in lipopolysaccharide-stimulated human monocytes through NF-kappaB down-regulation. J Immunol. 2007;179:6184-6192.

184. Pearce WH, Koch AE. Cellular components and features of immune response in abdominal aortic aneurysms. Ann N Y Acad Sci. 1996;800:175-185.

185. Wang Y, Krishna S, Golledge J. The calcium chloride-induced rodent model of abdominal aortic aneurysm. Atherosclerosis. 2013;226:29-39.

186. Meng X, Yang J, Dong M, Zhang K, Tu E, Gao Q, Chen W, Zhang C, Zhang Y. Regulatory T cells in cardiovascular diseases. Nat Rev Cardiol. 2016;13:167-179.

187. Cao Q, Wang Y, Zheng D, Sun Y, Wang Y, Lee VW, Zheng G, Tan TK, Ince J, Alexander SI, Harris DC. IL-10/TGF-beta-modified macrophages induce regulatory T cells and protect against adriamycin nephrosis. J Am Soc Nephrol. 2010;21:933-942.

188. Liu G, Ma H, Qiu L, Li L, Cao Y, Ma J, Zhao Y. Phenotypic and functional switch of macrophages induced by regulatory CD4+CD25+ T cells in mice. Immunol Cell Biol. 2011;89:130-142.

189. Lumeng CN, DelProposto JB, Westcott DJ, Saltiel AR. Phenotypic switching of adipose tissue macrophages with obesity is generated by spatiotemporal differences in macrophage subtypes. Diabetes. 2008;57:3239-3246.

190. Jenne CN, Kubes P. Immune surveillance by the liver. Nat Immunol. 2013;14:996-1006.

191. Hinek A, Rabinovitch M. 67-kD elastin-binding protein is a protective "companion" of extracellular insoluble elastin and intracellular tropoelastin. J Cell Biol. 1994;126:563-574.

192. Privitera S, Prody CA, Callahan JW, Hinek A. The 67-kDa enzymatically inactive alternatively spliced variant of beta-galactosidase is identical to the elastin/laminin-binding protein. J Biol Chem. 1998;273:6319-6326.

193. Wrenn DS, Griffin GL, Senior RM, Mecham RP. Characterization of biologically active domains on elastin: identification of a monoclonal antibody to a cell recognition site. Biochemistry. 1986;25:5172-5176.

194. Grosso L, Scott M. Peptide sequences selected by BA4, a tropoelastin-specific monoclonal antibody, are ligands for the 67-kilodalton bovine elastin receptor. 1993;32:13369-13374.

195. Klink A, Hyafil F, Rudd J, et al. Diagnostic and therapeutic strategies for small abdominal aortic aneurysms. Nat Rev Cardiol. 2011;8:338-347.

196. United Kingdom EVAR Trial Investigators, Greenhalgh RM, Brown LC, Powell JT, Thompson SG, Epstein D, Sculpher MJ. Endovascular versus open repair of abdominal aortic aneurysm. N Engl J Med. 2010;362:1863-1871.

197. Baird PA, Sadovnick AD, Yee IM, Cole CW, Cole L. Sibling risks of abdominal aortic aneurysm. Lancet. 1995;346:601-604.

198. Biros E, Norman PE, Walker PJ, Nataatmadja M, West M, Golledge J. A single nucleotide polymorphism in exon 3 of the kallikrein 1 gene is associated with large but not small abdominal aortic aneurysm. Atherosclerosis. 2011;217:452-457.

199. Deguara J, Burnand KG, Berg J, Green P, Lewis CM, Chinien G, Waltham M, Taylor P, Stern RF, Solomon E, Smith A. An increased frequency of the 5A allele in the promoter region of the MMP3 gene is associated with abdominal aortic aneurysms. Hum Mol Genet. 2007;16:3002-3007.

200. Annabi B, Shedid D, Ghosn P, Kenigsberg RL, Desrosiers RR, Bojanowski MW, Beaulieu E, Nassif E, Moumdjian R, Beliveau R. Differential regulation of matrix metalloproteinase activities in abdominal aortic aneurysms. J Vasc Surg. 2002;35:539-546.

201. Krettek A, Sukhova GK, Libby P. Elastogenesis in human arterial disease: a role for macrophages in disordered elastin synthesis. Arterioscler Thromb Vasc Biol. 2003;23:582-587.

202. Wagenseil JE, Mecham RP. New insights into elastic fiber assembly. Birth Defects Res C Embryo Today. 2007;81:229-240.

203. Clark JM, Glagov S. Transmural organization of the arterial media. The lamellar unit revisited. Arteriosclerosis. 1985;5:19-34.

204. Ait-Oufella H, Wang Y, Herbin O, Bourcier S, Potteaux S, Joffre J, Loyer X, Ponnuswamy P, Esposito B, Dalloz M, Laurans L, Tedgui A, Mallat Z. Natural regulatory T cells limit angiotensin II-induced aneurysm formation and rupture in mice. Arterioscler Thromb Vasc Biol. 2013;33:2374-2379.

205. Yodoi K, Yamashita T, Sasaki N, Kasahara K, Emoto T, Matsumoto T, Kita T, Sasaki Y, Mizoguchi T, Sparwasser T, Hirata K. Foxp3+ regulatory T cells play a protective role in angiotensin II-induced aortic aneurysm formation in mice. Hypertension. 2015;65:889-895.